Universidade de São Paulo
Instituto de Física

Termodinâmica e Transições de Fase de Buracos Negros

Andrés Felipe Cardona Jiménez

Carlos Molina Mendes

Orientador: Prof. Dr. Carlos Molina Mendes

Tese de doutorado apresentada ao Instituto de Física como requisito parcial para a obtenção do título de Doutor em Ciências.

Banca Examinadora:
Prof. Dr. Carlos Molina Mendes (EACH-USP)
Prof. Dr. Fernando T. C. Brandt (IF-USP)
Prof. Dr. Rodrigo Nemmen da Silva (IAG-USP)
Prof. Dr. Mario Cesar Baldiotti (UEL)
Prof. Dr. Olexandr Zhydenko (UFABC)

São Paulo
2020

FICHA CATALOGRÁFICA
Preparada pelo Serviço de Biblioteca e Informação
do Instituto de Física da Universidade de São Paulo

Cardona Jiménez, Andrés Felipe

Termodinâmica e transições de fase de buracos negros. São Paulo, 2020.

Tese (Doutorado) – Universidade de São Paulo. Instituto de Física. Depto. de Física Matemática

Orientador: Prof. Dr. Carlos Molina Mendes

Área de Concentração: Física

Unitermos: 1. Relatividade (Física); 2. Buracos negros; 3. Termodinâmica; 4. Teoria de campos.

USP/IF/SBI-045/2020

University of São Paulo
Physics Institute

Thermodynamics and Phase Transitions of Black Holes

Andrés Felipe Cardona Jiménez

Supervisor: Prof. Dr. Carlos Molina Mendes

Thesis submitted to the Physics Institute of the University of São Paulo in partial fulfillment of the requirements for the degree of Doctor of Science.

Examining Committee:
Prof. Dr. Carlos Molina Mendes (EACH-USP)
Prof. Dr. Fernando T. C. Brandt (IF-USP)
Prof. Dr. Rodrigo Nemmen da Silva (IAG-USP)
Prof. Dr. Mario Cesar Baldiotti (UEL)
Prof. Dr. Olexandr Zhydenko (UFABC)

São Paulo
2020

Resumo

Nesta tese estudamos aspectos da termodinâmica, dinâmica de campos e transições de fase de buracos negros assintoticamente não planos que são importantes no contexto das dualidades *gauge/gravidade*. Em geometrias Anti-Sitter são caracterizados os processos de evaporação e transições de fase de buracos negros. Consideramos o espaço-tempo Vaidya Anti-de Sitter como um modelo para evaporação ou colapso gravitacional, onde é introduzida uma dependência temporal mediante uma função de massa evoluindo no tempo. Para o estudo da termodinâmica de buracos negros evoluindo no tempo seguimos um formalismo adaptado a espaço-tempos não estacionários e com quantidades termodinâmicas associadas à propriedades geométricas dos chamados horizontes atrapantes. Para geometrias Anti-de Sitter comparamos os resultados termodinâmicos com a teoria de gauge dual estabelecido na correspondência AdS/CFT. Também é considerada a dinâmica de campos em certas geometrias onde os resultados perturbativos podem ser associados com um grupo de simetria não associado às isometrias do espaço-tempo de fundo.

Palavras chave: buracos negros, dualidade gauge/gravidade, transições de fase, termodinâmica.

Abstract

In this thesis we study aspects of thermodynamics, field dynamics and phase transitions of non-asymptotically flat black holes that are important in the context of *gauge/gravity* dualities. In Anti-de Sitter geometries the processes of black hole evaporation and phase transitions are characterized. We consider the Vaidya Anti-de Sitter spacetime as a model for evaporation or gravitational collapse, in which a time dependency is introduced by means of a mass function evolving in time. For the study of thermodynamics of black holes evolving in time we follow a formalism adapted to non-stationary spacetimes with thermodynamical quantities associated to geometric properties of the so called trapping horizons. For Anti-de Sitter geometries we compare the thermodynamical results with the corresponding dual gauge theory established in the AdS/CFT correspondence. It is also considered the field dynamics of certain geometries where perturbative results can be associated with a symmetry group not associated to the isometries of the background spacetime.

Keywords: black holes, gauge/gravity duality, phase transitions, thermodynamics.

Acknowledgements

First of all I want to dedicate this work to my dear mother and grandmother, for their unconditional love and continuous words of encouragement, and to my father who is no longer with us.

I would like to express my gratitude to my advisor, Prof. Dr. Carlos Molina Mendes, for his guidance and patience with me during all these years.

To all the friends from Brazil, my home country Colombia, and many other nationalities that I have met during all these years of graduate studies. Special thanks to my group colleagues Wallace, Fabián and Wayner.

To the CPG staff and the secretaries at the DFMA for their good disposition and kindness. Special thanks to Éber and Simone.

This work was financed by processo nº 2015/09221-5, Fundação de Amparo à Pesquisa do Estado de São Paulo (FAPESP) and the Coordenação de Aperfeiçoamento de Pessoal de Nível Superior - Brasil (CAPES) - Finance Code 001.

Contents

Chapter 1

Introduction

In our current understanding of the fundamental laws of nature, the theory of general relativity still remains as the best classical description of the gravitational interaction, with gravity interpreted not as a force but as a geometric property of spacetime. Behind the formulation of this theory lies the equivalence principle, establishing the impossibility for a local observer to distinguish between a gravitational field and a uniformly accelerated frame in a sufficiently small region. The base behind this principle is the equivalence between inertial and gravitational masses for all forms of matter, with the consequence that all physical bodies experience the same free fall in the presence of an external gravitational field. Gravity is unique in that it couples to all forms of matter and energy, establishing the impossibility to define a genuine inertial observer able to measure the physical properties of the gravitational field.

One of the most remarkable predictions of general relativity is the notion of a black hole. A black hole is understood as a compact region of spacetime with a gravitational pull of such magnitude that prevents infalling objects for ever escaping from its interior. On the classical level, black holes are considered as behaving like perfect absorbers, and if unable to radiate, devoid of properties such as temperature or entropy. However, the work of Bardeen, Bekenstein, Carter and Hawking in the early 1970s led to the realization that some properties of stationary black holes follow a close analogy to the laws of thermodynamics [1, 2]. It was only until Hawking showed that when quantum mechanical effects are taken into account in a semiclassical treatment (quantized fields on a classical background geometry), black holes could emit thermal radiation at a characteristic temperature, eventually leading the black hole to evaporate completely [3]. This led to a surprising connection between black hole physics and thermodynamics in which black holes are the systems with the maximum possible amount of entropy, but also to some additional conceptual problems regarding the laws of quantum mechanics and the nature of Hawking radiation.

Even though its is regarded as one of the most significant results in theoretical physics, black hole radiation has not been detected experimentally. If astrophysical black holes are able to evaporate not only would it be at very low temperatures but also it could take an evaporation time greater than the age of the universe [4].

On the order hand, for microscopical black holes, if they should exist, the evaporation time would be too fast to be realistically detected [5]. The thermodynamical behavior of black holes has some unique features when compared with what is expected from other thermodynamical systems. One of the main conclusions of black hole thermodynamics is that black hole entropy scales with the area and not with volume, as most usual thermodynamical systems do. Additionally, asymptotically flat black holes are found to be thermodynamically unstable. Such black holes increase temperature while losing mass eventually leading the black hole to evaporate completely.

With general relativity and quantum mechanics as the two cornerstones of modern theoretical physics, among the efforts that have been developed in order to bring both theories on the same level, a particular mention goes to the proposal of gauge/gravity dualities. The idea behind is that for certain gravitational phenomena it should be possible to find a description in terms of some gauge field theory which does not include gravitational interaction [6, 7]. The most celebrated realization of a gauge/gravity duality is the AdS/CFT correspondence, originally formulated by Maldacena [8], in which a particular gravity theory on an Anti-de Sitter (AdS) geometry can be described in terms of a conformal field theory (CFT) living on the boundary of the geometry. This conjecture has been the starting point of a vast research initiative pursuing the description of gravitational phenomena in terms of a quantum field theory.

The work presented in this thesis aims to explore aspects of thermodynamics and field dynamics of certain black holes geometries that take an important role in the study of gauge/gravity dualities. Even though the thermodynamical description of black holes is widely accepted, it is not yet understood the underlying principles behind such prescription. The exploration of thermodynamical properties of gravitational systems can provide insight on a more fundamental description of the gravitational interaction.

Even without considering their relevance to the AdS/CFT correspondence, the study of asymptotically flat black holes is very interesting on its own. Unlike asymptotically flat black holes asymptotically Anti-de Sitter black holes can be thermodynamically stable, and the evaporation process of an Anti-de Sitter black hole is heavily conditioned by the value of the black hole mass. Moreover, it is known that Anti-de Sitter black holes can undergo phase transitions [9]. Hawking and Page showed from a path integral formalism that although AdS black holes can be in thermal equilibrium with radiation, they are not the preferred state below a certain critical temperature, At this temperature there will be phase transition between thermal AdS and AdS black hole as the preferred state in the gravitational partition function.

In the study of thermodynamics of Anti-de Sitter black holes we are mostly interested in the behavior of time dependent solutions in order to gain additional insight in the details of the processes involved in the dynamics of black holes such as

black hole evaporation and phase transitions. The original formulation of black hole thermodynamics considered stationary black holes in asymptotically flat spacetimes where the event horizon of a black hole can be readily identified as a Killing horizon. If one is interested in study geometries beyond this kind of spacetimes, such as dynamical black holes or asymptotically (anti-)de Sitter black holes, the thermodynamic setting must be established with additional considerations.

In this work we follow the generalized thermodynamics introduced by Hayward, which attempts to formulate thermodynamical properties of black holes in terms of trapping horizons instead of event horizons [10, 11, 12]. In this formalism, adapted to spherically symmetric spacetimes, it is always possible to find a conserved quantity called the Misner-Sharp mass, interpreted as the gravitational energy inside a closed spherical region [13, 14].

With the setting of the thermodynamics for trapping horizons we will provide a description of evaporation and Hawking radiation of Anti-de Sitter black holes using time dependent geometries. We have employed a Vaidya in order to provide an specific model for the dynamical of Anti-de Sitter black holes. The Vaidya geometries are geometries describing massless null radiation [15, 16] and are used as model of black hole evaporation [17] In this type of geometries a time dependent black hole mass is introduced. In Anti-de Sitter geometries the black hole mass and the cosmological constant, it is expected that the dynamics of an evolving black hole depends on how the mass changes with respect to the cosmological constant.

Another incentive behind the formulation of gauge/gravity dualities is the possibility to relate properties of strongly coupled field theories in which a perturbative expansion is not possible with properties of weakly coupled dual theory that are well understood. In this sense the AdS/CFT correspondence is regarded as a promising theoretical tool for the treatment of otherwise difficult to solve problems in field theory. Even though the AdS/CFT is the most established example of a duality between different theories, many efforts have been made to expand such prescription to geometries other than asymptotically Anti-de Sitter. In this thesis we study certain geometries where the perturbative dynamics of relativistic field can be approximated by an effective potential such that the field equations of motion can be related to a differential representations of an underlying algebra that is not directly related to the isometries of the background geometry. As a result it is possible to obtain certain perturbative quantities such as quasinormal modes and frequencies by means of an algebra representation. The main appeal of gauge/gravity is to provide a quantum description of gravitational theories in terms of lower dimensional field theories. It is an open question if such equivalence only applies to a specific number of theories or if such correspondence is a general feature nature.

The outline of this thesis is as follows: In chapter 2 we present a review of the basic aspects of the theory of general relativity that are used in the remainder of the thesis, where we focus on generalities of spherical symmetry geometries. We introduce

the idea of trapping horizons as a characterization of the boundary non-stationary black holes and the generalized thermodynamics that constitutes the main formalism used in our work. In chapter 3 we present a review of some generalities of asymptotically Anti-de Sitter spacetimes and their role in the formulation of the AdS/CFT correspondence.

In chapter 4 we present results concerning field dynamics of near-extremal geometries and how elements of perturbative dynamics, namely quasinormal modes and frequencies can be related to the representation theory of a gauge group. Quasinormal modes are solutions in dynamics of relativistic fields with boundary conditions adapted to background geometries containing black holes and are expected to play a role in the description of gravitational waves associated to black holes. We specialize to geometries with dynamics that are approximated by Pöschl-Teller potentials and present a method that allows to obtain solutions to the equations of motions by a relation with a differential representation of the algebra $\mathfrak{sl}(2)$.

In chapter 5 we study the thermodynamics of Anti-de Sitter black holes with focus on a time-dependent generalization of the Schwarzchild Anti-de Sitter black hole. In order to analyze the time evolution of the Hawking radiation and phase transitions of Anti-de Sitter black holes we employ a Vaidya Anti-de Sitter solution where a time dependent mass function is introduced to model the evolution of such processes. The time-dependent behaviour of thermodynamical quantities such as temperature, free energy and heat capacity of the Vaidya-AdS black hole are analyzed in order to provide a characterization of the phase transitions between different equilibrium configurations. The thermodynamical results are compared with a semiclassical description of Hawking radiation. In particular, we study in detail a model of Hawking radiation of Anti-de Sitter black holes as a tunneling process and the time-dependent model for the evaporation process will provide additional insight on the thermodynamical behaviour of the black hole during the radiation process.

Finally, in chapter 6 we study the 5-dimensional Schwarzchild Anti-de Sitter black hole as a dual to the $\mathcal{N} = 4$ Super Yang-Mills theory in the AdS/CFT correspondence. We focus on study the behaviour of the free energy of the 5-dimensional Vaidya Anti-de Sitter black hole as an order parameter for the Hawking-Page phase transition and the results obtained are then compared with the free energy of the $\mathcal{N} = 4$ Super Yang-Mills theory in the strong and weak coupling limit.

In the development of this thesis, the signature of the metric tensor is $(-,+,+,+)$. We take units where $c = 1$, $G = 1$ and $\hbar = 1$.

Chapter 2

Gravity in Spherically Symmetric Spacetimes

In this chapter we introduce the generalized thermodynamics proposed by Hayward et al [18], which constitutes an extension of the original laws of black hole thermodynamics to non-stationary spacetimes. This formalism is applied for spherically symmetric spacetimes; where it is always possible to define a conserved charge, the Misner-Sharp mass and a conserved current, the Kodama vector field, that generalize the notions of static mass and Killing vector field to non-stationary spacetimes.

2.1 Elements of general relativity

The theory of general relativity is until now the most accepted description of the gravitational interaction and is central to the understanding of a great array of astrophysical phenomena such as black holes, gravitational waves, and the expansion of the universe [19]. Formulated by Albert Einstein in 1915 as an effort to reconcile Newton's gravitational theory with relativistic dynamics, general relativity treats gravity not as a force but as a consequence of a curved spacetime in which matter and radiation act as the source of curvature [20, 21].

The theory of general relativity is based upon two principles: the *equivalence principle* stating the impossibility for an observer to distinguish locally between an acceleration in his own reference frame and the effects of a gravitational field [21] and the *principle of general covariance*, as the requirement for all physics laws to have the same formulation in all reference frames, meaning that there is not such thing as a preferred reference frame. Moreover, special relativity should hold at least locally. The global Lorentz covariance of special relativity becomes a local Lorentz covariance when gravity is introduced [22]. The main property that sets apart gravity from the other known fundamental forces is that the gravitational field couples to all forms of matter and energy. The gravitational interaction possesses a universal character and every physical body or field will experience gravity. Because of that, it is not possible to define a proper inertial observer in the same sense as in special relativity, since every observer will experience the effects of gravity as well [23, 24].

The central idea of general relativity is the association between gravity and geometry, in particular, the relation between spacetime curvature and the content of energy-momentum of any form of matter and radiation present, which is described by the energy-momentum tensor $T_{\mu\nu}$ satisfying the conservation condition [21, 23],

$$\nabla^{\mu} T_{\mu\nu} = 0 \,. \tag{2.1}$$

In the geometric description the classical gravitational field is associated with the spacetime metric $g_{\mu\nu}$ on a Lorentzian manifold $\mathcal{M}$. The curvature is determined by the Riemann tensor, a (1,3) rank tensor whose components are given by

$$R^{\rho}{}_{\sigma\mu\nu} = \partial_{\mu}\Gamma^{\rho}{}_{\nu\sigma} - \partial_{\nu}\Gamma^{\rho}{}_{\mu\sigma} + \Gamma^{\rho}{}_{\mu\lambda}\Gamma^{\lambda}{}_{\nu\sigma} - \Gamma^{\rho}{}_{\nu\sigma}\Gamma^{\lambda}{}_{\mu\sigma} \,. \tag{2.2}$$

where $\{\Gamma^{\sigma}{}_{\mu\nu}\}$ are the connection coefficients associated with the covariant derivative ∇_{μ}. If the covariant derivative of the metric with respect to that connection is zero at every point, $\nabla_{\mu} g^{\mu\nu} = 0$, the associated connection coefficients are given uniquely in terms of the metric components and their first order derivatives by

$$\Gamma^{\sigma}{}_{\mu\nu} = \frac{1}{2} g^{\sigma\rho} \left(\partial_{\mu} g_{\nu\rho} + \partial_{\nu} g_{\rho\mu} - \partial_{\rho} g_{\mu\nu} \right) \,, \tag{2.3}$$

and are known as Christoffel symbols. If a coordinate system exists such that the components of the metric tensor are coordinate independent, the Riemann tensor will vanish. Another important tensor, known as the Ricci tensor, is defined from the Riemann tensor by contraction of indexes:

$$R_{\mu\nu} = R^{\lambda}{}_{\mu\lambda\nu} \,. \tag{2.4}$$

The trace of the Ricci tensor is called the Ricci scalar or curvature scalar and it is a quantity that remains invariant under coordinate changes

$$R = R^{\mu}{}_{\mu} \,. \tag{2.5}$$

In order to establish a mathematical relation between matter and curvature it is necessary to obtain a second rank contravariant tensor built from the metric tensor and its derivatives and satisfying the same conservation condition as the energy-momentum tensor. Even though the Ricci tensor is a second rank tensor containing information about curvature in general it does not have divergence zero. An appropriated choice is found from both the Ricci tensor (2.4) and the curvature scalar (2.5)

$$G_{\mu\nu} = R_{\mu\nu} - \frac{1}{2} R g_{\mu\nu} \,. \tag{2.6}$$

The tensor $G_{\mu\nu}$ is called the Einstein tensor and satisfies the requirement $\nabla^{\mu} G_{\mu\nu} = 0$. The Einstein's field equations of general relativity dictating the dynamics of the metric tensor are established as a directly proportional relation between the tensors

$G_{\mu\nu}$ and $T_{\mu\nu}$:

$$R_{\mu\nu} - \frac{1}{2} R\, g_{\mu\nu} = \frac{8\pi G}{c^4} T_{\mu\nu}\,. \tag{2.7}$$

An additional term proportional to the metric can be added to the field equation (2.7) such that both sides of the equation continue to satisfy the conservation condition,

$$R_{\mu\nu} - \frac{1}{2} R\, g_{\mu\nu} - \Lambda\, g_{\mu\nu} = \frac{8\pi G}{c^4} T_{\mu\nu}\,. \tag{2.8}$$

The constant Λ is known as the *cosmological constant*. Solutions of Einstein's field equation with non-zero cosmological constant represent geometries with a energy density associated to empty space.

Einstein's field equations can be derived using a variational method from the Einstein-Hilbert action:

$$S_{EH} = \frac{1}{16\pi G} \int d^4x \sqrt{-g}(R - 2\Lambda) + S_{matter}\,, \tag{2.9}$$

where S_{matter} represents the action of whatever form of matter is present. The Einstein's field equation (2.8) are obtained by variation of the action (2.9) with respect to the metric tensor $g_{\mu\nu}$, and the variation of the matter action with respect to the metric defines the energy-momentum tensor:

$$T_{\mu\nu} = -\frac{2}{\sqrt{-g}} \frac{\delta S_{matter}}{\delta g_{\mu\nu}}\,. \tag{2.10}$$

The Einstein-Hilbert action postulated in (2.9) is the only possible action if invariance under general coordinate transformations is demanded and involving at most second order derivatives of the metric tensor components [20]. Consider an infinitesimal coordinate transformation from a coordinate system x^μ to a new coordinate system $\tilde{x}^\mu$ of the form

$$\delta\tilde{x}^\mu = \delta x^\mu + \frac{\partial \lambda^\mu}{\partial x^\nu} dx^\nu\,, \tag{2.11}$$

where λ^μ is a variational parameter. Variation of the classical action under such general coordinate transformations gives

$$-\delta_\lambda S_{EH} = \int d^d x \sqrt{-g} \lambda^\nu \nabla_\mu T_\nu{}^\mu\,, \tag{2.12}$$

The principle of general covariance requires invariance of the action under such coordinate transformation, that is $\delta_\lambda S_{EH} = 0$, implying

$$\lambda^\nu \nabla_\mu T_\nu{}^\mu = 0\,, \tag{2.13}$$

which is nothing more than the requirement for the conservation of the energy-momentum tensor.

2.2 Spherically symmetric spacetimes

The non-linear character of Einstein's field equations implies the impossibility to obtain a general solution from an arbitrary energy-momentum tensor $T_{\mu\nu}$. The majority of known solutions in general relativity assume a certain number of symmetries and/or simplifications. A coordinate independent way to characterize a symmetry of the metric tensor with respect to a transformation generated by a vector field K is through the Lie derivative of the metric tensor:

$$\begin{aligned}\mathcal{L}_K g_{\mu\nu} &= K^\sigma \nabla_\sigma g_{\mu\nu} + (\nabla_\nu K^\lambda) g_{\lambda\nu} + (\nabla_\nu K^\lambda) g_{\mu\lambda} \\ &= \nabla_\mu K_\nu + \nabla_\nu K_\mu \,,\end{aligned} \tag{2.14}$$

where $\nabla_\sigma g_{\mu\nu} = 0$ is the covariant derivative associated to the metric affine connection of $g_{\mu\nu}$. If the metric $g_{\mu\nu}$ remains invariant under a transformation generated by a vector field K^μ then the Lie derivative of the metric is zero

$$\mathcal{L}_K g_{\mu\nu} = 0 \,, \tag{2.15}$$

and the components of the vector field K satisfy

$$\nabla_\mu K_\nu + \nabla_\nu K_\mu = 0 \,. \tag{2.16}$$

An invariance of the metric tensor under such transformation is called an an isometry. The vector field K is called Killing vector and equation (2.16) is known as Killing equation. If a spacetime has a Killing vector, it is always possible to find a coordinate system in which the metric is independent of one of the coordinates [20].

In general relativity, solutions without explicit time dependence, or better put, solutions in which there is a coordinate system in which the metric tensor is time-independent, are called *stationary* geometries. A stationary spacetime is characterized by possessing a Killing vector field that is globally timelike. In a a coordinate system (t, x^1, x^2, x^3), with t representing a temporal coordinate, the associated Killing vector is denoted ∂_t with components $\{\partial_t\}^\mu = (1, 0, 0, 0)$. A more general constraint to stationarity is *staticity*, in which a a physical system does not evolve at all over time. A spacetime is static if all of the metric components are time independent and invariant under temporal reflection. Static spacetimes are characterized in a coordinate independent way by the existence of a timelike Killing vector field orthogonal to a family of spatial hypersurfaces parameterized by t constant. A timelike Killing vector x^μ is orthogonal to a hypersurface if it satisfies the following equation

$$x_{[\mu} \nabla_\nu x_{\sigma]} = 0 \,, \tag{2.17}$$

which is a result following from the well known Frobenius's Theorem (the braces are a notation indicating an antisymmetric, linear combinations of terms with index

permutation) for details see for example appendix B of [23].

One of the most usual symmetries considered for solutions in general relativity is *spherical symmetry*, meaning that there is no preferred spatial direction. A coordinate-independent property of spherically symmetric spacetimes is the existence of three spacelike, linearly independent Killing vector fields $\{V_i\}_{i=1}^3$ satisfying the algebra of the group $SO(3)$

$$[V_i, V_j] = \epsilon_{ijk} V_k, \quad i, j, k = 1, 2, 3\,. \tag{2.18}$$

where ϵ_{ijk} is the Levi Civita symbol.

In a stationary, spherically symmetric spacetime the metric tensor can be described by a coordinate system (t, r, θ, ϕ), where t is a temporal coordinate associated with the timelike Killing vector defining staticity and (θ, ϕ) are the usual spherical coordinates parameterizing surfaces invariant under rotations (surfaces with area $A = 4\pi r^2$). In this coordinate system the metric tensor can be expressed as

$$ds^2 = -F(r)dt^2 + \frac{1}{G(r)}dr^2 + r^2 d\Omega^2\,, \tag{2.19}$$

where $d\Omega^2$ is the line element of the unit 2-sphere and $F(r)$ and $G(r)$ are positive definite functions of the radial coordinate r when defined on Lorentzian manifolds. The form of the metric tensor (2.19) considers the most general solution of Einstein's field equation satisfying the conditions of staticity and spherical symmetry [20].

2.3 Black hole thermodynamics

A black hole is formally understood as a spacetime region causally disconnected from infinity. If $(\mathcal{M}, g)$ is an asymptotically flat manifold, a black hole $\mathcal{B}$ is a region from which no null or timelike path can reach future null infinity $\mathcal{I}^+$, that is

$$\mathcal{B} = \mathcal{M} - J(\mathcal{I}^+)\,, \tag{2.20}$$

where $J(\mathcal{I}^+)$ is the causal past of $\mathcal{I}^+$. The boundary $\partial\mathcal{B}$ of the black hole is the event horizon and is a null hypersurface separating spacetime points that cannot be connected to infinity by a timelike path [23].

The first solution of Einstein's field equation that would characterize a black hole was found by Karl Schwarzschild in 1916, describing the spacetime geometry outside a spherical symmetric body of mass M [25] and that has come to be known as the Schwarzschild metric:

$$ds^2 = -\left(1 - \frac{2M}{r}\right)dt^2 + \left(1 - \frac{2M}{r}\right)^{-1} dr^2 + r^2 d\Omega^2\,, \tag{2.21}$$

In this solution the surface $r = 2M$ is known as the Schwarzschild radius. If a spherical object of mass M collapses under its Schwarzchild radius the surface $r =$

$2M$ demarcates what is known as the *event horizon*, representing the point past which light can no longer escape the gravitational field. To locate the event horizon for any given geometry would require to solve the geodesic equation and determine which geodesics cannot reach future null infinity from the past.

In stationary spacetimes, a characterization of the boundary of a black hole is possible from the notion of Killing horizons. A Killing horizon is a surface where the norm of a timelike Killing vector is zero. If a Killing vector field K^μ is null along some null hypersurface Σ, it is said that Σ is a Killing horizon of K^μ. In stationary, asymptotically flat spacetimes every event horizon is a Killing horizon for some Killing vector K^μ, but in general, not every Killing horizon is an event horizon [20]. To every Killing horizon there is an associated quantity called surface gravity κ. Since K^μ is normal to the Killing horizon, it obeys the geodesic equation along the Killing horizon

$$K^\mu \nabla_\mu K^\nu = -\kappa K^\nu \,. \tag{2.22}$$

Using Killing's equation (2.16) and Frobenius's' theorem (2.17), a formula that allows to find the value of the surface gravity associated to the Killing horizon can be found [23]

$$\kappa^2 = -\frac{1}{2} \left(\nabla_\mu K_\nu\right) \left(\nabla^\mu K^\nu\right) \,, \tag{2.23}$$

and it is meant to be evaluated only at the Killing horizon.

In a static, asymptotically flat spacetime, the surface gravity κ is interpreted as the acceleration (as seen by a static observer at infinity) needed to keep an object at rest at the horizon of events [20]. In the coordinate system (t, r, θ, ϕ) the associated Killing vector to the metric (2.19) has components

$$K^\mu = \frac{\partial}{\partial t} = (1, 0, 0, 0) \,. \tag{2.24}$$

such that the norm of the Killing vector is then given by $K_\mu K^\mu = -F(r)$. The Killing horizon will correspond to the surface $r = r_+$ where $F(r_+) = 0$. The surface gravity can be obtained from the covariant derivative of K^μ, in this case the only relevant Christoffel symbol is $\nabla_r K_t$, therefore

$$\nabla_\mu K_\nu = -\frac{1}{2} \frac{dF(r)}{dr} \,. \tag{2.25}$$

With this the surface gravity in equation (2.23) reads

$$\kappa^2 = \lim_{r \to r_+} \frac{1}{4} \frac{G(r)}{F(r)} \left(\frac{d}{dr} F(r)\right)^2 \,. \tag{2.26}$$

We use to following equality

$$\sqrt{\frac{G(r)}{F(r)}} \left(\frac{d}{dr} F(r)\right) = \frac{d}{dr} \left(\sqrt{F(r) G(r)}\right) - F(r) \frac{d}{dr} \left(\sqrt{\frac{G(r)}{F(r)}}\right) \,, \tag{2.27}$$

from which we can write

$$\kappa = \lim_{r\to r_+} \frac{1}{2}\left|\frac{d}{dr}\left(\sqrt{F(r)G(r)}\right) - F(r)\frac{d}{dr}\left(\sqrt{\frac{G(r)}{F(r)}}\right)\right| . \tag{2.28}$$

Taking this into account makes the second term in (2.28) equal to zero, as long as the fraction $G(r)/F(r)$ is differentiable in $r = r_+$. Then we obtain the following expression for the surface gravity of the metric (2.19)

$$\kappa = \lim_{r\to r_+} \frac{1}{2}\left|\frac{d}{dr}\sqrt{F(r)G(r)}\right| . \tag{2.29}$$

For the Schwarzschild black hole the surface gravity is equal to $\kappa = 1/4M$.

The work of Bardeen, Bekenstein, Carter and Hawking in the early 1970s suggested that some properties of stationary black holes follow a close analogy to the laws of thermodynamics [1, 2]. For perturbations in stationary black holes, an infinitesimal change of the black hole mass M is related with the variation of the event horizon area A, the angular momentum J and the electric charge Q by

$$\delta M = \frac{\kappa}{8\pi}\delta A + \Omega\delta J + \Phi\delta Q\,, \tag{2.30}$$

where Ω is the angular velocity of the black hole and Φ the electrostatic potential. This relation mirrors the law of thermodynamics relating the change of internal energy U of a system with the change of entropy S between two equilibrium states,

$$\delta U = T\delta S + \text{work terms}\,, \tag{2.31}$$

under the identifications $M \to U$, $T \propto \kappa$ and $S \propto A$. When quantum mechanical effects are taken into account in a semiclassical treatment black holes are predicted to radiate thermal radiation at a characteristic temperature proportional to the surface gravity of the black hole [3]:

$$T_{BH} = \frac{\kappa}{2\pi}\,, \tag{2.32}$$

called *Hawking temperature*, and with an entropy proportional to the event horizon area

$$S_{BH} = \frac{A}{4}\,. \tag{2.33}$$

This realization lead to the identification of black holes as thermodynamics objects. For a Schwarzchild black hole in asymptotically flat space the heat capacity $C = \partial M/\partial T$ turns out to be negative and inversely proportional to the squared mass, making asymptotically flat black hole thermodynamically unstable. Such black holes increase temperature while losing mass, eventually leading the black hole to evaporate completely.

2.4 Thermodynamics in non-stationary geometries

Albeit the characterization of a black hole in terms of an event horizon is a simple and elegant definition, it is from a certain point of view unsatisfactory when realistic black holes come into consideration. The location of the event horizon depends on the global structure of the spacetime; in principle it is not possible to determine from the geometry near the event horizon alone. Identifying the location of the event horizon would in principle require knowledge of the whole story of the spacetime, which is not possible for a local observer in a finite proper time. For a treatment of black holes as ordinary physical objects, it would be desirable a prescription in terms of local quantities. One such proposal comes from the idea of *trapping horizons*, which are surfaces enclosing a region where outgoing light rays actually move inwards, thus formalizing the intuitive idea of the boundary of a black hole as a surface preventing light rays from escaping from the interior of the black hole.

2.4.1 Trapping horizons

Let $\mathcal{S}$ be a 2-dimensional, closed, spacelike surface. If every null congruence orthogonal to $\mathcal{S}$ has negative expansion, then such surface is said to be a *trapping surface*. A 2-dimensional, closed, spacelike surface is said to be *marginal* if one of the null orthogonal congruences converges and the other either converges or diverges. Finally, a *trapping horizon* is defined as the boundary of a 3-dimensional surface foliated by a set of marginal surfaces [26]. For static and spherically symmetric vacuum solutions the trapping horizon coincides with the event horizon, but in general they are different. An important difference is that while the event horizon is always null, a trapping horizon can be timelike, spacelike or null.

We will assume spacetimes with spherical symmetry. In a coordinate system (x^+, x^-, θ, ϕ) adapted to the incoming and outgoing null congruences, the metric can be expressed as:

$$ds^2 = 2g_{+-}(x^+, x^-)dx^+dx^- + R^2(x^+, x^-)d\Omega^2\,, \tag{2.34}$$

where $R(x^+, x^-)$ is the "aerial radius" of spheres with area $A = 4\pi R^2$. The components of the metric (2.34) in matrix notation read

$$g_{ab} = \begin{bmatrix} 0 & -g_{+-} \\ -g_{+-} & 0 \end{bmatrix}\,, \quad g^{ab} = \begin{bmatrix} 0 & -g_{+-}^{-1} \\ -g_{+-}^{-1} & 0 \end{bmatrix}\,. \tag{2.35}$$

In this coordinate system the radial null vectors tangent to radial null geodesics are expanded by the basis $\{X_+, X_-\}$ where

$$X_\pm = \frac{\partial}{\partial x^\pm}\,. \tag{2.36}$$

It is assumed that these vectors are future-oriented. The convergence or divergence of these null vectors is characterized by the expansions $\theta_\pm$ of the associated geodesic congruences. In general, the expansion θ is a measure of the (fractional) rate of change of the cross-sectional area of a geodesic congruence:

$$\theta = \frac{\delta A}{A} \,. \tag{2.37}$$

Since we are considering spherical symmetry, the (total) cross section of radial null geodesics satisfies the area relation $A = 4\pi R^2$, with the area A being an invariant quantity under rotations for a surface of fixed R. From (2.36) we can obtain the expansions $\theta_\pm$ of the light rays congruences. In the coordinate system (x^+, x^-, θ, ϕ), the expansion of vectors $X_\pm$ is [11]

$$\theta_\pm = \frac{2}{R}\frac{\partial R}{\partial x^\pm} \,. \tag{2.38}$$

In general, if X^μ is a tangent vector to (an affinely parametrized) geodesic congruence, then the expansion of said congruence is given by

$$\theta = \nabla_\mu X^\mu = \frac{1}{\sqrt{-g}}\partial_\mu(\sqrt{-g}g^{\mu\nu}X_\nu) \,. \tag{2.39}$$

In terms of the light ray congruence expansions, a trapping surface satisfies $\theta_+\theta_- > 0$ and a marginal surface $\theta_+\theta_- = 0$. A (future exterior) trapping horizon is the boundary of a 3-surface foliated by marginal surfaces satisfying

$$\theta_+ = 0 \,, \tag{2.40}$$

$$\theta_- < 0 \,, \tag{2.41}$$

$$\mathcal{L}_-\theta_+ < 0 \,. \tag{2.42}$$

The last condition is used to define an outer future horizon. In this context, a black hole is understood as the region closed by an outer future trapping horizon, where ingoing light rays converge $\theta_+ > 0$, and outgoing light rays are parallel along the horizon and diverging outside it.

2.4.2 Kodama vector and geometric surface gravity

In non-stationary spacetimes there are no Killing horizons that can be associated to a timelike Killing vector field. In spherically symmetric spacetimes a generalization comes from the Kodama vector [27]. Any spherically symmetric 4-dimensional manifold $\mathcal{M}$ can be decomposed as $\mathcal{M} = \mathcal{M}_2 \times S_2$, where S_2 is the unit 2-sphere. In a general coordinate system the metric of $\mathcal{M}$ is:

$$ds^2 = h_{ab}dx^a dx^b + R^2(x^a, x^b)d\Omega^2 \,, a, b = 0, 1 \,, \tag{2.43}$$

with h_{ab} the induced metric on $\mathcal{M}_2$, the tangent space to the unit 2-sphere in $\mathcal{M}$. The Kodama vector is initially defined in the manifold $\mathcal{M}_2$, with components [28]:

$$K^a = \frac{1}{\sqrt{-h}}\epsilon^{ab}\nabla_b R, \quad a,b = 0,1\,, \tag{2.44}$$

where ϵ^{ab} is the 2-dimensional Levi-Civita symbol. The 2-dimensional Kodama vector on $\mathcal{M}_2$ can be extended to the 4-dimensional manifold $\mathcal{M}$ with components $K^\mu = (k^0, k^1, 0, 0)$. From the antisymmetric property of the Levi-Civita symbol, it follows that the Kodama vector has divergence equal to zero: $\nabla_a K^a = 0$. The Kodama vector does not necessarily satisfy Killing's equation and it is not necessarily geodesic on the horizon. In non-stationary spacetimes, the Kodama vector defines a privileged time direction.

In the coordinate system (x^+, x^-, θ, ϕ), the Kodama vector is given in terms of the basis $\{X^+, X^-\}$ as:

$$K = -g^{+-}\left(\frac{\partial R}{\partial x^+}\frac{\partial}{\partial x^-} - \frac{\partial R}{\partial x^-}\frac{\partial}{\partial x^+}\right), \tag{2.45}$$

with norm:

$$K^2 = K_a K^a = -2g^{+-}\frac{\partial R}{\partial x^+}\frac{\partial R}{\partial x^-} = \frac{R^2 g^{+-}}{2}\theta_+\theta_-\,, \tag{2.46}$$

where in the last expression we have used the expansions $\theta_\pm$ of the null geodesic congruences equation (2.38). The Kodama vector is spacelike, timelike or null for trapping, non-trapping and marginal surfaces respectively. From equation (2.46), it can be seen that a trapping horizon is the hypersurface where the Kodama vector is null.

In spacetimes admitting a Kodama vector, it is possible to generalize the concept of surface gravity. The geometric surface gravity κ_g of a Kodama vector K^a associated to a trapping horizon is defined by [12]:

$$\frac{1}{2}h^{ab}K^c(\nabla_c K_a - \nabla_a K_c) = \kappa_g K^b\,, \tag{2.47}$$

or, equivalently

$$\kappa_g = \frac{1}{2}\Box_{(h)}R = \frac{1}{2\sqrt{-h}}\partial_a(\sqrt{-h}h^{ab}\partial_b R)\,. \tag{2.48}$$

In the coordinate system (x^+, x^-, θ, ϕ) adapted to the light ray congruences

$$\kappa_g = g^{+-}\frac{\partial^2 R(x^+, x^-)}{\partial x^+ \partial x^-}\,. \tag{2.49}$$

In the formalism of generalized thermodynamics the geometric surface gravity κ_g is proportional to the temperature and is constant only if the trapping horizon is static.

2.4.3 Misner-Sharp mass

In a generalized formulation of thermodynamics for gravitational systems it is necessary a general notion of energy associated with the gravitational field. Since the Kodama vector has divergence zero it is always possible to define a conserved current $J^a = G^{ab}K_b$ satisfying $\nabla_a J^a = 0$. The Noether charge associated to the conserved current J^a of the Kodama vector K is called the Misner-Sharp mass M_{ms} [11, 18]:

$$M_{ms} = -\int_{\Sigma} d\Sigma T_{ab}K^b \, , a, b = 0, 1 \, . \tag{2.50}$$

In spherically symmetric geometries the Misner-Sharp mass is invariant for each symmetric sphere of radius R and represents the gravitational mass inside the sphere. In terms of the gradient $\nabla_a R \nabla^a R$ the Misner-Sharp mass is defined as [13, 14]:

$$M_{ms} = \frac{R}{2}\left(1 - h^{ab}\nabla_a R \nabla_b R\right) \, . \tag{2.51}$$

In the coordinate system (x^+, x^-, θ, ϕ) of metric (2.34) is possible to write the Misner-Sharp mass in terms of the norm of the Kodama vector (2.46) as

$$M_{ms} = \frac{R}{2}\left(1 - 2g^{+-}\frac{\partial R}{\partial x^+}\frac{\partial R}{\partial x^-}\right) = \frac{R}{2}(1 + K^2) \, . \tag{2.52}$$

At a trapping horizon the norm of the Kodama vector is zero, therefore the trapping horizon will be located at

$$R = 2M_{ms} \, . \tag{2.53}$$

The derivative of (2.52) with respect to $x^{\pm}$ gives us

$$\frac{\partial M_{ms}}{\partial x^{\pm}} = \frac{1}{2}\frac{\partial R}{\partial x^{\pm}}(1 + K^2) + \frac{R}{2}\frac{\partial K^2}{\partial x^{\pm}} \, . \tag{2.54}$$

At the horizon the norm of the Kodama vector is zero, therefore

$$\frac{\partial M_{ms}}{\partial x^{\pm}} = \frac{1}{2}\frac{\partial R}{\partial x^{\pm}} \, , \tag{2.55}$$

implying that at the trapping horizon the variation of the Misner-Sharp mass with respect to the null coordinates is proportional to the expansions $\theta_{\pm}$ of the respective null vectors.

2.4.4 Generalized first law

In usual thermodynamics the first law is defined from the variation of the internal energy δU between different equilibrium states. For the generalized thermodynamics of trapping horizons the corresponding first law is formulated from variations of the Misner-Sharp mass. To define the generalized first law the following quantities are introduced [12, 26]:

$$\omega = -\frac{1}{2} T_{ab} h^{ab} \,, \tag{2.56}$$

and

$$\psi_a = T_a{}^b \nabla_b R + \omega \nabla_a R \,, \tag{2.57}$$

that can be interpreted as energy density and energy flux respectively. In terms of the density (2.56) and flux (2.57), the generalized first law is formulated as [12]

$$\nabla_a M_{ms} = A \psi_a + \omega \nabla_a V \,, \tag{2.58}$$

with V the volume related to the area A of a sphere of symmetry with radius R by $\nabla_a V = A \nabla_a R$. The generalized first law (2.58) is valid for any spherical region of radius R, not just the trapping horizon of a black hole. To develop how equation (2.58) should apply to black holes we specialize to the coordinate system (x^+, x^-, θ, ϕ). In this coordinate system we can write Einstein field equations in terms of the expansions $\theta_\pm$ and their derivatives as :

$$\theta_\pm \frac{\partial \ln[(-g_{+-})]}{\partial x^\pm} - \frac{\partial \theta_\pm}{\partial x^\pm} - \frac{1}{2} (\theta_\pm)^2 = 8\pi T_{\pm\pm} \,, \tag{2.59}$$

$$\frac{\partial \theta_\pm}{\partial x^\mp} + \theta_+ \theta_- + \left(\Lambda - \frac{1}{r^2} \right) g_{+-} = 8\pi T_{+-} \,. \tag{2.60}$$

In particular, since at a trapping horizon the condition $\theta_+ \theta_- = 0$ holds, we get for equation (2.60) the following result

$$\frac{\partial \theta_\pm}{\partial x^\mp} + \left(\Lambda - \frac{1}{r^2} \right) g_{+-} = 8\pi T_{+-} \,. \tag{2.61}$$

On the other hand, in the coordinate system (x^+, x^-, θ, ϕ), the energy density ω and energy flux ψ defined in (2.56) and (2.57) read

$$\omega = -g^{+-} T_{+-} \,, \tag{2.62}$$

$$\psi = T^{++} \frac{\partial R}{\partial x^+} \frac{\partial}{\partial x^+} + T^{--} \frac{\partial R}{\partial x^-} \frac{\partial}{\partial x^-} \,. \tag{2.63}$$

With that, the generalized first law (2.58) reads

$$\frac{\partial M_{ms}}{\partial x^\pm} = -A g^{+-} \left(T_{+-} \frac{\partial R}{\partial x^\pm} - T_{\pm\pm} \frac{\partial R}{\partial x^\mp} \right) \,. \tag{2.64}$$

We can associate the quantity ω defined in (2.56) with the expansions $\theta_\pm$

$$\omega = -g_{+-}T^{+-} = -g^{+-}T_{+-} = \frac{-g^{+-}}{8\pi}\left[\frac{\partial\theta_\pm}{\partial x^\pm} + \left(\Lambda - \frac{1}{r^2}\right)g_{+-}\right] . \tag{2.65}$$

We can write this in terms of the geometric surface gravity κ_g given by (2.49). Taking into account the definitions for the expansions $\theta_\pm$ in (2.38), we have

$$\frac{\partial\theta_\pm}{\partial x^\mp} = -\frac{2}{R^2}\frac{\partial R}{\partial x^+}\frac{\partial R}{\partial x^-} + \frac{\partial^2 R}{\partial x^+\partial x^-} , \tag{2.66}$$

or

$$\frac{\partial\theta_\pm}{\partial x^\mp} = -\frac{1}{2}\theta_+\theta_- + \kappa_g(g^{+-})^{-1} . \tag{2.67}$$

In particular, at a trapping horizon we have

$$\frac{\partial\theta_\pm}{\partial x^\mp} = \kappa_g(g^{+-})^{-1} . \tag{2.68}$$

Thus, at the apparent horizon the derivative of the expansion is proportional to the geometric surface gravity. With this result

$$8\pi T_{+-} = \kappa_g(g^{+-})^{-1} + \left(\Lambda - \frac{1}{r^2}\right)g_{+-} . \tag{2.69}$$

Then, the quantity ω at a trapping horizon is

$$\omega = -\frac{\kappa_g}{4\pi R} - \frac{1}{8\pi}\left(\Lambda - \frac{1}{R^2}\right) , \tag{2.70}$$

providing a useful form for the energy density ω at the trapping horizon in terms of the geometrical surface gravity κ_g and the trapping horizon radius.

Now we can express the variation of the Misner-Sharp mass (2.58) in terms of the geometric properties of the trapping horizon. It will be useful to rearrange equation (2.58) as

$$A\psi_a = \nabla_a M_{ms} - \omega\nabla_a V . \tag{2.71}$$

We can write the variation $\nabla_a M_{ms}$ as

$$\nabla_a M_{ms} = R\nabla_a\left(\frac{M_{ms}}{R}\right) + \frac{M_{ms}}{R}\nabla_a R . \tag{2.72}$$

Taking into account $\nabla_a A = 8\pi R\nabla_a R$ eventually leads to

$$A\psi_a = R\nabla_a\left(\frac{M_{ms}}{R}\right) + \frac{1}{8\pi}\nabla_a A\left(\frac{M_{ms}}{R^2} - 4\pi\omega R\right) . \tag{2.73}$$

In the second term is identified from (2.70) the surface gravity in terms of the Misner-Sharp mass (there is a slight subtlety in absorbing the term depending on the cosmological constant in (2.70) into ω):

$$\kappa_g = \frac{M_{ms}}{R^2} - 4\pi\, R\, \omega\,. \tag{2.74}$$

With that, the term $A\psi_a$ becomes

$$A\psi_a = \frac{\kappa_g}{8\pi}\nabla_a A + R\nabla_a\left(\frac{M_{ms}}{R}\right)\,. \tag{2.75}$$

When this expression is evaluated at a trapping horizon, the quantity M_{ms}/R is constant and $\nabla_a R$ is null, making the second term equal to zero. Then we have that the variation of the Misner-Sharp mass in equation (2.58) at the trapping horizon is:

$$\nabla_a M_{ms} = \frac{\kappa_g}{8\pi}\nabla_a A + \omega\nabla_a V\,, \tag{2.76}$$

where the first term is the energy added to the black hole and the second term is interpreted as the work performed by the black hole to maintain its configuration. Comparing with the first law of usual thermodynamics (2.31), the Misner-Sharp mass takes the role of internal energy (not just the black hole mass M) and the temperature and entropy of the trapping horizon are

$$T = \frac{\kappa_g}{2\pi}\,, \quad S = \frac{A}{4}\,. \tag{2.77}$$

These expressions share the same form as the temperature (2.32) and entropy (2.33) of stationary back holes. One can take either the horizon radius r_+ or the entropy/horizon area as the independent thermodynamical variable and the Misner-Sharp mass and volume as the dependent variables. Here it is important to remember that these new quantities are associated with a trapping horizon and that unlike the case for Killing horizons they are valid for time dependent surface gravity and horizon area.

2.5 Field dynamics in spherically symmetric spacetimes

Solving Einstein's equation means finding the metric tensor $g_{\mu\nu}$ associated to a certain matter-radiation distribution given by the energy-momentum tensor $T_{\mu\nu}$. Once the background metric is established, a natural question is to determine its response to variations of the matter content. This is a highly non-linear problem, as variations in $T_{\mu\nu}$ imply an alteration of spacetime geometry, which at the same time involves a matter redistribution. Nevertheless, if one assumes small variations of the background metric one can treat the problem perturbatively, and in the lowest order, the background reaction can be ignored, implying that only the matter fields are treated dynamically in this approach [29].

2.5.1 Effective potential of scalar fields

In an approach where the backreaction of the metric is negligible, the dynamics of matter fields is introduced by means of a relativistic motion equation that depends on the spacetime metric. We will focus in developing the dynamics for a scalar field propagating on a fixed background geometry. A scalar field is the simplest example of a relativistic field and is often used in certain cosmology models or extensions to general relativity. We introduce as a test field a massless scalar field Φ in a background spacetime satisfying the (massless) Klein-Gordon equation [30]

$$g^{\mu\nu}\nabla_\mu\nabla_\nu\Phi = 0\,, \tag{2.78}$$

or equivalently

$$\frac{1}{\sqrt{-g}}\partial_\mu\left(\sqrt{-g}g^{\mu\nu}\partial_\nu\Phi\right) = 0\,. \tag{2.79}$$

Consider the general spherically symmetric and stationary geometry (2.19) with a coordinate system (t, r, θ, ϕ). In such geometry the field Φ is given by a multipole expansion of the form

$$\Phi(t, r, \theta, \phi) = \sum_{\ell,m}\frac{1}{r}\Psi_\ell(t, r)Y_{l.m}(\theta, \phi)\,, \tag{2.80}$$

where $Y_{\ell.m}$ are the spherical harmonics. Furthermore, if the background is stationary, the field equation for the function $\Psi(t, r)$ is

$$-\frac{\partial^2}{\partial t^2}\Psi_\ell(t, r) + \sqrt{F(r)G(r)}\frac{\partial}{\partial r}\left(\sqrt{F(r)G(r)}\frac{\partial}{\partial r}\Psi_\ell(t, r)\right) = V_{sc}(r)\Psi_\ell(t, r), \tag{2.81}$$

where we have defined the function $V_{sc}(r)$ as

$$V_{sc}(r) = \frac{\ell(\ell+1)}{r^2}F(r) + \frac{1}{2r}\left[F'(r)G(r) + F(r)G'(r)\right]\,. \tag{2.82}$$

Equation (2.81) can be expressed in a simpler way with the change of variables

$$\frac{\partial}{\partial r} = \frac{dx}{dr}\frac{\partial}{\partial x} = \frac{1}{\sqrt{F(r)G(r)}}\frac{\partial}{\partial x}\,. \tag{2.83}$$

where x is the tortoise coordinate. In the coordinate system $(t, x, \theta; \phi)$ the (2.81) reduces to

$$-\frac{\partial^2}{\partial t^2}\Psi_\ell(t,x) + \frac{\partial^2}{\partial x^2}\Psi_\ell(t,x) = \tilde{V}_{sc}(x)\Psi_\ell(t,x), \tag{2.84}$$

where we are using the notation

$$\Psi_\ell(t,x) = \Psi_\ell(t, r(x)), \tag{2.85}$$

$$\tilde{V}_{sc}(x) = V_{sc}(r(x)). \tag{2.86}$$

The functions $V_{sc}(r)$ in (2.82) and $\tilde{V}_{sc}(x)$ in (2.84) are *effective potentials* for the scalar perturbations, which depends on the details of the geometry from metric coefficients $F(r)$ and $G(r)$. Solutions of equation (2.84) are labeled by the integer ℓ, and depend on the explicit form of the effective potential $\tilde{V}_{sc}(r)$. This development for the dynamics of a scalar field in a curved spacetime can be extended to more complex perturbations, for example, electromagnetic or gravitational perturbations [31]. In those scenarios the particular details of the dynamics are captured by other forms for the effective potential in contrast with the scalar potential (2.82). Nevertheless, many features of scalar dynamics are carried to the other scenarios.

2.5.2 Quasinormal modes

In scattering problems involving propagation of fields in background geometries with a black hole, one is frequently interested in the solutions classified as *quasinormal modes* (QNMs), which are solutions to the relativistic field equations such as (2.78) with particular boundary conditions. On the horizon of a black hole it is specified a purely ingoing field, with modes always propagating towards the interior of the black hole, while, at spatial infinity it is imposed a purely outgoing boundary condition. A solution satisfying both conditions represents a field configuration that does not propagate from the interior of the black hole and is not reflected from spatial infinity. Related to a given quasinormal mode, there is a quasinormal frequency that is usually complex-valued. Quasinormal spectra are relevant since they do not depend on the details of the initial conditions, but rather on the parameters of the background geometry. They can be used in the construction of the Green function associated to the relevant equations of motion, and therefore they determine at least part of the dynamics in the considered systems [32].

In spherically symmetric and static spacetimes the perturbative dynamics of scalar, electromagnetic and gravitational fields are found as solutions of equations of the

form [32, 31]

$$\frac{\partial^2}{\partial t^2}\Psi(t,x) + \left(-\frac{\partial^2}{\partial^2 x} + V(x)\right)\Psi(t,x) = 0\,, \tag{2.87}$$

with $V(x)$ the effective potential, depending on the details of the (fixed) background spacetime. If one is interested in the evolution of a certain initial perturbation, one can write the problem as a Cauchy initial value problem of the form

$$\Psi(t=0,x), \quad \left.\frac{\partial\Psi(t,x)}{\partial t}\right|_{t=0}. \tag{2.88}$$

We will be interested in studying perturbations in spacetimes containing black holes. The property that the inner region of a black hole is casually disconnected from spatial infinity leads to impose the condition that near the event horizon perturbations should behave as purely ingoing waves (only entering into the black hole). Additionally, if perturbations coming from spatial infinity are disregarded, thus considering only localized perturbations, solutions at spatial infinity behave as purely outgoing waves. If the event horizon is located at $x \to -\infty$ and spatial infinity at $x \to \infty$ the boundary conditions for perturbations are

$$\Psi(x) \sim \begin{cases} e^{-i\omega x} & \text{as } x \to -\infty \\ e^{i\omega x} & \text{as } x \to \infty \end{cases}. \tag{2.89}$$

Perturbations satisfying these conditions are called *quasinormal modes* and the complex numbers $\{\omega_n\}$, for which both conditions are satisfied simultaneously are called *quasinormal frequencies*. If a solution with boundary condition (2.89) does exist, then an initial perturbation outside the event horizon of the black hole will be followed by exponentially damped oscillations, given the complex character of the frequencies [32, 31].

When the effective potentials $V(x)$ are defined only on the domain $x \in (-\infty, 0)$, it is usually introduced a modified version of the QNM boundary conditions, which can be expressed as

$$\psi(x) \sim \begin{cases} e^{-i\omega x} & \text{as } x \to -\infty \\ 0 & \text{as } x \to 0 \end{cases}. \tag{2.90}$$

In general, quasinormal modes do not constitute a complete set, and it is not possible to express a perturbation in terms of quasinormal modes only. For any given perturbation, and depending on the nature of the effective potential, other possible contributions may appear:

1. *Tail contributions*: These contributions appear for some potentials that decay faster than exponentials, for example, with a power-tail law. In [33] it was

found that for effective potentials of the form

$$V(r) = \frac{\ell(\ell+1)}{r^2} + \frac{1}{r^\alpha}\ln(r)^\beta\,, \quad \beta = 0, 1\,, \tag{2.91}$$

the Green function possesses singularities on the -$\mathrm{Im}\,\omega$ axis, and therefore a branch cut. The predominant late time behavior are power-law tails of the form

$$t^{-(2\ell+1)}\ln(t)^\beta\,. \tag{2.92}$$

The Schwarzschild black hole is a particular case of (2.91) with $\beta = 0$, and normally, after an initial perturbation there is a quasinormal mode oscillation followed by a power-tail law decaying behavior .

2. *Prompt-contributions*: This contribution corresponds from the integration over the semicircle $|\omega| = R$ with $R \to \infty$. These are large frequency $|\omega|$, or equivalent, short time contributions which vanishes after a certain time and does not affect the late time behavior of the field evolution [32].

Chapter 3

Anti-de Sitter Geometries and Gauge/Gravity Correspondence

3.1 Maximally symmetric spacetimes

An n-dimensional manifold with $\frac{1}{2}n(n+1)$ Killing vectors is said to be a maximally symmetric space, that is, a space with the maximum number of possible isometries. For a maximally symmetric space the curvature is constant everywhere, and the Riemann tensor is [20]

$$R_{\mu\nu\rho\sigma} = \frac{R}{n(n-1)} \left(g_{\mu\rho} g_{\nu\sigma} - g_{\mu\sigma} g_{\nu\rho} \right) . \tag{3.1}$$

Maximally symmetric spaces are characterized locally by the value of the Ricci tensor R, classified according to whether R is positive, negative or zero. For Euclidean spaces $R = 0$ corresponds to $\mathbb{R}^n$, $R > 0$ corresponds to S^n and $R < 0$ corresponds to an n-dimensional hyperboloid.

For Lorentzian manifolds the maximally symmetric spacetime with $R = 0$ is Minkowski space, which in addition to static and spherical symmetries possesses Poincaré invariance under Lorentz boosts and translations. Likewise, the maximally symmetric space with positive curvature is known as *de Sitter* spacetime (dS) and the negative curvature spacetime is called *Anti-de Sitter* spacetime (AdS). These two geometries are solutions to the Einstein's equation with non-zero cosmological constant (2.8).

The pure de Sitter geometry is the vacuum solution to Einstein's field equation with positive cosmological constant, $\Lambda > 0$. In four dimensions and in a coordinate system (t, r, θ, ϕ), the metric tensor of de Sitter spacetime is [34]

$$ds^2 = -\left(1 - \frac{r^2}{a^2}\right) dt^2 + \left(1 - \frac{r^2}{a^2}\right)^{-1} dr^2 + r^2 d\Omega^2 \, , \tag{3.2}$$

where $a = \sqrt{3/\Lambda}$ is called the de Sitter radius. As a particular feature as a metric of the form (2.19), the metric component $g_{rr} = G(r)^{-1}$ becomes singular at $r = a$ and $F(r), G(r) < 0$ for $r > a$. The domain of validity of the radial coordinate is $r \in [0, a)$,

in which the functions $F(r)$ and $G(r)$ are positive defined. The surface $r = a$ is said to be a *cosmological horizon*, a surface surrounding any observer and delimiting the space from which the observer can retrieve information.

Anti-de Sitter spacetime is the maximally symmetric solution of Einstein's equation with negative cosmological constant Λ, corresponding to a negative vacuum energy density and positive pressure. In the coordinate system (t, r, θ, ϕ) the AdS metric is given by [9]

$$ds^2 = -\left(1 + \frac{r^2}{l^2}\right) dt^2 + \left(1 + \frac{r^2}{l^2}\right)^{-1} dr^2 + r^2 d\Omega \,. \tag{3.3}$$

where $\Lambda = -3/l^2 < 0$ defines the Anti-de Sitter radius l The metric tensor is well-defined for $r \in [0, \infty)$. Anti-de Sitter resembles Minkowski spacetime for $r \ll l$ but has a different asymptotic behavior near l.

The Anti-de Sitter spacetime possesses very interesting features. Even though there is a well defined limit $r \to \infty$, AdS has the property that a light beam emitted from any point can reach spatial infinity and bounce back in a finite proper time. In that sense, it is said that Anti-de Sitter spacetime has a boundary at $r \to \infty$ (more formally, spatial infinity takes the form of a timelike hypersurface). The Anti-de Sitter geometry is non-globally hyperbolic, meaning that knowledge of equations of motion and of initial data in a Cauchy surface is not enough to uniquely determine the time evolution of a physical system, since information can always flow in from infinity. Additional boundary conditions in spatial infinity are required to determine the dynamics of a relativistic field satisfying an hyperbolic equation of motion [35].

3.2 Generalities of Anti-de Sitter spacetime

The Anti-de Sitter spacetime is a constant curvature solution of Einstein's field equation with negative cosmological constant. It can be viewed as a submanifold of $\mathbb{R}^{2,n-1}$, which is equipped with the metric:

$$ds^2 = -(dx^0)^2 - (dx^n)^2 + \sum_{i=1}^{n-1}(dx^i)^2 \,. \tag{3.4}$$

As a submanifold of $\mathbb{R}^{2,n-1}$, the n-dimensional AdS space is defined by set of points:

$$\{(x^0,\ldots,x^n| - (x^0)^2 - (x^n)^2 + \sum_{i=1}^{n-1}(x^i)^2 = -L^2\} \,. \tag{3.5}$$

Just as the Minkowski spacetime is the maximally symmetric spacetime of zero curvature with isometry group $SO(1,n)$, i.e, the Lorentz group, the corresponding isometry group of AdS is $SO(2,n-1)$. Consider the following set of coordinates

$$x_0 = L\cosh(\rho)\cos(\tau)\,, \quad x_n = L\cosh(\rho)\sin(\tau)\,, \quad x_i = R\sinh(\rho)\,\Omega_i\,, \tag{3.6}$$

where $\tau \in [0, 2\pi)$ and $\rho \geq 0$. The coordinates Ω_i with $i = 1,\ldots,n-1$ are the angles parameterizing the $(n-1)$ unit-sphere, such that $\sum_i \Omega_i^2 = 1$. In this coordinate system the induced metric for the submanifold defined by set of points (3.5) becomes

$$ds^2 = L^2(-\cosh^2(\rho)d\tau^2 + d\rho^2 + \sinh^2(\rho)\, d\Omega_{n-2}^2)\,. \tag{3.7}$$

The set of coordinates (τ,ρ,Ω_i) are called global coordinates, because they cover the entire space. Near $\rho = 0$ the metric (3.7) behaves as

$$ds^2 = L^2(-d\tau^2 + d\rho^2 + \rho^2 d\Omega_{n-2}^2)\,. \tag{3.8}$$

with a topology $S^1 \times \mathbb{R}^{n-1}$. Here S^1 is associated to closed time-like curves in the direction of the coordinate τ. Causality is recovered by going to the universal cover where $-\infty < \tau < \infty$.

In the coordinate system (τ,ρ,Ω_i) A conformal compactification of the metric (3.7) is achieved by setting $\tan\theta = \cosh\rho$, giving

$$ds^2 = \frac{L^2}{\cos\theta}\left(-d\tau^2 + d\theta^2 + \sinh^2\theta d\Omega_{n-2}^2\right)\,, \tag{3.9}$$

It is concluded that the conformal boundary of AdS_n is identical to the conformally compactified Minkowski spacetime in $(n-1)$ dimensions. This conclusion is relevant to the formulation of the AdS/CFT correspondence, where field theories are defined in the conformal boundary of the Anti-de Sitter geometry.

A set of coordinates that is used regularly in the description of the Anti-de Sitter space are the Poincaré coordinates $(t, \tilde{x}_i, z)$ with $i = 1, \ldots, n-1$, and defined by

$$\begin{aligned} x^0 &= \frac{1}{2z}\left(z^2 + L^2 + \sum_i (\tilde{x}^i)^2 - t^2\right), \quad x^i = \frac{R\tilde{x}^i}{z}, \\ x^{n-1} &= \frac{1}{2z}\left(z^2 - L^2 + \sum_i (\tilde{x}^i)^2 - t^2\right), \quad x^n = \frac{L\,t}{z}. \end{aligned} \tag{3.10}$$

In this coordinate system the metric is:

$$ds^2 = \frac{L^2}{z^2}\left(-dt^2 + \sum_i (d\tilde{x}^i)^2 + dz^2\right). \tag{3.11}$$

From the metric (3.7) the metric of Anti-de Sitter space can be expressed in static coordinates (t, r, θ, ϕ) by a coordinate change $t = L\tau$ and $r = L\sinh(\rho)$:

$$ds^2 = -\left(1 + \frac{r^2}{L^2}\right)dt^2 + \left(1 + \frac{r^2}{L^2}\right)^{-1} dr^2 + r^2 d\Omega^2. \tag{3.12}$$

Geometries that in the limit $r \to \infty$ approach the form (3.12) are said to be asymptotically Anti-de Sitter. One particular feature from such geometries is that the energy measured at asymptotic infinity is red-shifted from the locally measured energy. Consider a particle with 4-momentum $P^\mu = (-E, p^1, p^2, p^3)$ located at an arbitrary spacetime point with coordinates $(t_0, r_0, \theta_0, \phi_0)$. A static observer at infinity has four velocity

$$U^\mu = \frac{k^\mu}{\sqrt{-k^2}}, \quad k = \frac{\partial}{\partial\, t}. \tag{3.13}$$

Then the energy measured by the such observer is given in terms of the Tolman's law by

$$E_\infty = -g_{\mu\nu}U^\mu P^\nu = \frac{E}{\sqrt{-k^2}} = \frac{E}{\sqrt{-g_{00}}}, \quad -g_{00} = 1 + \frac{r^2}{L^2}. \tag{3.14}$$

This means that the energy E of a particle when measured by an observer in the spatial infinity of AdS is red-shifted by a factor $\sqrt{-g_{00}}$. At infinity the behavior of such factor is $-g_{00} \to \infty$, meaning that the energy is red-shifted to zero.

3.3 Schwarzschild Anti-de Sitter black hole

Anti-de Sitter geometries are solutions to Einstein's field equations with negative cosmological constant. The simplest black hole solution with negative cosmological constant is the Schwarzschild-Anti-de Sitter geometry. In four dimensions, the metric of a Schwarzschild-Anti-de Sitter black hole of mass M is a static, spherically symmetric spacetime of the form (2.19) with

$$ds^2 = -\left(1 - \frac{2M}{r} + \frac{r^2}{l^2}\right) dt^2 + \left(1 - \frac{2M}{r} + \frac{r^2}{l^2}\right)^{-1} dr^2 + r^2 d\Omega^2 \,. \tag{3.15}$$

The metric (3.15) is static with a Killing horizon given by the surface $r = r_+$ satisfying $f(r_+) = 0$, identified as the event horizon of the Schwarzschild-AdS black hole. The surface gravity for the Schwarzschild Anti-de Sitter black hole is

$$\kappa_g = \frac{1}{2}\frac{df(r)}{dr}\bigg|_{r=r_+} = \frac{3r_+^2 + l^2}{2r_+ l^2} \,, \tag{3.16}$$

giving a corresponding temperature to the horizon of the $SAdS$ black hole

$$T = \frac{\kappa_g}{2\pi} = \frac{3r_+^2 + l^2}{4\pi\, r_+ l^2} \,. \tag{3.17}$$

Unlike the temperature of a Schwarzschild black hole which is inversely proportional to the black hole mass M, there is a minimum for the temperature (3.17) given by

$$T_0 = \frac{\sqrt{3}}{2\pi l} \,, \tag{3.18}$$

corresponding to an horizon $r_+ = l/\sqrt{3}$. Anti-de Sitter black holes with horizons $r_+ < l/\sqrt{3}$ are referred to as *small* AdS black holes and their temperature is inversely proportional to the mass, much like in the case of a Schwarzschild black hole, whereas a Schwarzschild Anti-de Sitter black hole with horizon $r_+ > l/\sqrt{3}$ is referred to as a *large* AdS black hole, with their temperature increasing for large mass values.

Now we will concern ourselves with applying the thermodynamical formalism introduced in section 2.4 to the particular case of the Schwarzschild Anti-de Sitter black hole. The first step will be to determine an expression for the Misner-Sharp mass from the metric (3.15). From (2.51), the Misner-Sharp mass of an arbitrary sphere of radius $r = R$ is:

$$M_{ms} = \frac{R}{2}\left[1 - \left(1 - \frac{2M}{R} + \frac{R^2}{l^2}\right)\right] = M - \frac{R^3}{2l^2} \,. \tag{3.19}$$

With a cosmological constant equal to zero the Misner-Sharp mass is just the black hole mass M, whereas for the Schwarzschild-Anti-de Sitter black hole there is an

energy density associated with the cosmological constant. For vacuum Anti-de Sitter geometries there is an (effective) energy-momentum tensor proportional to the metric tensor. In the space orthogonal to S^2 with induced metric h_{ab} the effective energy-momentum tensor is:

$$T_{ab} = \frac{\Lambda}{8\pi} h_{ab} \,, \tag{3.20}$$

corresponding to the energy-momentum tensor of a perfect fluid of negative energy density ρ; with a equation of state of the form $\rho = -P = \Lambda/8\pi$, where P is the pressure of the perfect fluid. From this we have from equation (2.56)

$$\omega = -\frac{1}{2} h_{ab} T^{ab} = \frac{\Lambda}{8\pi} \,, \tag{3.21}$$

and $\psi_a = 0$. Evaluating the generalized first law (2.76) at the horizon, we have for the variation of the area and volume $\nabla_a A = 8\pi r_+ \nabla_a r_+$ and $\nabla_a V = 4\pi r_+^2 \nabla_a r_+$ respectively. Together with (3.16) and (3.21), we obtain on the right-hand side of (2.76)

$$\frac{\kappa_g}{8\pi} \nabla_a A + \omega \nabla_a V = \frac{1}{2} \nabla_a r_+ \,, \tag{3.22}$$

which is equal to the variation of the Misner-Sharp mass (3.19) evaluated at the trapping horizon

$$\nabla_a M_{ms}(r_+) = \nabla_a \left(M - \frac{r_+^3}{2l^2} \right) = \frac{1}{2} \nabla_a r_+ \,. \tag{3.23}$$

Thus the generalized thermodynamics holds for Schwarzschild-Anti-de Sitter at the horizon. This result reproduces what would be obtained from the usual formulation of black hole thermodynamics, given that for a stationary geometry the trapping horizon is equivalent to the Killing horizon. In chapter 5 we will elaborate on the generalized thermodynamics of a non-stationary generalization of the Schwarzchild Anti-de Sitter spacetime where the thermodynamical treatment for trapping horizons becomes more relevant.

From the equation satisfied by the horizon, $f(r_+) = 0$, follows that the mass M can be expressed as:

$$M = \frac{r_+}{2} \left(1 + \frac{r_+^2}{l^2} \right) \,. \tag{3.24}$$

The Misner-Sharp mass (3.19) evaluated at the horizon is equal to $M_{ms}(r_+) = r_+/2$. With $\rho = \Lambda/8\pi = -3/8\pi l^2$ we get from (3.24)

$$M_{ms}(r_+) = M + \rho V \,. \tag{3.25}$$

where $V = 4\pi r^3/3$ is the "thermodynamical volume" of the horizon. With the entropy as a function of the trapping horizon radius as $S = \pi r_+^2$, we write (3.24) as a function of entropy:

$$M = \frac{1}{2} \left(\frac{S}{\pi} \right)^{1/2} + \rho \frac{4\pi}{3} \left(\frac{S}{\pi} \right)^{3/2} \,, \tag{3.26}$$

such that temperature is

$$T = \frac{\partial M}{\partial S} = \frac{3r_+^2 + \ell^2}{4\pi r_+ \ell^2} = \frac{\kappa_g}{2\pi} \,. \tag{3.27}$$

The heat capacity of the Schwarzschild-Anti-de Sitter black hole is:

$$C = \frac{\partial M}{\partial T} = \left(\frac{\partial M}{\partial r_+}\right)\left(\frac{\partial T}{\partial r_+}\right)^{-1} = \frac{1}{4\pi}\left(\frac{1}{2} + \frac{3r_+^2}{2l^2}\right)\left(\frac{3}{l^2} - \frac{1}{r_+^2}\right)^{-1} . \tag{3.28}$$

At $r_+ = l/\sqrt{3}$, the heat capacity (3.28) diverges, with temperature

$$T_C = \frac{\sqrt{3}}{2\pi l} \,. \tag{3.29}$$

The heat capacity is positive for black holes with $r_+ > l/\sqrt{3}$ and negative for $r_+ < l/\sqrt{3}$, indicating that only Anti-de Sitter black holes at temperature $T > T_C$ are thermodynamically stable. The free energy is obtained from the thermodynamical potential $F = M - TS$ as a function of either the entropy S or horizon r_+:

$$F = \frac{1}{4}\left(\frac{S}{\pi}\right)^{1/2} - \frac{1}{4l^2}\left(\frac{S}{\pi}\right)^{3/2} = \frac{r_+}{4}\left(\frac{l^2 - r_+^2}{l^2}\right) , \tag{3.30}$$

with a zero at an horizon radius of $r_+ = l$, corresponding to a temperature:

$$T_1 = \frac{1}{l} \,. \tag{3.31}$$

Unlike the heat capacity, the free energy is continuous for every value of entropy S.

3.4 The Hawking-Page phase transition

In their study of the thermodynamics of Anti-de Sitter spacetime, Hawking and page considered a path integral approach [9]. The partition function considers the propagation of field with initial configuration ϕ_1 on a hypersurface S_1 with metric g_1 to a final field configuration ϕ_2 on a hypersurface S_2 with metric g_2. The path integral is carried over all configurations

$$Z = \int \mathcal{D}[\phi, g] e^{iI[\phi]} \,, \tag{3.32}$$

where I is the gravitational action

$$I = \frac{1}{16\pi} \int d^4x \sqrt{-g}(R - 2\Lambda) \,. \tag{3.33}$$

In order to ensure convergence of the path integral (3.32) it is considered the Euclidean integral by Wick rotation $\tau = it$

$$Z = \int \mathcal{D}[\phi, g] e^{-I[\phi]} \,. \tag{3.34}$$

The path integral is carried over all fields that are periodic in complex time with period β; The dominant contribution to the partition function comes from the minima of the action where $\delta I = 0$. Under approximation $\log Z = -I$. Free energy $F = -T \log Z = -T\, I$. When multiple minima the partition function is dominated by the one with the lowest free energy.

For asymptotically Anti-de Sitter geometries the integral (3.33) reduces to a volume integral given that $R = 4\Lambda$

$$I = \frac{\Lambda}{8\pi} \int d^4x \sqrt{-g} \,. \tag{3.35}$$

This allows to compare the free energies of the pure AdS and Schwarzschild-AdS geometries. This integral diverges over all space take a $r = r'$ For the pure Anti-de Sitter geometry we have

$$I_{AdS} = \frac{\Lambda}{8\pi} \int_0^{\beta_1} dt \int_0^{r'} r^2 \int_{S^2} d\Omega^2 = \frac{\Lambda}{6} \beta_1 r'^3 \,. \tag{3.36}$$

For the Schwarzschild-AdS black hole the radial integral starts at the horizon surface $r = r_+$:

$$I_{SAdS} = \frac{\Lambda}{8\pi} \int_0^{\beta_0} dt \int_{r_+}^{r'} r^2 \int_{S^2} d\Omega^2 = \frac{\Lambda}{6} \beta_1 (r'^3 - {r_+}^3) \,. \tag{3.37}$$

The relation between β_0 and β_1 by matching of both metrics at the $r = r'$ surface:

$$\beta_1 \sqrt{1 + \frac{r'^2}{l^2}} = \beta_0 \sqrt{1 - \frac{2M}{r'} + \frac{r'^2}{l^2}} \,. \tag{3.38}$$

With that the difference between the two actions is:

$$I = I_{SAdS} - I_{AdS} = \frac{\pi r_+^2 (l^2 - r_+^2)}{3r_+^2 + l^2} \,. \tag{3.39}$$

The Hawking Page transition determines which state between thermal AdS and an AdS black hole will become the dominant contribution to the path integral (3.34) For $l < r_+$ the quantity (3.39) is positive, and the preferred state in the partition function is thermal AdS. The horizon surface $r_+ = l$ marks the point of the phase transition between the two geometries, and the corresponding temperature of the Hawking-Page transition is

$$T_H = \frac{1}{\pi l} \,. \tag{3.40}$$

For temperatures below T_H and greater than T_0 in (3.18), an AdS black holes can be

in stable thermal equilibrium with radiation but thermal AdS will be the the preferred state. For temperatures above T_H the difference between actions in (3.39) will be negative and the AdS black hole will become the dominant contribution to the path integral (3.34). The Hawking-Page temperature corresponds to the temperature T_1 obtained in equation (3.31) in which the free energy (3.30) of an Anti-de Sitter black hole is zero. This means that the thermodynamical free energy can be taken as a criterion to determine the occurrence of the Hawking-Page phase transition.

3.5 Overview of AdS/CFT correspondence

The AdS/CFT correspondence is one of the most well-known realizations of a *gauge-gravity* duality; a conjecture suggesting that certain gauge field theories can be described in terms of a proper gravitational theory and vice versa. The AdS/CFT correspondence suggests that a strongly coupled gauge theory in the d-dimensional conformal boundary of an asymptotically Anti-de Sitter spacetime can be described in terms of a low energy gravitational theory on the $d+1$-dimensional Anti-de Sitter space.

In its initial formulation, the AdS/CFT correspondence establishes a duality between a $\mathcal{N}=4$ supersymmetric Yang-Mills theory (SYM) with gauge group $SU(N)$ in the large N limit and type IIB supergravity on $AdS_5 \times S^5$, where $\mathcal{N}=4$ denotes the number of supercharges and N is the color number of the gauge theory. As a gravitational theory, supergravity is the low energy limit of string theory, in which the coupling constant g_s and string length l_s of string theory are taken to zero. The $\mathcal{N}=4$ SYM theory is a conformal field theory (CFT) living in the 4-dimensional boundary of AdS_5 [8].

An element featured in the formulation of the AdS/CFT correspondence are Dp-branes. In string theory, a Dp-brane is a $p+1$ dimensional hypersurface on which endpoints of open strings can be attached given appropriated boundary conditions . A feature of Dp-branes is that they can be used to define to gauge theories. Consider N incidental extremal D_3-branes; each end point of an open string can be attached to one of the N branes. The open string states can be labeled by their endpoints, thus constituting an $N \times N$ unitary $U(N)$ matrix, with open string states living in the adjoint representation of $U(N)$. In the limit $l_s \to 0$ this construction gives rise to a $SU(N)$ Yang-Mills theory where the gauge fields are open string modes on the D_p-branes.

A particular set of solutions to supergravity are called p-branes, which are given by the metric:

$$ds^2 = H_p(r)^{-1/2}\left(-f(r)dt^2 + \sum_{i=1}^{p}(dx^i)^2\right) + H_p(r)^{1/2}\left(\frac{1}{f(r)}dr^2 + r^2 d\Omega^2_{n-p-2}\right), \tag{3.41}$$

where

$$f(r) = 1 - \frac{r_0^4}{r^4}\,, \quad H_p(r) = 1 + \left(\frac{r_p}{r}\right)^{n-p-3}\,. \tag{3.42}$$

The p-brane solution represents a black hole with horizon $r = r_0$ extending into p spatial dimensions. In the AdS/CFT correspondence it is considered the near horizon limit of extremal 3-branes. The extremal limit of 3-branes in $n = 10$ dimensions is given by the limit $r_0 \to 0$ of (3.41), in which the metric reduces to:

$$ds^2 = H(r)^{-1/2}\left(-dt^2 + \sum_{i=1}^{p}(dx^i)^2\right) + H(r)^{1/2}\left(dr^2 + r^2 d\Omega_5^2\right)\,, \tag{3.43}$$

with

$$H(r) = 1 + \frac{L^4}{r^4}\,. \tag{3.44}$$

In string theory Dp-branes are equivalent to extremal p-branes in supergravity. In the low energy limit open and closed string modes decouple. Closed strings correspond to free type IIB supergravity in the bulk and open strings on the D_3-brane give rise to the $\mathcal{N} = 4\ SYM$. In the near horizon limit, equivalent to the low energy limit, the supergravity metric becomes:

$$ds^2 = \frac{r^2}{L^2}(-dt^2 + dx^2) + \frac{L^2}{r^2}(dr^2 + r^2 d\Omega_5^2)\,. \tag{3.45}$$

Under a coordinate change $z = L^2/r$ it is obtained the metric

$$ds^2 = \frac{L^2}{z^2}(-dt^2 + dx^2 + dz^2) + L^2 d\Omega_5^2\,, \tag{3.46}$$

which is the metric of $AdS_5 \times S^5$ in Poincaré coordinates with L as the Anti-de Sitter radius. Thus, the low energy limit of D_p-branes is simply asymptotic Anti-de Sitter space.

The AdS/CFT correspondence establishes a relation between the coupling constants that mediate the strength of the interaction in both theories. Equating the gravitational tension of the extremal 3-brane to N times the tension of a single D_3-brane gives:

$$\frac{L^4 Vol(S^5)}{4\pi G_{10}} = \frac{N}{\sqrt{8G_{10}}}\,, \tag{3.47}$$

where $G_{10} = 8\pi^6 g_s^2 l_s^8$ is the 10 dimensional Newton constant in terms of the string length l_s and string coupling g_s. What follows in terms of the parameters of the theories is:

$$\frac{L^4}{l_s^4} = 4\pi g_s N = g_{YM}^2 N = \lambda\,. \tag{3.48}$$

The constant λ is called the t'Hooft coupling. In the low energy limit the Anti-de Sitter radius is much larger than the string length, $L \gg l_s$, implying $\lambda \gg 1$. In the low energy limit of string theory $g_s \to 0$, in order to keep λ large in (3.48), it is requires a

large number of colors, that is $N \to \infty$. Thus, the AdS/CFT correspondence establishes that both theories are equivalent in the limit $N \to \infty$ and $g_{YM} \to 0$ while the t'Hooft parameter $\lambda = N g_{YM}^2$ remains fixed.

A further property behind the formulation of the AdS/CFT correspondence is that the symmetries on both sides of the correspondence are coincident. The global bosonic symmetry of the $\mathcal{N}=4$ SYM theory is generated by the conformal group $SO(2,4)$, while the R-symmetry group is $SU(4) \cong SO(6)$. In the $AdS_5 \times S^5$ background the isometry groups are $SO(2,4)$ for AdS_5 and $SO(6)$ for S^5.

3.6 Temperature and entropy of $\mathcal{N}=4$ SYM theory

In the AdS/CFT correspondence an asymptotically Anti-de Sitter black hole on the gravity theory is dual to a gauge theory at finite temperature in the AdS boundary. Specifically, the dual to the five dimensional Schwarzchild Anti-de Sitter black hole is the $\mathcal{N}=4$ supersymmetric Yang-Mills theory with gauge group $SU(N)$ in the large N limit living in the four dimensional boundary of AdS. In four dimensions, the field content of the $\mathcal{N}=4$ SYM theory consists of a gauge field A_μ, six scalar fields Φ_i and four Weyl fermions λ_i living in the adjoint representation of the gauge group [36]. The Lagrangian of theory is

$$\mathcal{L} = \frac{1}{g_{YM}^2} tr\left[-\frac{1}{2}F_{\mu\nu}F^{\mu\nu} - (D_\mu\Phi)^2 - i\bar{\lambda}\gamma^\mu D_\mu\lambda + V(\Phi)\right], \tag{3.49}$$

where g_{YM}^2 is the coupling constant of the supersymmetric Yang-Mills theory. With a large number of colors N the perturbative theory of the Lagrangian (3.49) is controlled by the t'Hooft parameter $\lambda = g_{YM}^2 N$. A perturbative series is only feasible in the weak coupling regime $\lambda \ll 1$. In the zero coupling and high temperature the free field limit of the Yang-Mills theory corresponds to $8N^2$ bosonic and $8N^2$ fermionic degrees of freedom [36, 37].

In the AdS/CFT correspondence the thermodynamical quantities of an Anti-de Sitter black hole are mapped to the $\mathcal{N}=4$ super Yang-Mills theory. The temperature of the conformal field theory is taken as equivalent to the temperature of the AdS black hole. As reviewed in chapter 3 the original formulation of the AdS/CFT correspondence considers p-brane representing black hole solutions. Consider the near extremal limit of a 3-brane (3.43) in Euclidean space

$$ds^2 = \frac{r^2}{L^2}\left(f(r)d\tau^2 + \sum_{i=1}^{3}(dx^i)^2\right) + \frac{r^2}{L^2 f(r)}dr^2 + L^2 d\Omega_5^2\,. \tag{3.50}$$

with

$$f(r) = 1 - \frac{r_0^4}{r^4}\,. \tag{3.51}$$

Taking the near horizon approximation $r \to r_0$ gives

$$\frac{r^2}{L^2} f(r) = \frac{r^4 - r_0^4}{L^2 r^2} = \frac{(r^2 + r_0^2)(r^2 - r_0^2)}{L^2 r^2} = \frac{2(r + r_0)(r - r_0)}{L^2} = \frac{4r_0(r - r_0)}{L^2} . \quad (3.52)$$

Define a coordinate $r = r_0 + \rho^2$. The (τ, r) part of the metric is

$$ds^2 = \frac{4r_0(r - r_0)}{L^2} d\tau^2 + \frac{L^2}{4r_0(r - r_0)} dr^2 = \frac{L^2}{r_0} \left(4\frac{r_0^2}{L^4} \rho^2 d\tau^2 + d\rho^2 \right) . \quad (3.53)$$

To avoid a conical singularity at r_0 the τ coordinate needs to be periodic with period $\beta = \pi L^2 / r_0$. Then, the Hawking temperature is given by the inverse of the period:

$$T_H = \frac{1}{\beta} = \frac{r_0}{\pi L^2} . \quad (3.54)$$

The entropy of the 10-dimensional 3-brane is $S = A/4G_{10}$, where A is the eight-dimensional area of the black 3-brane [36]

$$A = \left(\frac{r_0}{L} \right)^3 V_3 \, L^5 \, Vol(S^5) = \pi^6 L^8 \, V_3 \, T_H^3 , \quad (3.55)$$

with $Vol(S^5) = \pi^3 L^3$ and $G_{10} = L^8 \pi^4 / 2N^2$. The entropy is

$$S_{BH} = \frac{1}{2} \pi^2 N^2 \, V_3 \, T_H^3 . \quad (3.56)$$

The black hole entropy (3.56) is identified as the entropy of the strongly coupled $\mathcal{N} = 4$ Yang-Mills theory. The entropy of the conformal theory in the large N and weak coupling limit is equivalent to the entropy of $8N^2$ massless bosons and fermions:

$$S_{CFT} = \frac{2}{3} \pi^2 N^2 \, V_3 \, T_{CFT}^3 . \quad (3.57)$$

The temperature T_{CFT} is the black hole temperature red-shifted to the conformal boundary:

$$T_{CFT} = \frac{T_H}{\sqrt{-g_{tt}}} = \frac{T_H}{L r_0} . \quad (3.58)$$

Using the volume $V_{CFT} = 2\pi^2 r_0^3$ and the relation between parameters L and N it is obtained

$$S_{CFT} = \frac{1}{12} \frac{\pi^2}{L^6 G_5} \left(\frac{1 + 2r_+^2 L^2}{r_+} \right)^3 , \quad (3.59)$$

which in the high temperature limit reduces to:

$$S_{CFT} = \frac{2}{3} \frac{\pi^2 r_+^3}{G_5} = \frac{4}{3} S_{BH} \quad (3.60)$$

The entropy of the conformal theory in the weak coupling limit agrees with the entropy of the strong coupling limit obtained via the gravitational dual up to a factor of $3/4$. It is speculated that the entropy of the Yang-Mills theory is a function of the

coupling λ of the form

$$S_{BH} = \frac{2}{3} f(\lambda) \pi^2 N^2 \, V_3 \, T_H^3 \,, \tag{3.61}$$

with $f(\lambda) = 1$ for $\lambda \to 0$ and $f(\lambda) = 3/4$ for $\lambda \to \infty$. Whether the function $f(\lambda)$ is a continuous function of λ or if there exists a phase transition between the strong and weak coupling limit for a certain value of λ is still an unresolved question.

Chapter 4

Algebraic Description of Perturbatively Dynamics

In this chapter we present work concerning a potential application of the concepts behind the idea of gauge/gravity dualities to geometries aside from Anti-de Sitter. We study geometries where the field dynamics can be approximated by effective potentials in a way that a relation can be established between perturbative elements such as quasinormal modes and representations of a Lie algebra. Results of this chapter have been published in [38].

4.1 Near-extremal geometries

Spacetimes admitting a Killing horizon are said to be *extremal geometries* if the Killing horizon has a surface gravity equal to zero. Following the same line, *near-extremal geometries* are spacetimes admitting a Killing horizon with a surface gravity very close but not exactly zero. We consider spherically symmetric and static metrics of the form (2.19), where the functions $F(r)$ and $G(r)$ have one of the following properties:

- $F(r)$ and $G(r)$ share two simple roots r_1 and r_2.
- $F(r)$ has a single simple root r_1 and $G(r)$ has two simple roots r_1 and r_2.

The near-extremal limit will be given when both horizons r_1 and r_2 get arbitrarily close. To characterize this limit it is useful to define a dimensionless parameter δ in terms of r_1 and r_2

$$\delta = \frac{r_2 - r_1}{r_1}\,, \tag{4.1}$$

such that the near-extremal limit is characterized by

$$0 < \delta \ll 1\,. \tag{4.2}$$

In the following sections we will introduce some spacetimes with Killing horizons admitting a near-extremal limit and we will get as a result that they can be described

in the coordinate system (t, x, θ, ϕ) by a metric of the form

$$ds^2 = \tilde{F}_0 \operatorname{sech}^2(\kappa x)\left[-dt^2 + (dx)^2\right] + [r(x)]^2 d\Omega_2^2 . \tag{4.3}$$

where the surface gravity κ of the black hole is proportional to the dimensionless parameter δ. Spacetimes described by (4.3) can be seen as a region delimited by the horizons r_1 and r_2, extended to the limit $x \to \pm\infty$.

4.1.1 Near-extremal Schwarzschild-de Sitter spacetime

The Schwarzschild-de Sitter is a prime example of a geometry admitting a near-extremal limit [39, 40]. In four dimensions, the metric of the Schwarzschild-de Sitter black hole with positive cosmological constant Λ is of the form:

$$ds^2 = -\left(1 - \frac{2M}{r} - \frac{\Lambda}{3}r^2\right)dt^2 + \left(1 - \frac{2M}{r} - \frac{\Lambda}{3}r^2\right)^{-1} dr^2 + r^2 d\Omega^2 , \tag{4.4}$$

where M is the black hole mass. Provided this condition the geometry (4.4) possesses two horizons $r = r_1$ and $r = r_2$ corresponding to the two positive solutions of the polynomial

$$F(r) = 1 - \frac{2M}{r} - \frac{\Lambda}{3}r^2 = 0 , \tag{4.5}$$

along with a third negative solution $r_M = -r_1 - r_2$. There is a maximum value the cosmological constant can take for which the geometry actually admits a black hole, given by $\Lambda_{ext} = 1/9M^2$. The surface $r = r_1$ corresponds to a black hole horizon while the surface $r = r_2$ is the cosmological horizon of the spacetime. The black hole temperature is given in terms of the surface gravity κ_1 of the black hole horizon as:

$$T_1 = \frac{\kappa_1}{2\pi} = \frac{1 - \Lambda r_1^2}{4\pi r_1} . \tag{4.6}$$

Likewise, it is possible to assign a temperature to the cosmological horizon

$$T_2 = -\frac{\kappa_2}{2\pi} = \frac{-1 - \Lambda r_2^2}{4\pi r_2} . \tag{4.7}$$

As Λ approaches Λ_{ext}, the two horizons r_1 and r_2 become arbitrarily close and the temperatures T_1 and T_2 approach the same value. Defining the following dimensionless parameter δ

$$\delta = \frac{r_2 - r_1}{r_1} , \tag{4.8}$$

allows to characterize the near-extremal limit of the Schwarzschild-de Sitter metric (4.4), with $\delta \to 0$ as the horizons become arbitrarily close with $\Lambda \to \Lambda_{ext}$. Since r_1 and r_2 are simple roots, we can write $F(r)$ as

$$F(r) = G(r) = R(r)(r_2 - r)(r - r_1) ; \tag{4.9}$$

We expand the function $F(r)$ in a Taylor series around $r_0 = (r_1 + r_2)/2$, the midpoint of r_1 and r_2,

$$F(r) = F(r_0) + r_1 \left.\frac{dF(r)}{dr}\right|_{r=r_0} \left(\frac{r - r_0}{r_1}\right) + \frac{r_1^2}{2} \left.\frac{d^2F(r)}{d^2r}\right|_{r=r_0} \left(\frac{r - r_0}{r_1}\right)^2 + \mathcal{O}(\delta^3)\,. \quad (4.10)$$

Now we develop each term we have. For the zeroth-order term we have

$$F(r_0) = R(r_0)(r_2 - r_0)(r_0 - r_1) = R(r_0)\left(\frac{r_2 - r_1}{2}\right)^2\,, \quad (4.11)$$

whereas we obtain that the first order term is zero up to higher order in δ^3

$$r_1 \left.\frac{dF(r)}{dr}\right|_{r=r_0} \left(\frac{r - r_0}{r_1}\right) = 0 + \mathcal{O}(\delta^3)\,, \quad (4.12)$$

and for the second order term we get

$$\frac{r_1^2}{2} \left.\frac{d^2F(r)}{d^2r}\right|_{r=r_0} \left(\frac{r - r_0}{r_1}\right)^2 = -R(r_0)(r - r_0)^2 + \mathcal{O}(\delta^3)\,. \quad (4.13)$$

With this we write

$$F(r) = R(r_0)(r_2 - r)(r - r_1) + \mathcal{O}(\delta^3)\,, \quad (4.14)$$

where $R(r_0)$ is a constant given by

$$R(r_0) = \frac{2\kappa_1}{r_2 - r_1}\,. \quad (4.15)$$

The near-extremal surface κ_1 of r_1, obtained from (4.14) is

$$\kappa_1 = \frac{1}{2}R(r_0)(r_2 - r_1) = \frac{1}{2}R(r_0)r_1\delta + \mathcal{O}(\delta^3)\,, \quad (4.16)$$

which effectively approaches zero in the near-extremal limit. From the simplified expression of $F(r)$ in (4.14), the tortoise coordinate is found to be

$$x = \frac{1}{2\kappa_1}\ln\left(\frac{r - r_1}{r_2 - r}\right) + \mathcal{O}(\delta^3)\,, \quad (4.17)$$

and this allows us to obtain an explicit expression for the function $r(x)$

$$r(x) = \frac{r_1 e^{-\kappa_1 x} + r_2 e^{\kappa_1 x}}{e^{-\kappa_1 x} + e^{\kappa_1 x}} + \mathcal{O}(\delta^3)\,. \quad (4.18)$$

The form of (4.18) is illustrated in figure 4.1. It is to be noted that (4.18) is monotonic increasing, implying that there are no additional horizons aside from r_1 and r_2. The

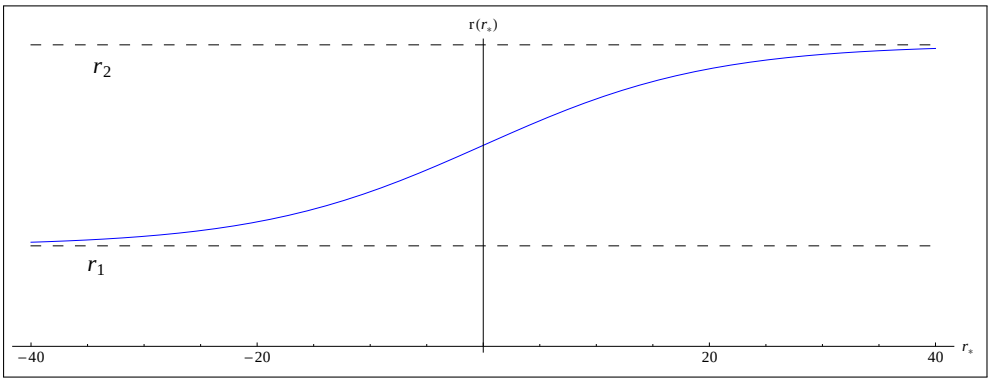

FIGURE 4.1: Behavior of $r(x)$ in near-extremal SdS geometry.

function $\mathcal{F}(x) = F(r(x))$, with the result (4.18), is given by

$$\mathcal{F}(x) = \frac{2\kappa_1}{r_2 - r_1} \frac{\left(r_2 e^{-\kappa_1 x} - r_1 e^{-\kappa_1 x}\right)\left(r_2 e^{\kappa_1 x} - r_1 e^{\kappa_1 x}\right)}{\left(e^{-\kappa_1 x} + e^{\kappa_1 x}\right)^2} + \mathcal{O}(\delta^3)\,, \tag{4.19}$$

which can be simplified to

$$\mathcal{F}(x) = \frac{(r_2 - r_1)\kappa_1}{2} \operatorname{sech}^2(\kappa x) + \mathcal{O}(\delta^3)\,. \tag{4.20}$$

4.1.2 Near-extremal wormholes

A second case of interest which admits a near-extremal limit are the geometries introduced in [41] as *near-extremal wormholes*. Wormholes are compact spacetimes with non trivial topological interiors and topologically simple boundaries, which can be seen as connections between otherwise distant or disconnected parts of the universe [42]. Near-extremal wormholes typically appear in spacetimes with a positive cosmological constant, analogous to the near-extremal Schwarzschild-de Sitter, and can be interpreted as limits of static and spherically symmetric solutions in brane world scenarios [41].

In the coordinate system (t, r, θ, ϕ) the near-extremal limit of this spacetimes is given by

$$F(r) = \tilde{F}_0(r_2 - r)\,, \tag{4.21}$$

$$G(r) = \tilde{G}_0(r_2 - r)(r - r_0)\,, \tag{4.22}$$

where $\tilde{F}_0$ and $\tilde{G}_0$ are positive constants which are defined explicitly in [41]. The coordinate system (t, r, θ, ϕ) is only valid in the region $r_0 < r < r_2$, where r_2 is a Killing horizon assuming the role of a cosmological horizon. We define again a dimensionless parameter δ in terms of r_2 and r_0

$$\delta = \frac{r_2 - r_0}{r_0}\,, \tag{4.23}$$

we have that the surface gravity at $r = r_2$ is given by

$$\kappa = \frac{1}{2}\sqrt{\tilde{F}_0\tilde{G}_0(r_2 - r_0)} = \frac{1}{2}\sqrt{\tilde{F}_0\tilde{G}_0 r_0}\,\delta^{1/2}\,. \tag{4.24}$$

The near-extremal limit is obtained when $r_0 \to r_2$, that is, $0 < \delta \ll 1$, and the surface gravity κ at r_2 approaches zero. Now we extend the coordinate system in the region $r_0 < r < r_2$ by means of the tortoise coordinate (t, x, θ, ϕ), solving the following integral

$$x(r) = \frac{1}{\sqrt{\tilde{F}_0\tilde{G}_0}}\int \frac{dr}{(r_2 - r)\sqrt{(r - r_0)}}\,. \tag{4.25}$$

The solution of this integral is (based on [43])

$$x(r) = \frac{1}{\sqrt{\tilde{F}_0\tilde{G}_0(r_2 - r_0)}}\ln\left(\frac{\sqrt{r_2 - r_0} - \sqrt{r - r_0}}{\sqrt{r_2 - r_0} + \sqrt{r - r_0}}\right)\,, \tag{4.26}$$

which can be reformulated as

$$x(r) = \frac{1}{2\kappa}\ln\left[\frac{(r_2 - r_0) - (r - r_0)}{r - r_0 + (r_2 - r_0) + 2\sqrt{r_2 - r_0}\sqrt{r - r_0}}\right]\,, \tag{4.27}$$

where the result (4.24) was used. The interval $r_0 < r < r_2$ is mapped to $-\infty < x < \infty$, with $r = r_0$ corresponding to $x = 0$. In the near-extremal limit we can simplify the denominator in equation (4.27) with the following assumption

$$\sqrt{r_2 - r_0}\sqrt{r - r_0} \approx r_2 - r_0\,, \tag{4.28}$$

since r is assumed to be smaller but close to r_2 for any r in the interval $r_0 < r < r_2$. With this consideration the tortoise coordinate takes a simpler form

$$x(r) = \frac{1}{2\kappa}\ln\left(\frac{r_2 - r}{r + 3r_2 - 4r_0}\right)\,. \tag{4.29}$$

Expression (4.29) is invertible, and an analytic expression for $r(x)$ is available

$$r(x) = \frac{r_2 - (3r_2 - 4r_0)e^{2\kappa x}}{1 + e^{2\kappa x}}\,, \tag{4.30}$$

which can be written as

$$r(x) = \frac{4r_2\cosh^2(\kappa x) - 4(r_2 - r_0)\left(1 + e^{2\kappa x}\right)}{4\cosh^2(\kappa x)}\,. \tag{4.31}$$

Further simplification of (4.31) leads to

$$r(x) = r_2 - r_0\,\delta\,\mathrm{sech}^2\left(\kappa x\right)\,. \tag{4.32}$$

The form of (4.32) is illustrated in figure 4.2. Reminding that in the near-extremal

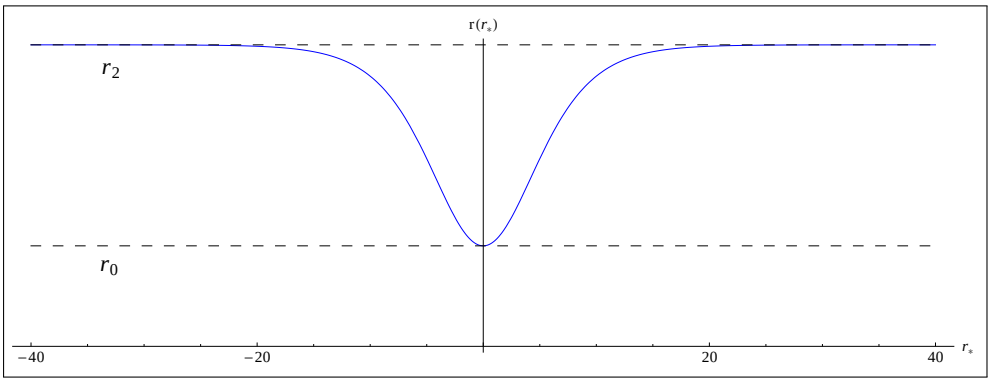

FIGURE 4.2: Behavior of $r(x)$ in near-extremal wormhole geometry.

limit we have $r_0 \to r_2$ we can write

$$r(x) = r_0 - r_0\,\delta\,\mathrm{sech}^2\,(\kappa x)\ , \tag{4.33}$$

and this allows us to write the function $\mathcal{F}(x)$ as

$$\mathcal{F}(x) = \tilde{F}_0 r_0 \delta \mathrm{sech}^2(\kappa x)\,. \tag{4.34}$$

In this extension of coordinates spacetime limited by two Killing horizons $x \to \pm\infty$, both of them corresponding to $r = r_2$. The surface $x = 0$ $(r = r_0)$ is a local minimum of $r(x)$, and corresponds to an outer trapping horizon [42], which can be seen as a throat of a wormhole. Spacetimes described by (4.21) and (4.22) are interpreted as a wormhole joining two regions delimited by cosmological horizons.

4.2 Perturbative dynamics of the Schwarzschild-de Sitter spacetime

Now we proceed to discuss on the perturbative dynamics of the Schwarzschild-de Sitter black hole. In a Schwarzschild-de Sitter spacetime, the effective potential associated with a massless scalar field perturbation is of the form

$$V(r) = F(r)\left[\frac{\ell(\ell+1)}{r^2} + \frac{2M}{r^3} - \frac{2}{a^2}\right] . \tag{4.35}$$

where $a = \sqrt{3/\Lambda}$ is the de Sitter radius and

$$F(r) = 1 - \frac{2M}{r} - \frac{r^2}{a^2} \tag{4.36}$$

has two roots r_1 and r_2, with r_1 corresponding to a black hole horizon and r_2 to a cosmological horizon. The effective potential (4.35) is zero at both r_1 and r_2 and it is positive defined as long as $\ell > 0$. As in section 4.1.1, the function $F(r)$ is approximated by equation (4.14) in the near extremal limit. We define $\Omega(r)$ as the factor

$$\Omega(r) = \frac{\ell(\ell+1)}{r^2} + \frac{1}{r}\frac{dF(r)}{dr} . \tag{4.37}$$

We will expand the function $\Omega(r)$ around r_0 at the lowest order

$$\Omega(r) = \Omega(r_0) + \mathcal{O}(\delta) . \tag{4.38}$$

From (4.12) we have that the first derivative of $F(r)$ at r_0 is zero at the leading order

$$\left.\frac{dF(r)}{dr}\right|_{r=r_0} = 0 + \mathcal{O}(\delta^2) , \tag{4.39}$$

and the function $\Omega(r)$ reduces to

$$\Omega(r) = \frac{\ell(\ell+1)}{r_0^2} + \mathcal{O}(\delta) . \tag{4.40}$$

Now, in the near-extremal limit we have the following relation between r_0 and r_1

$$r_0 = r_1 + \mathcal{O}(\delta) , \tag{4.41}$$

and then, at the lowest order in δ, the effective potential in the near extremal limit becomes

$$V(r) = \left[\frac{\ell(\ell+1)}{r_1^2}\right]\frac{2\kappa_1(r_2-r)(r-r_1)}{r_2-r_1} + \mathcal{O}(\delta) , \tag{4.42}$$

which we note is only meaningful for $\ell > 0$. In the near-extremal approximation, in terms of the tortoise coordinate x given in equation (4.17), the radial function $r(x)$ is of the form (4.18), and the effective potential in the tortoise coordinate obtains the

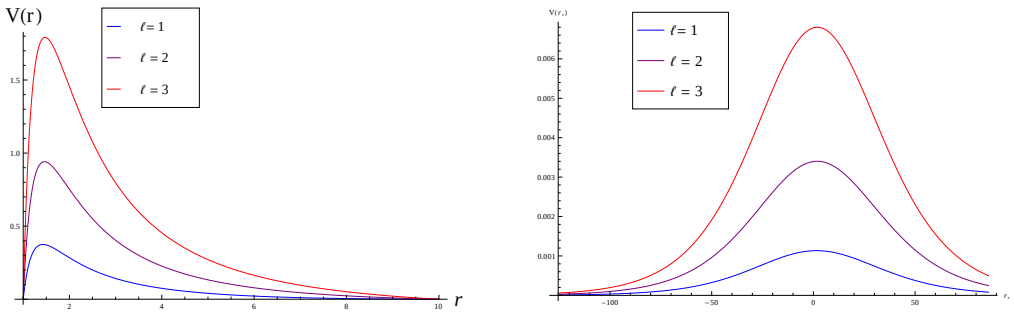

FIGURE 4.3: (a) Effective potential for Schwarzschild-de Sitter spacetime as a function of the radial coordinate. Parameters $r_1 = 1$, $r_2 = 10$. (b)Effective potential for near-extremal Schwarzschild-de Sitter as a function of x. Parameters: $r_1 = 1$, $r_2 = 1.05$, $\ell = 1$.

following form

$$V(x) = \left[\frac{\ell(\ell+1)}{r_1^2}\right] \frac{2\kappa_1}{\left(e^{-\kappa x} + e^{\kappa x}\right)^2} + \mathcal{O}(\delta)\,. \tag{4.43}$$

We can write (4.43) in terms of an hyperbolic cosine function as,

$$V(x) = \frac{V_0}{\cosh^2(\kappa x)}\,, \tag{4.44}$$

where the constant V_0 is the peak of the potential, given by

$$V_0 = \left[\frac{\ell(\ell+1)}{r_1^2}\right] \frac{\kappa_1}{2}\,. \tag{4.45}$$

Potential (4.44) is known in the literature as *Pöschl-Teller* potential. In the following section we present a development in which perturbation of relativistic fields are solved by exploiting the symmetries of the perturbative equations when considering potentials of the form (4.44).

4.3 Algebraic treatment of the Pöschl-Teller potential

The Pöschl-Teller potential was originally introduced as a potential for which the Schrödinger equation is exactly solvable, but as seen in the example of perturbations in the Schwarzschild-de Sitter spacetime, this potential also appears in the description of scattering problems in gravitational physics. We extend from (4.44) to consider a generalized form for the Pöschl-Teller potentials

$$V(x) = \frac{V_0}{\cosh^2(\kappa x + \alpha)} \,. \tag{4.46}$$

The parameter α is allowed to be complex. Naturally, a particular case of $V(x)$ in equation (4.46) is the usual Pöschl-Teller potential in equation (4.44), obtained by setting $\kappa > 0$ and $\alpha = 0$. Still, other interesting cases are possible if quasinormal modes are to be considered. For example, with $V_0 = -V_- < 0$, $\kappa > 0$ and $\alpha = i\pi/2$ we have

$$V(x) = \frac{V_-}{\sinh^2(\kappa x)} \,, \tag{4.47}$$

where the domain of $V(x)$ in this case is defined to be the half real line,$x \in (-\infty, 0)$. The modified form of Pöschl-Teller effective potential in equation (4.47) is relevant when the gravitational perturbative dynamics on anti-de Sitter or de Sitter spacetimes is treated [44, 45].

We are mainly interested in solutions of the scalar wave equation (2.87) with the form

$$\Psi(t, x) = \psi(x) e^{-i\omega t} \,, \tag{4.48}$$

where ω is extended to the complex plane. With the sign convention in the argument of the exponential stable solutions are those with $\mathrm{Im}(\omega) < 0$. Considering wave functions with the time-dependence in equation (4.48), we obtain the so-called time-independent version of the equation of motion:

$$\frac{d\psi(x)}{dx^2} + \left[\omega^2 - V(x)\right] \psi(x) = 0 \,. \tag{4.49}$$

It should be noticed that equation (4.49) has the same form of the time-independent version of Schrödinger equation, a relevant point when the original work of Pöschl and Teller is considered [46].

4.3.1 Lie algebra representations and quasinormal modes

In our approach, we study the relation between the scalar field equation with generalized forms of the Pöschl-Teller potential and differential representations of the Lie algebra $\mathfrak{sl}(2)$. We find a direct relation between the equations of motion and an invariant of the algebra, namely the Casimir element, allowing us to obtain solutions in a closed form by means of a highest weight representation.

As we shall see, another symmetry described by the Lie algebra $\mathfrak{sl}(2)$, the algebra of 2×2 traceless matrices. We propose the following representation of $\mathfrak{sl}(2)$ acting on functions (4.48)

$$\hat{L}_0 = \frac{2}{\kappa}\frac{\partial}{\partial t}\,, \tag{4.50}$$

$$\hat{L}_+ = \frac{1}{\kappa}e^{\kappa t}\left[-\sinh(\kappa x+\alpha)\frac{\partial}{\partial t} - \cosh(\kappa x+\alpha)\frac{\partial}{\partial x}\right]\,, \tag{4.51}$$

$$\hat{L}_- = \frac{1}{\kappa}e^{-\kappa t}\left[-\sinh(\kappa x+\alpha)\frac{\partial}{\partial t} + \cosh(\kappa x+\alpha)\frac{\partial}{\partial x}\right]\,. \tag{4.52}$$

preserving the Lie bracket structure

$$[\hat{L}_0,\hat{L}_+] = 2\hat{L}_+\,,\quad [\hat{L}_0,\hat{L}_-] = -2\hat{L}_-\,,\quad [\hat{L}_+,\hat{L}_-] = \hat{L}_0\,. \tag{4.53}$$

Since quasinormal modes have the time dependence indicated in equation (4.48), we select $\hat{L}_0$ as our diagonalizable operator. In representation theory language, $\hat{L}_0$ is chosen to be a Cartan operator. In this way, a quasinormal mode must be an eigenvalue of $\hat{L}_0$,

$$\hat{L}_0\left[\psi(x)e^{-i\omega t}\right] = -i\frac{2\omega}{\kappa}\left[\psi(x)e^{-i\omega t}\right]\,. \tag{4.54}$$

The Casimir invariant of the representation will be important in the development. The Casimir is an operator which commutes with all the operators associated to the basis in equations(4.50)-(4.52), being given by

$$\hat{L}^2 = \frac{1}{2}\,\hat{L}_0\,\hat{L}_0 + \hat{L}_-\,\hat{L}_+ + \hat{L}_+\,\hat{L}_-\,. \tag{4.55}$$

In the present case, from equation (4.55), the Casimir operator associated with the representation in equations (4.50)-(4.52) is

$$\hat{L}^2 = -\frac{2}{\kappa^2}\cosh^2(\kappa x+\alpha)\left(-\frac{\partial^2}{\partial t^2}+\frac{\partial^2}{\partial x^2}\right)\,. \tag{4.56}$$

It follows from result (4.56) that the equation of motion (2.87) can be written as a constraint in the proposed representation of the algebra $\mathfrak{sl}(2)$:

$$\hat{L}^2\Psi(t,x) = -2\frac{V_0}{\kappa^2}\Psi(t,x)\,. \tag{4.57}$$

Thus, the value of the Casimir is directly related with the height of the potential.

To obtain the solution of the equations (4.54) and (4.57), we will consider what is known as a highest weight representation [47, 48]. Having selected a diagonalizable operator on the representation, our solutions will be eigenvalues of both $\hat{L}_0$ and $\hat{L}^2$. With the highest weight representation technique, it is introduced a function $\Psi^{(0)}(t,r)$ satisfying the highest weight conditions,

$$\hat{L}_0\Psi^{(0)}(t,x) = h\Psi^{(0)}(t,x)\,, \tag{4.58}$$

$$\hat{L}_+\Psi^{(0)}(t,x) = 0\,, \tag{4.59}$$

where h is the highest weight. From this fundamental state, an infinite number of solutions is obtained by successive applications of the lowering operator $\hat{L}_-$. Another set of solutions could be found by applying the operator L_+ on the fundamental mode $\Psi^{(0)}(t,x)$ instead, but it is later verified that only the solutions obtained from the action of the operator $\hat{L}_-$ satisfy the boundary conditions (2.89) characterizing quasinormal modes solutions.

Since the action of $\hat{L}_0$ on a quasinormal mode is given by equation (4.54), it follows that the quasinormal frequency ω_0 associated to $\Psi^{(0)}$ is related to the constant h as

$$\omega_0 = i\frac{\kappa h}{2}\,. \tag{4.60}$$

In terms of the highest weight h, the action of the Casimir $\hat{L}^2$ on $\Psi^{(0)}(t,r)$ is given by

$$\hat{L}^2\Psi^{(0)}(t,x) = \left(\frac{h^2}{2} + h\right)\Psi^{(0)}(t,x)\,. \tag{4.61}$$

Direct comparison between equations (4.57) and (4.61) allows one to solve h in terms of V_0 and κ,

$$h = -1 \pm 2i\sqrt{\frac{V_0}{\kappa^2} - \frac{1}{4}}\,. \tag{4.62}$$

Using equations (4.60) and (4.62), the fundamental frequency ω_0 can now be expressed in terms of the potential parameters κ and V_0 as

$$\omega_0 = \kappa\left(-i\frac{1}{2} \pm \sqrt{\frac{V_0}{\kappa^2} - \frac{1}{4}}\right)\,. \tag{4.63}$$

To find the explicit form of the corresponding fundamental mode $\Psi^{(0)}(t,r)$ associated to ω_0, we use the highest weight conditions in equations (4.58) and (4.59), which are translated to the following differential equations:

$$\frac{2}{\kappa}\frac{\partial\Psi^{(0)}(t,x)}{\partial t} = h\Psi^{(0)}(t,x)\,, \tag{4.64}$$

$$-\sinh(\kappa x+\alpha)\frac{\partial\Psi^{(0)}(t,x)}{\partial t} - \cosh(\kappa x+\alpha)\frac{\partial\Psi^{(0)}(t,x)}{\partial x} = 0\,. \tag{4.65}$$

The pair of equations (4.64) and (4.65) can be solved exactly, with

$$\Psi^{(0)}(t,x) = Ce^{-i\omega_0 t}\cosh(\kappa x+\alpha)^{i\omega_0/\kappa}\,, \tag{4.66}$$

where C is an integration constant.

The complete spectrum $\{\omega_n\}$ can be expressed in a closed form. For this purpose, it is useful the following property,

$$[\hat{L}_0,(\hat{L}_\pm)^n] = \pm 2n(\hat{L}_\pm)^n\,, \tag{4.67}$$

which can be proved by induction. In equation (4.67), n is a non-negative integer. The frequency associated to the mode $\Psi^{(n)}(t,x)$ is given by the action of the operator $\hat{L}_0$. Using equation (4.67), we obtain that

$$\begin{aligned}\hat{L}_0\Psi^{(n)}(t,x) &= \left([\hat{L}_0,\hat{L}_-^n]+\hat{L}_-^n\hat{L}_0\right)\Psi^{(0)}(t,x)\\ &= (h-2n)\,\Psi^{(n)}(t,x)\,.\end{aligned} \tag{4.68}$$

With equation (4.68), the fundamental and overtone frequencies are given by

$$\omega_n = i\frac{\kappa}{2}(h-2n) = \kappa\left[-i\left(n+\frac{1}{2}\right)\pm\sqrt{\frac{V_0}{\kappa^2}-\frac{1}{4}}\right]\,,\ n=0,1,2\ldots\,. \tag{4.69}$$

Higher order solutions can be obtained by the successive application of the operator $\hat{L}_-$ to the fundamental mode $\Psi^{(0)}(t,x)$,

$$\Psi^{(n)}(t,x) = (\hat{L}_-)^n\Psi^{(0)}(t,x)\,, \tag{4.70}$$

and there will be an infinite number of them. For instance, considering the second mode, one has

$$\Psi^{(1)}(t,x) = Ce^{-i\omega_1 t}\sinh(\kappa x+\alpha)\cosh(\kappa x+\alpha)^{i\frac{\omega_0}{\kappa}}\,. \tag{4.71}$$

For the third mode, it is obtained that

$$\Psi^{(2)}(t,x) = Ce^{-i\omega_2 t}\cosh(\kappa x+\alpha)^{i\frac{\omega_0}{\kappa}}\left[\cosh(\kappa x+\alpha)+(1+h)\sinh^2(\kappa x+\alpha)\right]\,, \tag{4.72}$$

and so on.

4.3.2 Boundary conditions

A boundary condition analysis is essential in the characterization of quasinormal modes. Besides being solutions of the wave equation (2.87), they must satisfy the appropriate boundary conditions (2.89) or (2.90). Let us consider the case $\alpha = 0$ and $V_0 = V_+ > 0$ in the development from the previous section. This case corresponds

to the usual Pöschl-Teller potential (4.44). For latter convenience, we will introduce some new notation. We denote the wave functions with $\alpha = 0$ as $\psi^{(n)}(t,x)$. The basis operators will be denoted $\{\hat{P}_0, \hat{P}_+, \hat{P}_-\}$ for $\alpha = 0$. Explicitly, we have for the fundamental mode

$$\psi^{(0)}(t,x) = Ce^{-i\omega_0 t}\cosh(\kappa x)^{i\omega_0/\kappa}\,, \tag{4.73}$$

and for the higher overtones,

$$\psi^{(n)}(t,x) = (\hat{P}_-)^n\psi^{(0)}(t,x)\,. \tag{4.74}$$

The frequencies have always non-null imaginary components:

$$\omega_n = \kappa\left[-i\left(n+\frac{1}{2}\right) \pm \sqrt{\frac{V_+}{\kappa^2}-\frac{1}{4}}\right]\,,\ n = 0,1,2,\dots\ . \tag{4.75}$$

Considering the limits $x \to \pm\infty$ for the solutions in equation (4.73), one verifies that the functions $\psi^n(t,x)$ have the correct quasinormal mode asymptotic behavior

$$\psi^{(n)}(t,x) \sim \begin{cases} e^{i\omega x} & \text{as } x \to \infty \\ e^{-i\omega x} & \text{as } x \to -\infty \end{cases}\,, \tag{4.76}$$

matching the standard quasinormal mode boundary conditions (2.89).

For the case $\alpha = i\,\pi/2$ and $V_0 = -V_- < 0$, we obtain the modified Pöschl-Teller potential in equation (4.47), proportional to $\sinh^{-2}(\kappa x)$. Also for latter convenience, we will denote the wave functions with $\alpha = i\pi/2$ as $\varphi^n(t,x)$. The basis operators will be denoted $\{\hat{M}_0, \hat{M}_+, \hat{M}_-\}$ when $\alpha = i\pi/2$. For this particular representation the Casimir operator is given by

$$\hat{M}^2 = \frac{2}{\kappa^2}\sinh^2(\kappa x)\left(-\frac{\partial^2}{\partial t^2}+\frac{\partial^2}{\partial x^2}\right)\,. \tag{4.77}$$

General results from previous subsection give us

$$\varphi^{(0)}(t,x) = Cbe^{-i\omega_0 t}\sinh(\kappa x)^{i\frac{\omega_0}{\kappa}} \tag{4.78}$$

for the fundamental mode and

$$\varphi^{(n)}(t,x) = (\hat{M}_-)^n\varphi^{(0)}(t,x) \tag{4.79}$$

for the higher overtones. As an important characteristic of this case, the spectrum turns out to be purely imaginary. We have two non-equivalent sets of solutions of the wave equation, $(+)$ and $(-)$, characterized by the frequencies

$$i\kappa\left[-\left(n+\frac{1}{2}\right) \pm \sqrt{\frac{V_-}{\kappa^2}+\frac{1}{4}}\right]\ ,\ n = 0,1,2,\dots\ . \tag{4.80}$$

The $(-)$ solutions are necessarily stable. But the $(+)$ solutions could describe unstable modes, with positive imaginary parts (for large enough values of V_-/κ^2). We will show in the following that only stable solutions are quasinormal modes.

Let us consider the boundary conditions to be satisfied. Functions $\{\varphi^{(n)}(t,x)\}$ in equations (4.78)-(4.79) are defined only on the half real line, $x \in (-\infty, 0)$, and therefore they cannot satisfy the standard quasinormal boundary condition (2.89). But they could satisfy the modified quasinormal mode conditions in (2.90). On the other hand, only the $(-)$ solutions satisfy the Dirichlet boundary condition prescribed in (2.90). That is, only for those solutions we have

$$\lim_{x\to 0^-} \varphi^{(n)}(t,x) \to 0\,, \tag{4.81}$$

as can be straightforwardly verified. Therefore, the unstable $(+)$ solutions are not quasinormal modes. The quasinormal frequencies associated to the modified Pöschl-Teller potential are then given by

$$\omega_n = -i\kappa \left[\left(n + \frac{1}{2}\right) + \sqrt{\frac{V_-}{\kappa^2} + \frac{1}{4}} \right] \,, \; n = 0, 1, 2, \dots \,. \tag{4.82}$$

4.3.3 Further generalization of the Pöschl-Teller potential

We consider now a further generalization of the Pöschl-Teller potential, combining both terms $\cosh^{-2}(\kappa x)$ and $\sinh^{-2}(\kappa x)$ as

$$V(x) = \frac{V_+}{\cosh^2(\kappa x)} + \frac{V_-}{\sinh^2(\kappa x)} \,, \tag{4.83}$$

with $V_+ > 0$ and $V_- > 0$, and defined on the half real line, $x \in (-\infty, 0)$. Motivations for considering this potential can be found in the study of the perturbative dynamics of different types of fields [45, 35, 49]. Regarding the domain of the the full Pöschl-Teller potential, $V(x)$ diverges in the limit $x \to 0$, since the term proportional to $\sinh^{-2}(\kappa x)$ becomes dominant. It follows that the potential is defined on $x \in (-\infty, 0)$.

In sections 4.3 and 4.3.2, we considered two particular representations of the algebra $\mathfrak{sl}(2)$: `(Rep1)`, as the operators $\{\hat{P}_0, \hat{P}_+, \hat{P}_-\}$, obtained setting $\alpha = 0$ in equations (4.50)-(4.52); and `(Rep2)`, as the operators $\{\hat{M}_0, \hat{M}_+, \hat{M}_-\}$, obtained setting $\alpha = i\pi/2$ in equations (4.50)-(4.52). Both representations `(Rep1)` and `(Rep2)` share the same Cartan operator $\hat{L}_0 = \hat{P}_0 = \hat{M}_0$. However, their Casimir operators, denoted by $\hat{P}^2$ and $\hat{M}^2$,

$$\hat{P}^2 = \frac{1}{2}\,\hat{P}_0\,\hat{P}_0 + \hat{P}_-\,\hat{P}_+ + \hat{P}_+\,\hat{P}_- \,, \tag{4.84}$$

$$\hat{M}^2 = \frac{1}{2}\,\hat{M}_0\,\hat{M}_0 + \hat{M}_-\,\hat{M}_+ + \hat{M}_+\,\hat{M}_- \,, \tag{4.85}$$

and given explicitly by expressions (4.56) and (4.77), do not commute. Hence the eigenvalues of one of the Casimir do not constitute solutions for the other case. Nevertheless, a solution for the full Pöschl-Teller potential in equations (4.83) can be constructed from the particular solutions $\psi^{(n)}(t,x)$ and $\varphi^{(n)}(t,x)$, associated to the potentials in equations (4.44) and (4.47) respectively.

We will denote the product of the highest weight solution of both representations in equations (4.73) and (4.78) by $\Psi^{(0)}$. One obtains that

$$\begin{aligned}\Psi^{(0)}(t,x) &= \psi^{(0)}(t,x)\varphi^{(0)}(t,x) \\ &= A\cosh(\kappa x)^{-\frac{1}{2}h_+}\sinh(\kappa x)^{-\frac{1}{2}h_-}e^{\frac{\kappa}{2}(h_++h_-)t}\,, \end{aligned} \tag{4.86}$$

where h_+ and h_- are the highest weight constants of `(Rep1)` and `(Rep2)` respectively:

$$\hat{P}_0\psi^{(0)}(t,x) = h_+\psi^{(0)}(t,x)\,, \tag{4.87}$$

$$\hat{M}_0\varphi^{(0)}(t,x) = h_-\varphi^{(0)}(t,x)\,. \tag{4.88}$$

In the following, it will be shown that $\Psi^{(0)}(t,x)$ is a solution of the wave equation with the full Pöschl-Teller (4.83) is considered. Acting with the D'Alambertian operator $(-\partial_t^2+\partial_x^2)$ on $\Psi^{(0)}(t,x)$ and taking into account the relation between the Casimir elements and the height of the potentials, one has

$$\left(-\frac{\partial^2}{\partial t^2}+\frac{\partial^2}{\partial x^2}\right)\Psi^{(0)}(t,x) = V(x)\varphi^{(0)}\psi^{(0)} + 2\left[\varphi'^{(0)}\psi'^{(0)} - \dot{\varphi}^{(0)}\dot{\psi}^{(0)}\right]\,. \tag{4.89}$$

In equations (4.89), φ' denotes derivative with respect to x, and $\dot{\varphi}$ denotes derivative with respect to t. Also, we can show that the additional term on the right hand side of equations (4.89) is identically zero given the properties of the highest weight functions. Indeed, from the highest weight conditions, we obtain the following equalities,

$$\tanh(\kappa x)\frac{\partial}{\partial t}\psi^{(0)}(t,x) = \frac{\partial}{\partial x}\psi^{(0)}(t,x)\,, \tag{4.90}$$

$$\operatorname{cotanh}(\kappa x)\frac{\partial}{\partial t}\varphi^{(0)}(t,x) = \frac{\partial}{\partial x}\varphi^{(0)}(t,x)\,. \tag{4.91}$$

Taking the product of the expressions in equations (4.90) and (4.91), we have

$$\varphi'^{(0)}\psi'^{(0)} = \dot{\varphi}^{(0)}\dot{\psi}^{(0)}\,, \tag{4.92}$$

from which the second term in the right-hand side of equations (4.89) is canceled. Hence,

$$\left[-\frac{\partial^2}{\partial t^2}+\frac{\partial^2}{\partial x^2}\right]\Psi^{(0)}(t,x) = V(x)\Psi^{(0)}(t,x)\,, \tag{4.93}$$

and therefore $\Psi^{(0)} = \varphi^{(0)}\psi^{(0)}$ solves the wave equation (2.87) with the potential (4.83), as we wanted to show.

We can now obtain the fundamental quasinormal frequency for the mode $\Psi^{(0)}(t,x)$. The action of the Cartan operator $\hat{L}_0 = \hat{P}_0 = \hat{M}_0$ on $\Psi^{(0)}(t,x)$ is

$$\hat{L}_0\Psi^{(0)}(t,x) = (h_+ + h_-)\Psi^{(0)}(t,x)\,. \tag{4.94}$$

It follows that the fundamental frequency of $\Psi^{(0)}(t,x)$ is given by the sum of the frequencies of the fundamental modes associated to $\hat{P}_0$ and $\hat{M}_0$:

$$\frac{\partial}{\partial t}\Psi^{(0)}(t,x) = \frac{\kappa}{2}(h_+ + h_-)\Psi^{(0)}(t,x) = -i\omega_0\Psi^{(0)}(t,x)\,, \tag{4.95}$$

with

$$\omega_0 = \kappa\left[\pm\sqrt{\frac{V_+}{\kappa^2} - \frac{1}{4}} - i\left(1 + \sqrt{\frac{V_-}{\kappa^2} + \frac{1}{4}}\right)\right]. \tag{4.96}$$

It can be readily verified that the function $\Psi^{(0)}(t,x)$ in equation (4.86) satisfies the modified boundary conditions presented in equation (2.90). Therefore, $\Psi^{(0)}(t,x)$ and the associated ω_0 are proper quasinormal modes and frequencies of the full Pöschl-Teller potential.

4.3.4 Quasinormal modes in an initial value problem

Quasinormal solutions of the generalized Pöschl-Teller potentials can also be investigated through the analysis of an associated initial value problem. In fact, quasinormal modes dominate the intermediate and (possibly) the late-time field evolution. Let us consider the Cauchy initial value problem associated to the hyperbolic equation (2.87). In this formulation, initial data are given by two functions F and G, where

$$\Psi(0,x) = F(x) \ , \ \frac{\partial \Psi}{\partial t}(0,x) = G(x) \, . \tag{4.97}$$

Since we are interested in a quasinormal mode evolution, we will consider initial conditions with a sharp peak and fast decay [32, 31]. For most of the development presented here, the initial data have the form

$$F(x) = A_1 \, e^{-\sigma_1 x^2} \ , \ G(x) = A_2 \, e^{-\sigma_2 x^2} \, . \tag{4.98}$$

An issue to be considered is the eventual existence of a late-time tail. That tail, if it exists, would dominate the field decay for the late-time regime, supplanting the quasinormal mode phase. The problem can be analytically addressed considering the asymptotic form of the effective potential. Asymptotically, with $-x$ large, one obtains that

$$V(x) = 4 \, (V_+ + V_-) \, e^{-2\kappa x} + o\left(e^{2\kappa x}\right) \, . \tag{4.99}$$

That is, the potential decreases like an exponential. It is then shown in [50] that a potential with this form do not generate tails.

Therefore, we arrive at a qualitative description of the time evolution of the field at a fixed position. After an initial transient, which depends on the initial conditions, follows the quasinormal mode phase. The late-time field evolution is then dominated by the fundamental quasinormal mode. The field decay can be oscillatory or non-oscillatory, depending on the existence of a non-null real part in the fundamental quasinormal frequency. The dynamics is always stable, that is, the function $\Psi(t,x)$ is bounded. These qualitative features of the field dynamics are illustrated in Figs. 4.4 and 4.5.

For a quantitative comparison between the analytic expressions found for the quasinormal frequencies and the results from the time evolution, we employ numerical techniques. We use an explicit finite difference scheme to numerically integrate the field equation (2.87). A discretized version of equation (2.87) is obtained with

$$t \to t_i = t_0 + i \, \Delta t \ , \ \ i = 0, 1, 2, \dots \, , \tag{4.100}$$

$$x \to x_j = x_0 + j \, \Delta x \ , \ \ j = 0, 1, 2, \dots \, . \tag{4.101}$$

With this discretization, the wave equation is approximated by the difference equation

$$\psi_N = \left(2 - \Delta t^2\, V_C\right)\, \psi_C - \psi_S + \frac{\Delta t^2}{\Delta x^2}\left(\psi_E - 2\psi_C + \psi_W\right)\ , \tag{4.102}$$

where

$$\begin{aligned} \Psi_N = \Psi\left(t_{i+1}, x_j\right)\ &,\ \Psi_E = \Psi\left(t_i, x_{j+1}\right)\ , \\ \Psi_C = \Psi\left(t_i, x_j\right)\ &,\ \Psi_W = \Psi\left(t_i, x_{j-1}\right)\ , \\ \Psi_S = \Psi\left(t_{i-1}, x_j\right)\ &,\ V_C = V_\ell\left(t_i, x_j\right)\ . \end{aligned} \tag{4.103}$$

The numerical evolution of the field is evaluated at a fixed point x_i. With the described method for the numerical treatment of the Cauchy problem, we performed an extensive exploration on the parameter space of the generalized Pöschl-Teller potentials.

We first consider the usual Pöschl-Teller potential ($V_+ > 0$ and $V_- = 0$) defined on the whole real line. One characteristic of the time evolution generated by the usual Pöschl-Teller potential is the existence of oscillatory and non-oscillatory late-time field decay.[1] From the results of section 4.3.2, if $V_+/\kappa^2 > 1/4$ and $V_- = 0$, the real and imaginary parts of the fundamental frequencies are non-null, being given by

$$\mathrm{Re}\left(\omega_0^{\pm}\right) = \pm\sqrt{\frac{V_+}{\kappa^2} - \frac{1}{4}}\,, \tag{4.104}$$

$$\mathrm{Im}\left(\omega_0^{\pm}\right) = -\frac{\kappa}{2}\,. \tag{4.105}$$

In this case, the sign choice is not relevant. The late-time decay is oscillatory and exponentially attenuated. This is the usual picture of the time evolution with the usual Pöschl-Teller potential. But in the regime where $0 < V_+/\kappa^2 \leq 1/4$ and $V_- = 0$, the fundamental quasinormal frequencies are purely imaginary:

$$\mathrm{Re}\left(\omega_0^{\pm}\right) = 0\,, \tag{4.106}$$

$$\mathrm{Im}\left(\omega_0^{+}\right) = -\kappa\left(\frac{1}{2} + \sqrt{\frac{1}{4} - \frac{V_+}{\kappa^2}}\right)\ , \tag{4.107}$$

$$\mathrm{Im}\left(\omega_0^{-}\right) = -\kappa\left(\frac{1}{2} - \sqrt{\frac{1}{4} - \frac{V_+}{\kappa^2}}\right)\ . \tag{4.108}$$

Both $(\pm)$ modes are stable, but the $(-)$ mode has the lowest absolute value of its imaginary part, and therefore dominates the late-time decay. The existence of oscillatory and non-oscillatory modes for the usual Pöschl-Teller potential can be readily seen in the numerical evolution. We illustrate this point in Fig. 4.4.

Considering the modified Pöschl-Teller potential ($V_+ = 0$ and $V_- > 0$), it is

[1] In the analysis of near-extremal geometries, a non-oscillatory decay never appears because in those scenarios $V_+/\kappa^2 > 1/4$ [40, 39, 51, 52, 53, 41].

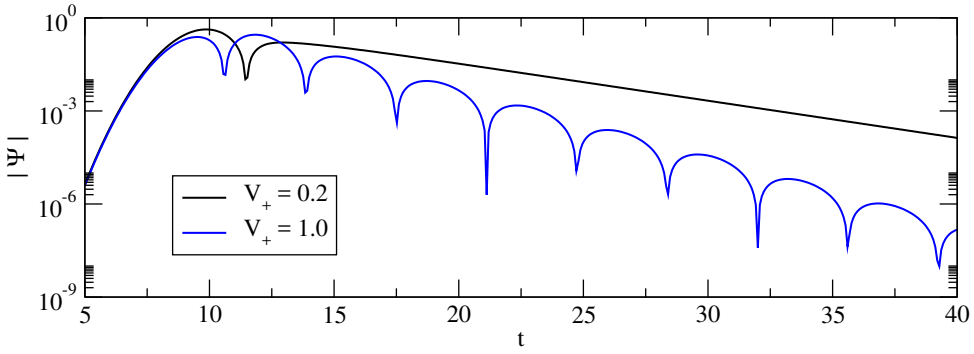

FIGURE 4.4: Semi-log graphs for the field evolution with the usual Pöschl-Teller potential. The oscillatory ($V_+/\kappa^2 > 1/4$) and non-oscillatory ($0 < V_+/\kappa^2 \leq 1/4$) regimes are shown. We used $V_+ = 1$ and $V_- = 0$.

apparent from the results of section 4.3.2 that the late-time decay is always non-oscillatory, with an exponential coefficient given by

$$\mathrm{Im}\,(\omega_0) = -\kappa\left(\frac{1}{2} + \sqrt{\frac{V_-}{\kappa^2} + \frac{1}{4}}\right) . \tag{4.109}$$

We present typical results for the field evolution with the modified Pöschl-Teller potential in Fig. 4.5. From the data, the numerical evaluation for the fundamental frequency ω_0^{num} can be made. The comparison between the analytical and numerical results are presented in Table 4.1. The concordance of the two approaches is very good.

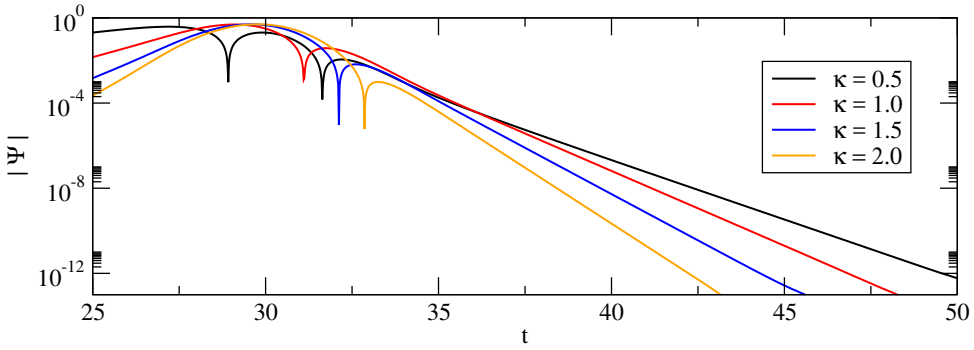

FIGURE 4.5: Semi-log graphs for the field evolution with the modified Pöschl-Teller potential. The late-time decay is always exponential and non-oscillatory. We used $V_- = 1$ and $V_+ = 0$.

The field evolution with the full Pöschl-Teller potential ($V_+ > 0$ and $V_- > 0$) combines elements from the dynamics associated to the usual and modified Pöschl-Teller potentials. We observe oscillatory and non-oscillatory regimes. Considering the results in section 4.3.3, we observe that if $V_+/\kappa^2 > 1/4$ the late-time

TABLE 4.1: Analytical and numerical results for the fundamental quasinormal frequencies associated to the modified Pöschl-Teller potential. The relative differences $\Delta\%$ between the results are also indicated. We use $V_- = 1$ and $V_+ = 0$.

κ	$\mathrm{Im}(\omega_0)$	$\mathrm{Im}(\omega_0^{num})$	$\Delta\%$
0.25	-1.1328	-1.1607	2.46
0.50	-1.2808	-1.2965	1.23
1.00	-1.6180	-1.6196	0.10
1.50	-2.0000	-2.0018	0.09
2.00	-2.4142	-2.4174	0.13

decay is characterized by an oscillatory behavior,

$$\mathrm{Re}\omega_0^{\pm} = \pm\sqrt{\frac{V_+}{\kappa^2} - \frac{1}{4}}\,, \tag{4.110}$$

$$\mathrm{Im}\omega_0^{\pm} = -\kappa\left(1 + \sqrt{\frac{V_-}{\kappa^2} + \frac{1}{4}}\right)\,. \tag{4.111}$$

If $0 < V_+/\kappa^2 \leq 1/4$, the field decays monotonically, with

$$\mathrm{Re}\omega_0^{-} = 0\,, \tag{4.112}$$

$$\mathrm{Im}\omega_0^{-} = -\kappa\left(1 + \sqrt{\frac{V_-}{\kappa^2} + \frac{1}{4}} - \sqrt{\frac{1}{4} - \frac{V_+}{\kappa^2}}\right)\,. \tag{4.113}$$

The numerical results for the full Pöschl-Teller potential are compared with the analytical formulas in Table 4.2, showing very good agreement between the two methods.

TABLE 4.2: Analytical and numerical results for the fundamental quasinormal frequencies associated to the full Pöschl-Teller potential. The relative differences $\Delta\%$ between the results are also indicated. We use $V_- = 1$ and $\kappa = 1$.

V_+	Re (ω_0)	Im (ω_0)	Re (ω_0^{num}) $(\Delta\%)$	Im (ω_0^{num}) $(\Delta\%)$
0	0	-1.6180	0	-1.6204 (0.15)
0.05	0	-1.6708	0	-1.6750 (0.25)
0.1	0	-1.7307	0	-1.7386 (0.46)
0.2	0	-1.8944	0	-1.9352 (2.15)
0.5	0.5000	-2.1180	0.5061 (1.21)	-2.1288 (0.51)
1.0	0.8660	-2.1180	0.8664 (0.05)	-2.1190 (0.05)
2.0	1.3229	-2.1180	1.3243 (0.11)	-2.1003 (0.84)
5.0	2.1794	-2.1180	2.1634 (0.74)	-2.1139 (0.19)
10.0	3.1225	-2.1180	3.1145 (0.26)	-2.1305 (0.59)

Chapter 5

Thermodynamics of Anti-de Sitter Black Holes

In this chapter we study the behavior of thermodynamical variables in the processes of evaporation and phase transition of Anti-de Sitter black holes. We employ the Vaidya Anti-de Sitter metric as non-stationary geometry with a time-dependent mass function that can be used to characterize the radiation process of a black hole and the phase transitions between different asymptotically Anti-de Sitter configurations.

5.1 Vaidya spacetime

In general relativity, the Vaidya metric constitutes a non-stationary generalization of the Schwarzschild metric (2.21) with a time dependent mass [15, 16]. The geometry no longer describes a vacuum solution of Einstein's field equation; instead the energy-momentum tensor corresponds to some form of null matter emitted from or absorbed by a spherically symmetric body. For a general spherically symmetric spacetime in $(3+1)$ dimensions, the metric can always be specified in terms of only two independent functions [20]. In Eddington-Finkelstein coordinates such specification can be given by:

$$ds^2 = -\left(1 - \frac{2M(v,r)}{r}\right) \mathrm{e}^{2\Psi} dv^2 \pm 2\, \mathrm{e}^{\Psi}\, dvdr + r^2 d\Omega^2\,, \tag{5.1}$$

with $\pm$ indicating either the advanced or retarded Eddington-Finkelstein time (see appendix A for a definition of the coordinate system). From the independent functions ψ and $M(v,r)$ the components of the energy-momentum tensor read [54]

$$\frac{\partial M(v,r)}{\partial r} = 4\pi r^2 T^{v}{}_{v}\,, \quad \frac{\partial M(v,r)}{\partial v} = 4\pi r^2 T^{r}{}_{v}\,, \quad \frac{\partial \Psi}{\partial r} = 4\pi r e^{\Psi} T^{v}{}_{r}\,. \tag{5.2}$$

The total energy-momentum tensor can be expressed as a superposition of the energy-momentum tensors corresponding to a null fluid, that is, a fluid with a traceless

energy-momentum tensor, and a perfect fluid [54]

$$T_{\mu\nu} = u l_\mu l_\nu + P\, g_{\mu\nu} + (\rho + P)(l_\mu n_\nu + l_\nu n_\mu)\,, \tag{5.3}$$

where l_μ and n_μ are the components of future-oriented null vectors. In this form u is the energy density of a radial null fluid and ρ and P are the energy density and pressure of a perfect fluid. These quantities depend on the derivatives of the function $M(v,r)$ in the following form:

$$u = \pm\frac{1}{4\pi r^2}\frac{\partial M(v,r)}{\partial v}\,, \quad \rho = \frac{1}{4\pi r^2}\frac{\partial M(v,r)}{\partial r}\,, \quad P = -\frac{1}{8\pi r^2}\frac{\partial^2 M(v,r)}{\partial r^2}\,. \tag{5.4}$$

As a non-stationary geometry, a black hole in the spacetime (5.1) will be delimited by a time evolving horizon that is not compatible with a Killing horizon. Therefore, we characterize the boundary of the black hole as corresponding to a trapping horizon, as it was discussed in section 2.4. In terms of the metric (5.1), the the future-oriented null vectors read:

$$n = -\frac{1}{2}\left(1 - \frac{2M(v,r)}{r}\right)\mathrm{e}^{2\Psi} dv + dr\,, \qquad l = -dv\,, \tag{5.5}$$

and the product of the corresponding outgoing geodesic expansion θ_+ and ingoing geodesic expansion θ_- is:

$$\theta_+\theta_- = \frac{2}{r}\left(1 - \frac{2M(v,r)}{r}\right)\mathrm{e}^{2\Psi}\,. \tag{5.6}$$

The metric (5.1) possesses a trapping horizon if the product $\theta_+\theta_-$ is zero. From (5.6), the trapping horizon of the metric (5.1) corresponds to the surface $r = 2M(v,r)$. In such case the surface gravity of the trapping horizon is:

$$\kappa_g = \frac{M(v,r_+)}{r_+^2} - \frac{M'(v,r_+)}{r_+} = \frac{1}{4M(v,r_+)} - \frac{M'(v,r_+)}{2M(v,r_+)} \tag{5.7}$$

where

$$M'(v,r_+) = \left.\frac{dM(v,r)}{dr}\right|_{r=r_+}\,. \tag{5.8}$$

5.1.1 Vaidya Anti-de Sitter black hole

The Vaidya Anti-de Sitter geometry is a a particular case of (5.1) with $\psi = 0$ and a mass function $M(v)$ depending only on the Eddington–Finkelstein time. This geometry is the non-stationary generalization of the Schwarzschild-Anti-de Sitter geometry (3.15); in advanced Eddington–Finkelstein coordinates the components of the Vaidya AdS metric read

$$ds^2 = -\left(1 - \frac{2M(v)}{r} + \frac{r^2}{l^2}\right) dv^2 + 2dvdr + r^2 d\Omega^2 \,, \tag{5.9}$$

corresponding to a non-vacuum solution of Einstein's field equations with negative cosmological constant and an energy-momentum tensor $T_{\mu\nu}$ describing a massless null fluid given by

$$T_{\mu\nu} = \frac{1}{4\pi r^2} \frac{\partial M(v)}{\partial v} \, l_\mu l_\nu \,, \tag{5.10}$$

where $l_\mu = -\partial_\mu v$ is the 4-vector along the null fluid with normalization $l_\mu l^\mu = 0$.

The metric (5.9) does not possess either a time-like Killing vector field or a Killing horizon, therefore a more adequate characterization of the geometric and thermodynamical quantities of the Vaidya-AdS black hole is given in terms of the corresponding trapping horizon. Following (5.6), the trapping horizon of the Vaidya-AdS black hole (5.9) is located at the surface $r = r_+(v)$ that is solution of the polynomial

$$r^3 + l^2 r - 2M(v) l^2 = 0 \,. \tag{5.11}$$

In the formalism of the generalized thermodynamics the function $M(v, r)$ in (5.1) corresponds to the Misner-Sharp mass. At the trapping horizon $r = r_+(v)$ we have

$$M_{ms}(v)_{r=r_+} = M(v) - \frac{r_+^3}{2l^2} = \frac{r_+(v)}{2} \,. \tag{5.12}$$

The variation of the Misner-Sharp mass obeys the generalized first law (2.76). To obtain the quantity ω in equation (2.56), we consider an effective energy-momentum tensor with contributions from both the null radiation (5.10) and the cosmological constant (3.20). We write

$$T'_{ab} = T_{ab} - \frac{\Lambda}{8\pi} h_{ab} \,. \tag{5.13}$$

Since the trace of the energy-momentum tensor (5.10) is null we get

$$\omega = -\frac{1}{2}\left(T^a{}_a - \frac{\Lambda}{8\pi} h^a{}_a\right) = \frac{\Lambda}{8\pi} \,, \tag{5.14}$$

$$\omega \nabla_a V = -\frac{3}{8\pi l^2} \nabla_a \left(\frac{4\pi r_+^3}{3}\right) = -\frac{3r_+^2}{2l^2} \nabla_a r_+ \,, \tag{5.15}$$

giving a work term corresponding to the pressure associated with the cosmological constant. From equation (2.57), the components of the vector ψ corresponding to the

energy flux are:

$$\psi_v = T_v{}^c \partial_c r + \omega \partial_v r = \frac{1}{4\pi r^2} \frac{dM(v)}{dv}\,, \tag{5.16}$$

$$\psi_r = T_r{}^c \partial_c r + \omega \partial_r r = -\frac{\Lambda}{8\pi} + \omega = 0\,. \tag{5.17}$$

None of these components depend on the cosmological constant Λ, since the energy associated with the cosmological constant does not radiate. The radiative term in equation (2.58) is:

$$\mathcal{A}\psi_v = 4\pi r^2 \left(\frac{1}{4\pi r^2} \frac{dM(v)}{dv} \right) = \frac{dM(v)}{dv}\,, \tag{5.18}$$

being equivalent with the derivative of the function $M(v)$ respect to the advanced time v. Differentiating on both sides of equation (5.11) and rearranging terms gives us:

$$\frac{dM(v)}{dv} = \left(\frac{3r_+^2 + l^2}{2l^2} \right) \frac{dr_+}{dv}\,. \tag{5.19}$$

The variation of the trapping horizon area is $dA = 8\pi dr_+$, then we have

$$\left(\frac{3r_+^2 + l^2}{2l^2} \right) \frac{dr}{dv} = \left(\frac{3r_+^2 + l^2}{2l^2} \right) \frac{1}{8\pi r_+} \frac{dA}{dv} = \frac{\kappa_g}{8\pi} \frac{dA}{dv}\,, \tag{5.20}$$

then it follows that the term (5.18) is:

$$A\psi_v = \frac{dM(v)}{dv} = \frac{\kappa_g}{8\pi} \nabla_a A = T \nabla_a S\,. \tag{5.21}$$

The quantity $\mathcal{A}\psi_v$ corresponds to the "heat" added to or subtracted from the black hole, with temperature $T = \kappa_g / 2\pi$ proportional to the geometric surface gravity of the trapping horizon. After adding both terms (5.21) and (5.15) we get:

$$\nabla_a M_{ms} = \frac{dM(v)}{dv} - \frac{3r_+^2}{2l^2} \frac{dr_+}{dv}\,. \tag{5.22}$$

which is equivalent to the derivative of equation (5.12). This result implies that in the case of the Vaidya-Anti-de Sitter black hole the variation of the Misner-Sharp mass corresponds not only to the variation of the function $M(v)$ but also from the work performed by the black hole to sustain an horizon of radius $r_+(v)$ when a vacuum energy density is present.

5.2 Mass functions for evaporation and phase transitions of AdS black holes

In this section we employ specific mass functions $M(v)$ in the $(3+1)$ Vaidya-AdS black hole in order to study the time dependency of the processes of evaporation and phase transitions in Anti-de Sitter black holes. For a given mass function $M(v)$, the trapping horizon of the Vaidya-AdS black hole is given by the real solution $r = r_+(v)$ of the polynomial (5.11). A polynomial of the form $r^3 + pr = q$ has three solutions, one real and two complex conjugated. The real solution corresponding to the horizon, can be expressed in terms of hyperbolic functions as [55]:

$$r_+ = \sqrt{\frac{4|p|}{3}}\sinh\left[\frac{1}{3}\text{arcsinh}\left(\frac{3q}{2p}\sqrt{\frac{3}{|p|}}\right)\right] \quad \text{if} \quad p > 0\,. \tag{5.23}$$

With $p = l^2$ and $q = 2M(v)l^2$ we have

$$r_+ = r_+(M(v)) = \sqrt{\frac{4l^2}{3}}\sinh\left[\frac{1}{3}\text{arcsinh}\left(3M(v)\sqrt{\frac{3}{l^2}}\right)\right]\,. \tag{5.24}$$

With an input mass function $M(v)$ we can obtain the time evolution of thermodynamical quantities such as temperature, entropy and heat capacity. The free energy is defined as a thermodynamical potential. with respect to a given energy reference; in this case we will work with the following forms for the free energy defined in terms of the mass function $M(v)$ and the Misner-Sharp mass $M_{ms}(v)$:

$$F = M(v) - TS, \qquad G = M_{ms}(v) - TS\,. \tag{5.25}$$

In an evaporating black hole the luminosity is the measure of radiated energy emitted per unit time, and is equal to (minus) the mass loss rate. If the a black hole is treated as a perfect blackbody the luminosity of a $(d+1)$ dimensional black hole would be given in terms of the horizon area and the temperature by the Stefan-Boltzmann's law:

$$L_{SB} = \sigma_{(d+1)}A_{d-1}T^{d+1} = -\frac{dM(v)}{dv}\,, \tag{5.26}$$

with $\sigma_{(d+1)}$ the $(d+1)$-dimensional Boltzmann constant

$$\sigma_{(d+1)} = (2\pi)^d\mathcal{A}_{d-1}\,\zeta(d-1)\,d! \tag{5.27}$$

where $\mathcal{A}_{d-1}$ is the area of a $(d-1)$ sphere [56].

5.2.1 Radiation of small and large Anti-de Sitter black holes

Small Anti-de Sitter black holes have negative heat capacity, therefore they are unstable under perturbation, they radiate away their mass just like a Schwarzschild black hole in asymptotically flat spacetime. For small Anti-de Sitter black holes $(M \ll l)$ the temperature and entropy scale with the mass as:

$$T = \frac{1}{8\pi M}, \quad S = 4\pi M^2 \,. \tag{5.28}$$

The thermodynamics of small Anti-de Sitter black holes is very similar to their asymptotically flat counterparts. From the Stefan-Boltzmann law (5.26) we have:

$$L_{SB} = \sigma 16\pi M^2 \left(\frac{1}{8\pi M}\right)^4 = \frac{\sigma}{256\pi^3 M^2} \,. \tag{5.29}$$

Solving for $M(v)$ gives the following mass function:

$$M(v) = \left[M_0^3 - b(v - v_0)\right]^{1/3} \,, \tag{5.30}$$

with $b = \sigma/256\pi^3$. This function describes a black hole of initial mass M_0 at $v = v_0$, with evaporation time $v_{evap} = M_0^3/3b$ and mass loss rate of proportional to the inverse of the square mass:

$$\frac{dM(v)}{dv} = -\frac{b}{M(v)^2} \,. \tag{5.31}$$

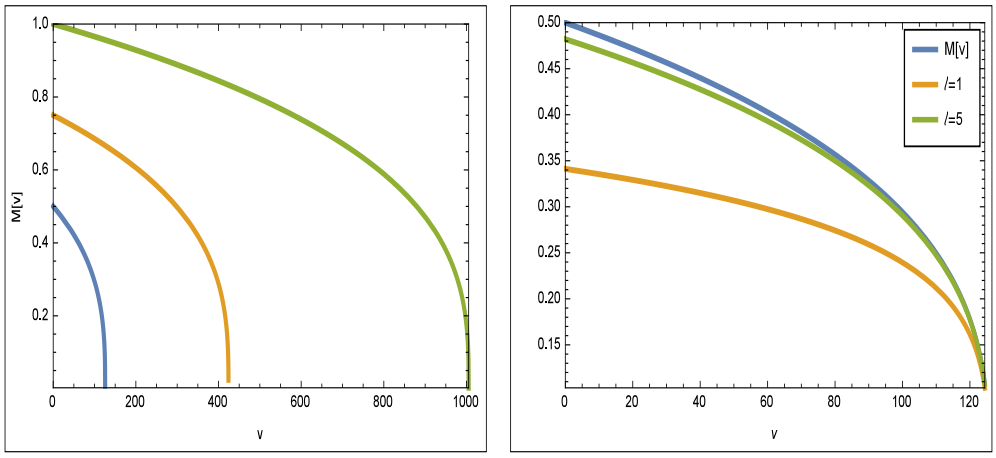

(A) (B)

FIGURE 5.1: (A) Function $M(v)$ for different initial mass values. (B) Misner-Sharp mass for $M_0 = 0.5$.

The black hole evaporates faster for smaller masses and temperature increases as the black hole radiates away its mass. In figure 5.2 we display the behavior of the temperature and luminosity for different values of l, near v_{evap} the temperature of

the black hole diverges. The mass loss rate of the black hole deviates from the Stefan-Boltzmann law for large values of the cosmological constant (equivalently for small values of l).

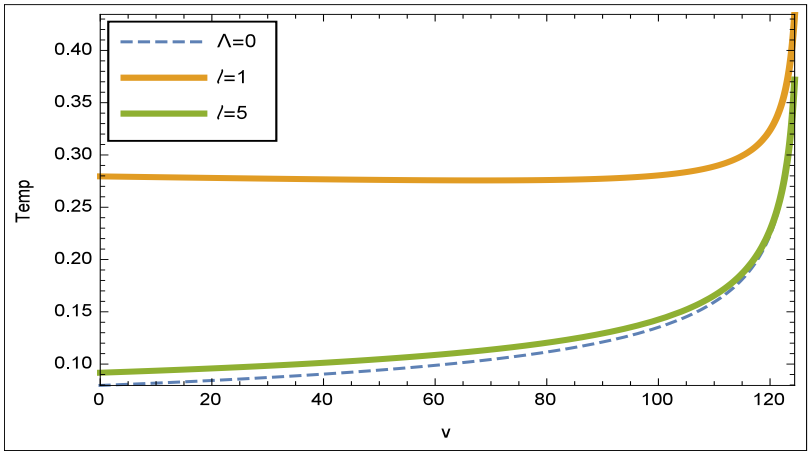

(A)

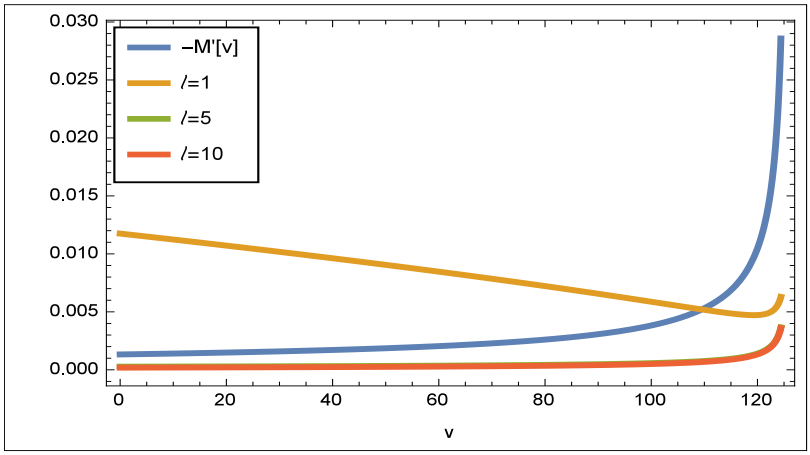

(B)

FIGURE 5.2: (A) Temperature as a function of advanced time for $M_0 = 0.5$. (B) Radiated mass with $M_0 = 0.5$.

On the other hand, large Anti-de Sitter black holes are thermodynamically stable. A difficulty for the study of the evaporation process of Anti-de Sitter black holes follows from their non-globally hyperbolic property, meaning that is also dependends on the boundary conditions imposed at infinity. If typical reflective boundary conditions are imposed at the conformal boundary of the AdS space, a large AdS black hole will tend to not evaporate but to reach thermal equilibrium with its Hawking atmosphere [57]. However, if different boundary conditions are imposed there is the possibility for large AdS black holes to evaporate.

For large Anti-de Sitter black holes the radius approximates as a function of the mass as

$$r_+ = (2l^2 M)^{1/3}\,, \tag{5.32}$$

and the temperature and entropy scale with the black holes mass M as

$$T = \frac{3(2l^2)^{1/3}}{4\pi l^2} M^{1/3}, \quad S = \pi(2l^2)^{2/3} M^{2/3}\,. \tag{5.33}$$

Following the arguments of [56, 58, 59, 60], for large black holes we can take an effective area on the Stefan-Boltzmann law that does not correspond to the horizon radius but to the Anti-de Sitter radius l instead. This implies an effective area $A = 4\pi l^2$. The black hole luminosity is then:

$$\frac{dM(v)}{dv} = \sigma 4\pi l^2 \left(\frac{3(2l^2)^{1/3}}{4\pi l^2} M^{1/3} \right)^4 = -\frac{\sigma 3^4 2^{4/3}}{(4\pi)^3 l^{10/3}} M^{4/3}\,. \tag{5.34}$$

Solving gives a mass function of the form:

$$M(v) = \left[\frac{3}{a(v - v_0) + 3M_0^{-\frac{1}{3}}} \right]^3, \quad a = \frac{\sigma 3^4}{2^6 \pi^3 l^{10/3}}\,. \tag{5.35}$$

This establishes a difference between large black holes in AdS and asymptotically flat. Whereas a large Schwarzschild black hole takes a time to evaporate of the order of M^3 ; the evaporation time for a large Anti-de Sitter black hole depends on the cosmological constant and is of order l^3

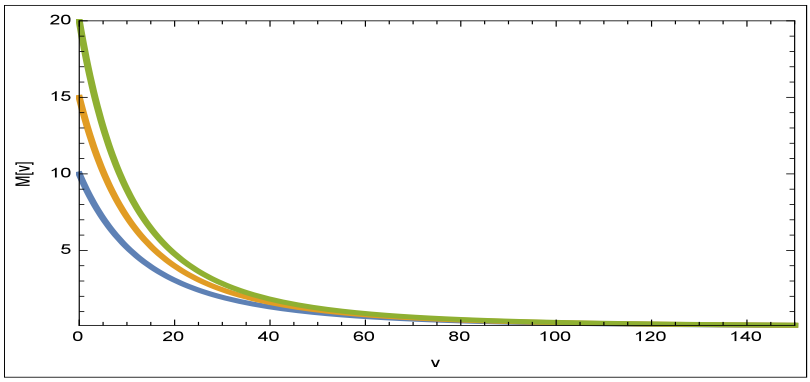

(A)

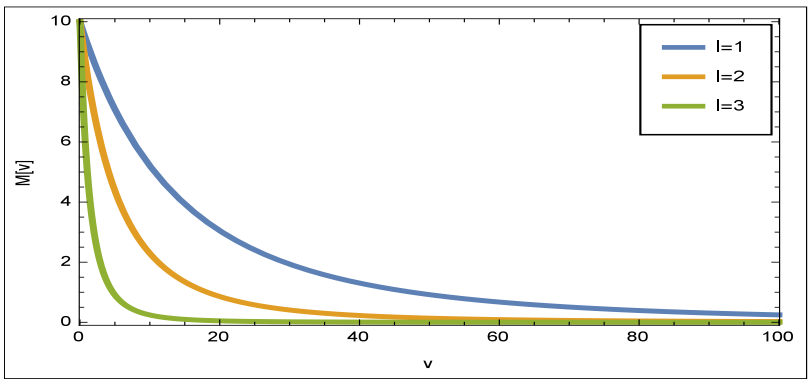

(B)

FIGURE 5.3: (A) Mass function (5.35) for different initial masses. (B) Mass function (5.35) for different values of L

5.2.2 Phase transitions

As a more general mass function $M(v)$ that allows to characterize the change of a black hole between two different mass values we consider the following

$$M(v) = M_0 + \frac{M_f - M_0}{2}\left[1 + \tanh\left(\frac{v - v_0}{b}\right)\right], \tag{5.36}$$

representing a black hole with initial mass M_0 and final mass M_f. The parameter b will serve as a control parameter for how fast or how slow the change between the two different mass values occurs . To study phase transitions of black holes we consider $M_f > M_0$. We can consider either M_f larger or smaller than l.

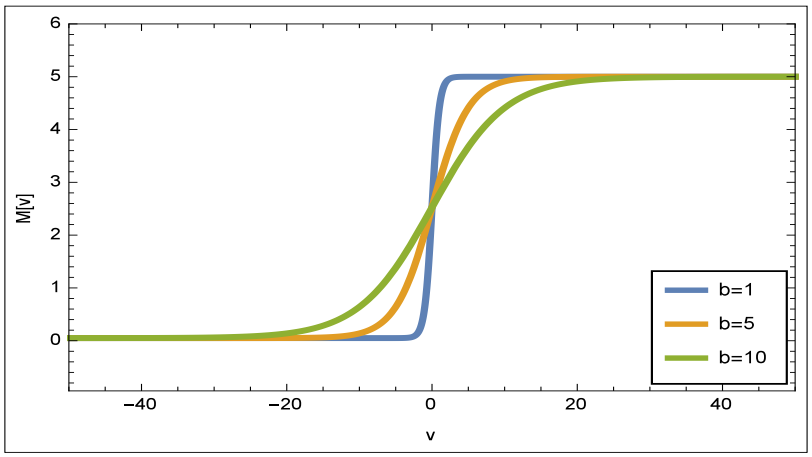

(A)

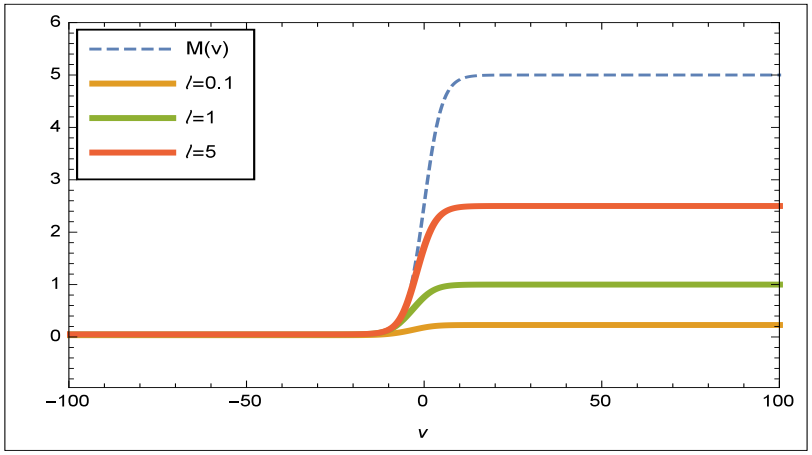

(B)

FIGURE 5.4: (A) Mass for different values of b. (B) Mass function and Misner-Sharp mass for different values of l.

In the numerical analysis we can, for a fixed value of b, either take a constant Anti-de Sitter radius l and different initial values of masses M_f or choose a fixed value for the initial mass and to different values of l. For a black hole with initial mass smaller than l we have that the temperature decreases as the black hole increases mass. If the mass function is such that the final mass becomes larger than l then the temperature will increase as the black hole. If the black hole never transitions from the small mass regime to the large mass regime the temperature will be always decreasing (see figure 5.5).

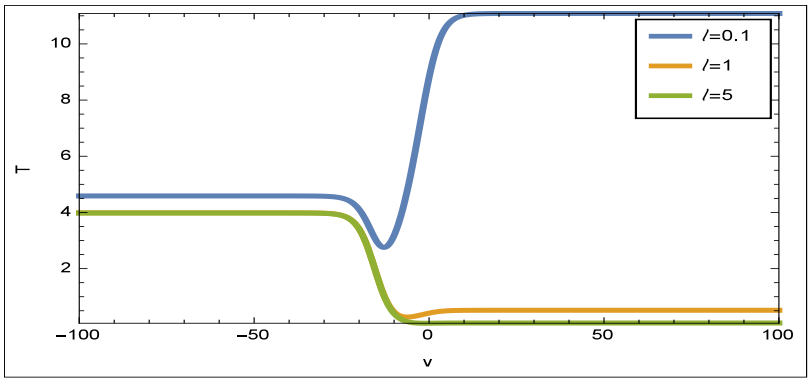

(A)

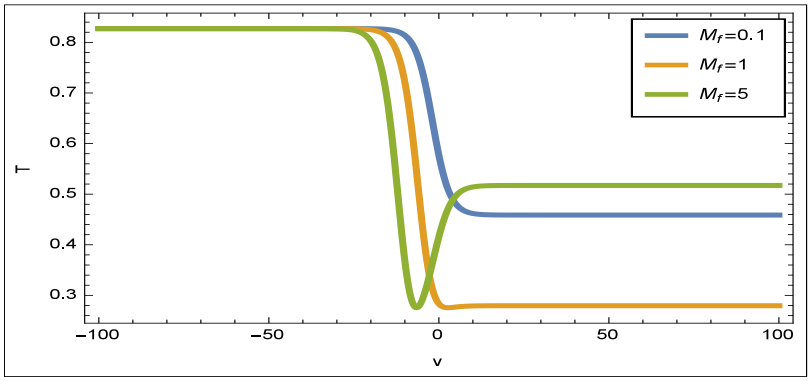

(B)

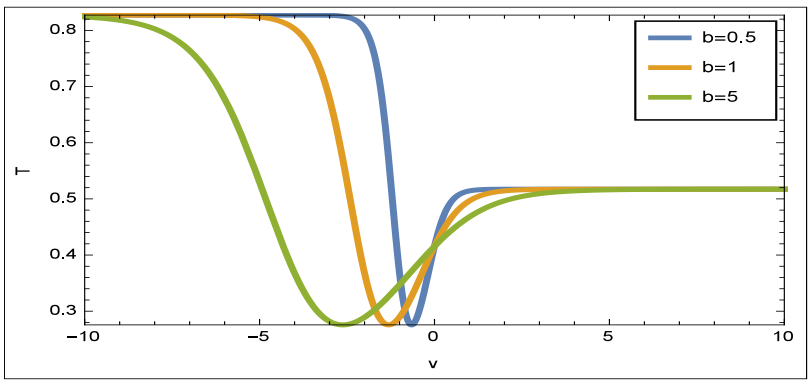

(C)

FIGURE 5.5: (A) Temperature as a function of advanced time for $l = \{0.1, 1, l = 5\}$ with $M_0 = 5$ and $M_f = 0.01$. (B) Temperature for $M_0 = \{1, 5, 10\}$ with $l = 1$. (C) Temperature for different values of b with $M_0 = \{1, 5, 10\}$ with $l = 0.1$.

In general, phase transitions and thermal instabilities can be identified by discontinuities of physical quantities or their derivatives with respect to certain thermodynamical variables [61]. In figure 5.6 we show the heat capacity as a function of temperature and entropy. If the initial black hole mass is smaller than l and the final mass is larger the heat capacity presents a discontinuity both as a function of temperature and entropy

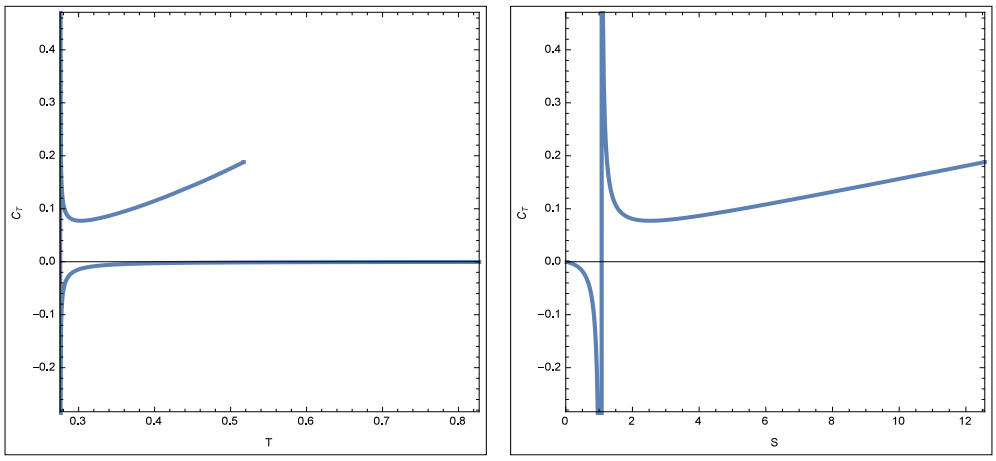

(A) (B)

FIGURE 5.6: (A) Heat capacity as a function of temperature for $M_0 = 0.01$, $M_f = 5$ and $l = 1$. (B) $M_0 = 0.05$, $M_f = 5$. Heat Capacity as a function of entropy for (C) $M_0 = 0.01$, $M_f = 5$ and (C)$l = 1$.

In figure (5.7) we obtain the time dependency of the free energy for different values of mass and AdS radius. When a phase transition occurs the free energy goes from positive to negative values.

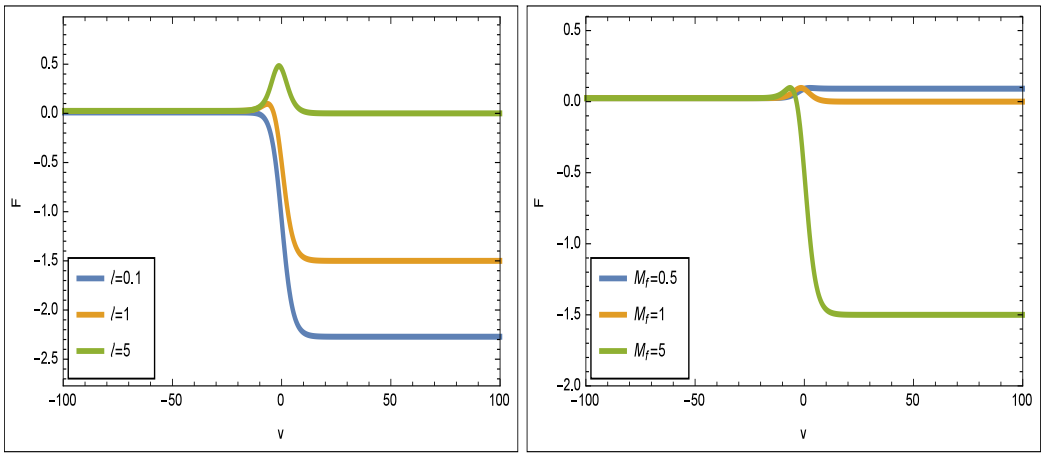

(A) (B)

FIGURE 5.7: Free energy as a function of advanced time. (A) Fixed masses $M_0 = 0.05$, $M_f = 5$. (B) Fixed radius $l = 1$.

As illustrated in figure 5.8, the free energy F defined in (5.25) as as a function of temperature has two branches representing the small and large mass regimes, with the upper branch corresponding to the small mass regime; there is also a point when the derivative of the free energy is discontinuous corresponding to the minimum value of the temperature of the AdS black hole. This behaviour indicatates a first order phase transition. The free energy as a function of entropy is always continuous. The Hawking-page transition occurs when the free energy goes from positive to negative as the entropy entropy increases.

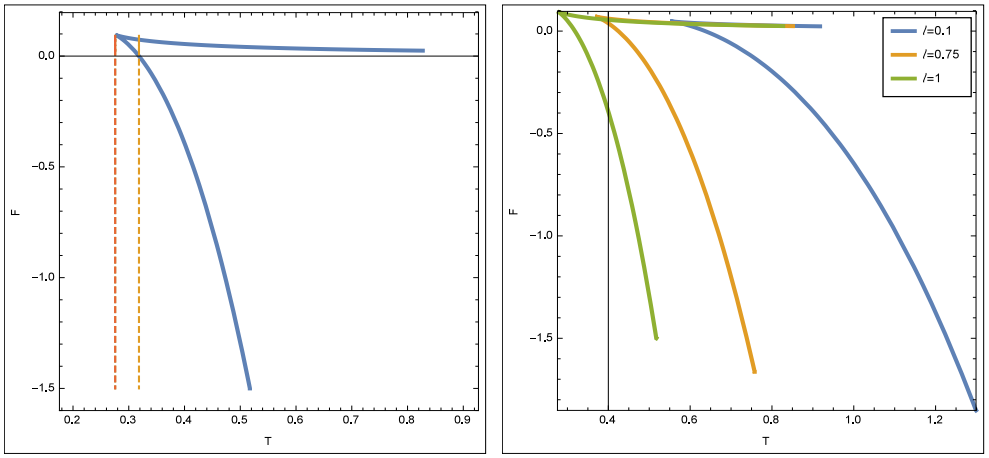

(A) (B)

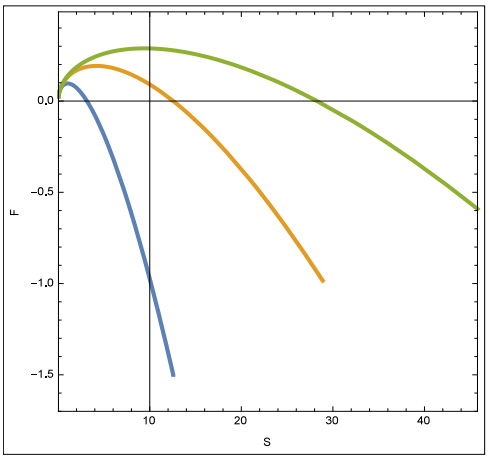

(C)

FIGURE 5.8: (A) Free energy as a function of temperature. (B) Free energy as a function of temperature for different values of l. (C) Free energy as a function of entropy for different values of l. Values $M_0 = 0.05$, $M_f = 5$.

5.3 Semiclassical description of Hawking atmosphere of Anti-de Sitter black holes

In asymptotic Anti-de Sitter black holes, the Hawking radiation that escapes the black hole is reflected back from spatial infinity and the evaporation process is conditioned to the initial condition of the black hole as either a black hole of small or large mass. A small AdS black hole radiates at a faster rate that it reabsorbs the radiation reflected from infinity and eventually evaporates, much like an asymptotically flat Schwarzschild black hole. On the contrary, a large AdS black hole is able to reabsorb most of the reflected Hawking radiation and eventually reaches equilibrium with the surrounding Hawking atmosphere [57]. In general, a full description of the evaporation process of a black hole through emission of Hawking radiation is a complex task, since a realistic scenario needs to consider the spacetime backreaction, as the energy-momentum tensor of the radiation field modifies the background geometry. A common approach to the backreaction problem is taken in the context of semiclassical gravity, where the classic gravitational field couples to the expected value of the energy-momentum tensor of quantized matter fields in the semiclassical Einstein's equations:

$$G_{\mu\nu} + \Lambda\, g_{\mu\nu} = 8\pi \langle T_{\mu\nu} \rangle. \tag{5.37}$$

As an approximation, the Hawking radiation emitted by a black hole can be treated as a atmosphere of particles with an energy-momentum tensor that acts as a source on Einstein field equations [62, 54].

5.3.1 Renormalized energy-momentum tensor

A semiclassical treatment of the evolution of the Hawking atmosphere produced by the radiation of an evaporating black hole considers a quantum field propagating in a classical background from which a renormalized quantum energy-momentum tensor is obtained [63]. In asymptotically Anti-de Sitter black holes massive particles cannot reach infinity and fall into the black hole instead, meaning that only massless particles need to be considered as contributing to the evaporation process. A simple model of the Hawking atmosphere considers the dynamics of a massless scalar field Φ satisfying the Klein-Gordon equation (2.79). Classically, the energy-momentum tensor of a scalar field Φ is

$$T_{\mu\nu} = \nabla_\mu \nabla_\nu \Phi - \frac{1}{2} g_{\mu\nu} g^{\rho\sigma} \nabla_\rho \Phi \nabla_\sigma \Phi \,. \tag{5.38}$$

For a quantized field, the quantized energy-momentum tensor (5.38) is a divergent quantity and a renormalization scheme must be implemented. Explicit expressions for the renormalized energy-momentum tensor in 4 dimensions are hard to come by. In spherically symmetric spacetimes it is possible to implement an optic geometric approximation, in which the renormalized 4-dimensional energy-momentum is

related to the two-dimensional energy-momentum tensor of the induced metric tangent to S^2 as [63, 64]:

$$\langle T_{\mu\nu}\rangle_{(4D)} = \frac{1}{4\pi r^2}\langle T_{\mu\nu}\rangle_{(2D)}\,. \tag{5.39}$$

where the 4-dimensional energy-momentum tensor is:

$$\langle T_{\mu\nu}\rangle_{(4D)} = \alpha R^2 + \beta R_{\mu\nu}R^{\mu\nu} + \gamma R_{\mu\nu\rho\sigma}R^{\mu\nu\rho\sigma}\,. \tag{5.40}$$

We follow the procedure outlined in [65]. Classically, the trace $T_\mu{}^\mu$ of the energy-momentum tensor of a massless scalar field is zero. For a quantized scalar field in two dimensions the renormalized energy-momentum tensor is proportional to the scalar curvature R of the background geometry:

$$\langle T_\mu{}^\mu\rangle_{(2D)} = \alpha R\,, \tag{5.41}$$

where $\alpha = 1/24\pi$.

For the two-dimensional Vaidya-AdS metric the trace of the energy - momentum tensor is then

$$T_v{}^v + T_r{}^r = \alpha\left(\frac{4M}{r^3} - \frac{2}{l^2}\right)\,. \tag{5.42}$$

Now we obtain the different components of the renormalized energy-momentum tensor. From the conservation of the energy-momentum tensor $\nabla_\mu T_\nu{}^\mu = 0$ we have

$$\begin{aligned}\partial_v T_v{}^v + \partial_r T_v{}^r + (T_r{}^r - T_v{}^v)\left(\frac{M}{r^2} + \frac{r}{l^2}\right)\\ - \left[\left(\frac{M}{r^2} + \frac{r}{l^2}\right)\left(1 - \frac{2M}{r} + \frac{r^2}{l^2}\right) + \frac{\dot{M}}{r}\right] T_r{}^v = 0\,,\end{aligned} \tag{5.43}$$

$$\partial_v T_r{}^v + \partial_v T_r{}^r + T_r{}^v\left(\frac{M}{r^2} + \frac{r}{l^2}\right) = 0\,, \tag{5.44}$$

where the non-trivial Christoffel coefficients are:

$$\begin{aligned}\Gamma^v{}_{vv} &= \frac{M}{r^2} + \frac{r}{l^2}, \quad \Gamma^r{}_{vr} = -\frac{M}{r^2} - \frac{r}{l^2}\,,\\ \Gamma^r{}_{vv} &= \left[\left(\frac{M}{r^2} + \frac{r}{l^2}\right)\left(1 - \frac{2M}{r} + \frac{r^2}{l^2}\right) + \frac{\dot{M}}{r}\right], \quad .\end{aligned} \tag{5.45}$$

Symmetry of the energy-momentum tensor $T_{\mu\nu} = T_{\nu\mu}$ implies that

$$T_r{}^r - T_v{}^v = \left(1 - \frac{2M}{r} + \frac{r^2}{l^2}\right) T_r{}^v\,. \tag{5.46}$$

The time reversal invariance $T_{tr} = T_{rt} = 0$ of the energy-momentum tensor in the coordinates (v, r) is $T_v{}^r = 0$. Replacing equations (5.46) and (5.42) in equation (5.43)

we have

$$\partial_v T_r{}^v = \alpha \left(1 - \frac{2M}{r} + \frac{r^2}{l^2}\right)^{-1} \partial_v R\,, \tag{5.47}$$

and consequently we have from equation (5.44) a differential equation for the component $T_r{}^r$:

$$\begin{aligned} \partial_r T_r{}^r + \left(\frac{2M}{r^2} + \frac{2r}{l^2}\right)\left(1 - \frac{2M}{r} + \frac{r^2}{l^2}\right)^{-1} T_r{}^r \\ = \alpha \left(1 - \frac{2M}{r} + \frac{r^2}{l^2}\right)^{-1} \left[\frac{4\dot{M}}{r^3} - \frac{4M^2}{r^5} - \frac{2M}{r^2 l^2} + \frac{2r}{l^4}\right]. \end{aligned} \tag{5.48}$$

The solution of equation (5.48) is

$$\begin{aligned} T_r{}^r = \alpha \left(1 - \frac{2M}{r} + \frac{r^2}{l^2}\right)^{-1} \times \\ \left[\int_{r_+}^{r} \left(\frac{4\dot{M}}{r'^3} - \frac{4M^2}{r'^5} + \frac{2M}{r'^2 l^2} - \frac{4M}{r'^2 l^2} + \frac{2r'}{l^4}\right) dr' + C(v)\right]. \end{aligned} \tag{5.49}$$

The integration constant $C(v)$ can be taken to be equal to zero since it just shifts the energy value, and the integral can be solved giving:

$$\begin{aligned} T_r{}^r = \alpha \left(1 - \frac{2M}{r} + \frac{r^2}{l^2}\right)^{-1} \times \\ \left[-\frac{2\dot{M}}{r^2} + \frac{2\dot{M}}{r_+^2} + \frac{M^2}{r^4} - \frac{M^2}{r_+^4} + \frac{2M}{r l^2} - \frac{2M}{r_+ l^2} + \frac{r^2}{l^4} - \frac{r_+^2}{l^4}\right]. \end{aligned} \tag{5.50}$$

Now we obtain the remaining components of the energy-momentum tensor from (5.42). The component $T_v{}^v$ is

$$\begin{aligned} T_v{}^v = \alpha \left(1 - \frac{2M}{r} + \frac{r^2}{l^2}\right)^{-1} \left[\frac{2\dot{M}}{r^2} - \frac{2\dot{M}}{r_+^2} + \frac{7M^2}{r^4} + \frac{M^2}{r_+^4} + \frac{r^2}{l^4} + \frac{r_+^2}{l^4}\right. \\ \left. - \frac{10M}{r l^2} + \frac{2M}{r_+ l^2} - \frac{4M}{r^3} + \frac{2}{l^2}\right]. \end{aligned} \tag{5.51}$$

The component $T_v{}^v$ is proportional to the mass density of the scalar field. In (5.51) polarization terms proportional to M/r^2 and radiation terms proportional to $\dot{M}$. The component $T_v{}^v$ in the limit $r \to \infty$ is given by:

$$T_v{}^v = \frac{1}{24\pi}\left(-\frac{2\dot{M}}{r_+^2} + \frac{M^2}{r_+^4} + \frac{2M}{r_+ l^2} + \frac{r_+^2}{l^4} + \frac{2}{l^2}\right). \tag{5.52}$$

Since the Vaidya-Ads temperature can be expressed as:

$$T = \frac{1}{2\pi}\left(\frac{M}{r_+^2} + \frac{r_+}{l^2}\right), \tag{5.53}$$

we can write

$$T_v{}^v = \frac{\pi}{6}T^2 - \frac{\dot{M}}{12\pi r_+^2} + \frac{1}{12\pi l^2}\,. \tag{5.54}$$

We can compare the result (5.54) with the two-dimensional version of the Stefan-Boltzmann law describing the the energy density of a boson gas propagating in the radial direction: $u = \sigma\pi\beta T^2$, where $\sigma = \pi/12$ is the Boltzmann constant in two dimensions. In the Vaidya-Anti-de Sitter metric, from the energy-momentum tensor (5.10) it is obtained the following energy density:

$$u = \frac{1}{4\pi r^2}\frac{dM(v)}{dv}\,. \tag{5.55}$$

In figure 5.9 we compare the energy density (5.55) as a function of advanced time with the component of the renormalized energy-momentum obtained in (5.54). For large AdS radius (small cosmological constant) both quantities present the same behavior, whereas for small AdS radius the effect of the additional terms in (5.54) is more evident.

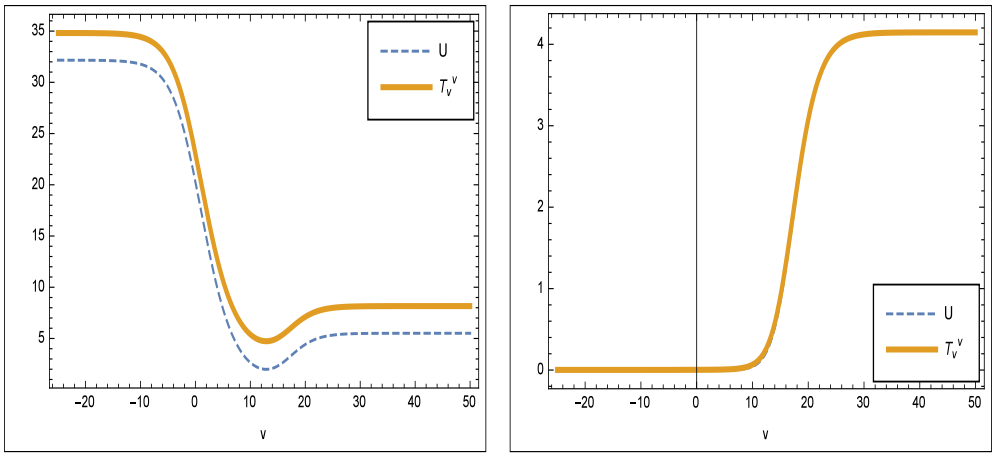

(A) (B)

FIGURE 5.9: Two-dimensional energy density for the Vaidya-Anti-de Sitter (A) $l = 0.1$ and (B) $l = 5$.

5.3.2 Hawking radiation as a trace anomaly

A more recent approach to the description of Hawking's radiation of an evaporating black hole is based in the work of Robinson and Wilczek [66]. In this approach the Hawking radiation is interpreted as a flux that cancels the anomaly appearing in the conservation condition of the energy-momentum tensor when a relativistic field is quantized. Classically, variation of the gravitational action 2.9 under a general coordinate transformation implies conservation of the energy-momentum tensor, as it was developed in section 2.1. In a semiclassical theory when a quantized field is considered the requirement of covariance under general coordinate transformations is transferred to the effective action $W[g_{\mu\nu}]$ [66, 67].

$$iW[g_{\mu\nu}] = \ln\left(\int \mathcal{D}g_{\mu\nu} e^{iS[matter, g_{\mu\nu}]}\right), \tag{5.56}$$

with variation

$$-\delta_\lambda W = \int d^2x\sqrt{-g}\lambda^\nu \nabla_\mu T_\nu{}^\mu . \tag{5.57}$$

General covariance of the quantum theory requires $\delta_\lambda W = 0$. In this variation the energy-momentum tensor is decomposed in the following form

$$T_\nu{}^\mu = T_\nu{}^\mu{}_{(in)}\Theta_- + T_\nu{}^\mu{}_{(out)}\Theta_+ + T_\nu{}^\mu{}_{(\chi)}\, H\,, \tag{5.58}$$

where $\theta_\pm = \theta(\pm r \mp r_H - \epsilon)$ is a step function inside/outside the black hole horizon and $H = 1 - \theta_+ - \theta_-$ is a hat function between $-r_H - \varepsilon$ and $r_H + \varepsilon$. The tensors $T_\nu{}^\mu{}_{(in)}$ and $T_\nu{}^\mu{}_{(out)}$ are conserved inside/outside the horizon respectively. It is in the component $T_\nu{}^\mu{}_{(\chi)}$ where the trace anomaly is manifested [66]

$$\nabla_\mu T_\nu{}^\mu{}_{(\chi)} \equiv A_\nu \equiv \frac{1}{\sqrt{-g}}\partial_\mu N^\mu_\nu, \qquad N^\mu_\nu = \frac{1}{96\pi}\epsilon^{\beta\mu}\partial_\alpha \Gamma^\alpha_{\nu\beta}\,. \tag{5.59}$$

With this decomposition of the energy-momentum tensor equation (5.57) reads

$$\begin{aligned} -\delta_\lambda W = \int d^2x\sqrt{-g}\{\lambda^r\left[\left(T^r_{r(out)} - T^r_{r(\chi)}\right)\partial\theta_+ + \left(T^r_{t(in)} - T^r_{r(\chi)}\right)\partial\theta_-\right] + \\ \lambda^t[\partial_r(N^r_t H) + \left(T^r_{t(out)} - T^r_{t(\chi)} + N^r_t\right)\partial\theta_+ + \left(T^r_{t(in)} - T^r_{t(\chi)} + N^r_t\right)\partial\theta_-]\}\,. \end{aligned} \tag{5.60}$$

Consider initially a stationary spacetime of the form (2.19) with $F(r) = G(r)$. The requirement for general covariance $\delta_\lambda W = 0$ yields

$$T^t_t = -\frac{K+Q}{F(r)} - \frac{B(r)}{F(r)} - \frac{I(r)}{F(r)} + T^\alpha_\alpha(r)\,, \tag{5.61}$$

$$T^r_r = \frac{K+Q}{F(r)} + \frac{B(r)}{F(r)} + \frac{I(r)}{F(r)}\,, \tag{5.62}$$

$$T^r_t = -K + C(r)\,, \tag{5.63}$$

where

$$\begin{aligned} C(r) &= \int_{r_+}^{r} A_t(x)dx\,, \quad B(r) = \int_{r_+}^{r} F(x)A_r(x)dx\,, \\ I(r) &= \frac{1}{2}\int_{r_+}^{r} T^{\alpha}_{\alpha}F'(x)dx\,, \end{aligned} \tag{5.64}$$

and K, Q are integration constants. Taking the limit $\epsilon \to 0$ and using

$$\partial_\mu \Theta_\pm = \delta^r_\mu \left(\pm 1 - \epsilon\partial_r \pm \frac{1}{2}\epsilon^2\partial_r^2 - \dots \right) \delta(r - r_H)\,, \tag{5.65}$$

equation (5.60) takes the form:

$$\begin{aligned} -\delta_\lambda W = \int d^2x\lambda^t [&(K_{out} - K_{in})\delta(r - r_H) \\ &- \epsilon(K_{out} + K_{in} - 2K_\chi - 2N_t^r)\partial\delta(r - r_H) + \dots] \\ &- \int d^2x\lambda^r \left[\left(\frac{K_{out} + Q_{out} + K_{in} + Q_{in} - 2K_\chi - 2Q_\chi}{F} \right) \delta(r - r_H) \right. \\ &\left. -\epsilon \left(\frac{K_{out} + Q_{out} - K_{in} - Q_{in}}{F} \right) \partial\delta(r - r_H) + \dots \right] \end{aligned} \tag{5.66}$$

Conservation of the effective action $W[g_{\mu\nu}]$ is satisfied with the following conditions

$$K_{out} = K_{in} = K_\chi + \Phi\,, \tag{5.67}$$

$$Q_{out} = Q_{in} = Q_\chi + \Phi\,, \tag{5.68}$$

where $\Phi = N_t{}^r|_{r_H}$ is the anomaly flux at the horizon. With this, the energy-momentum tensor becomes

$$T_\mu{}^\nu = T^\nu{}_{\mu(C)} + T^\nu{}_{\mu(\Phi)}\,, \tag{5.69}$$

where $T^\nu{}_{\mu(C)}$ is the component of the energy-momentum tensor that is conserved classically and $T^\nu{}_{\mu(\Phi)}$ is the energy-momentum tensor associated with the flux $\Phi = K = -Q$.

For the Vaidya-Anti-de Sitter metric (5.9) we have for the component $N_v{}^r$:

$$\begin{aligned} N_v{}^r &= \frac{1}{96\pi}\epsilon^{\beta r}\partial_\alpha \Gamma^\alpha{}_{v\beta} \\ &= \frac{1}{96\pi}\epsilon^{vr}\left(\partial_r \Gamma^r{}_{vv} + \partial_v \Gamma^v{}_{vv}\right) \\ &= \frac{1}{96\pi}\left[\left(-\frac{2M}{r^3} + \frac{1}{l^2} \right) \left(1 - \frac{2M}{r} + \frac{r^2}{l^2} \right) + \left(\frac{M}{r^2} + \frac{r}{l^2} \right) \left(\frac{2M}{r^2} + \frac{2r}{l^2} \right) \right]. \end{aligned} \tag{5.70}$$

Terms depending on $\dot{M}$ are canceled. The gravitational anomaly on the trapping horizon is

$$\Phi = N_v^r|_{r_+} = \frac{1}{96\pi}\left[\left(\frac{M(v)}{r_+^2} + \frac{r_+}{l^2} \right) \left(\frac{2M(v)}{r_+^2} + \frac{2r_+}{l^2} \right) \right] = \frac{\pi}{12}T^2\,, \tag{5.71}$$

corresponding to the flux expected from the Hawking radiation in two dimensions, implying that the trace anomaly is in fact canceled by emission of Hawking radiation. A similar result is obtained for stationary and spherically symmetric spacetimes [66, 67]. In reference [67] is concluded that if the anomaly is evaluated at the event horizon and not at the trapping horizon additional correction terms to (5.71) depending on the time variation of the horizon might appear.

5.3.3 Hawking radiation as tunneling

Another approach for the study of the Hawking radiation of a black hole considers the tunneling effect of particles through a black hole horizon [68]. In the Eikonal approximation, solutions of the massless Klein-Gordon equation (2.79) are spherically symmetric solutions of the form

$$\Phi = \Phi_0 e^{(iS)}\,, \tag{5.72}$$

where S is the action of a massless particle associated with the scalar field and Φ_0 is a term that varies slowly while S varies rapidly. Replacing (5.72) into the Klein Gordon equation (2.79) gives the Hamilton- Jacobi equation:

$$g^{ab}\frac{\partial S}{\partial x^a}\frac{\partial S}{\partial x^b} = 0\,, \tag{5.73}$$

which in has a general solution of the form

$$S = \int_\gamma \frac{\partial S}{\partial x^a} dx^a\,, \tag{5.74}$$

where γ is a null curve representing the trajectory of the massless particles. In a semiclassical treatment S is allowed to be complex valued. The tunneling probability is proportional to the amplitude of the field $\Phi^*\Phi$, which, considering the approximation (5.72) becomes

$$\Gamma \sim e^{(-2\mathrm{Im}S)}\,. \tag{5.75}$$

In order to solve (5.74) we consider the propagation of massless scalar particles through the horizon. Particles associated with a massless scalar field propagating in the radial direction obey the radial null geodesic equation, which for the Vaidya-Anti de Sitter spacetime is given by:

$$\frac{dr}{dv} = \frac{1}{2}\left(1 - \frac{2M(v)}{r} + \frac{r^2}{l^2}\right)\,. \tag{5.76}$$

Following the Hamilton-Jacobi formalism, the imaginary part of the action of a particle of frequency ω traveling from r_{in} inside the horizon to r_{out} outside the horizon is given by

$$\mathrm{Im}S = \mathrm{Im}\int_{r_{in}}^{r_{out}} p_r\, dr = \mathrm{Im}\int_{r_{in}}^{r_{out}}\int_0^{p_r} dp_r'\, dr\,. \tag{5.77}$$

Using Hamilton's equation $\dot{r} = dH/dp_r$, with H the Hamiltonian of the tunneled particle, we have

$$\mathrm{Im}S = \mathrm{Im}\int_{r_{in}}^{r_{out}}\int_0^H \frac{2}{dr/dv} dH'_r\, dr\,. \tag{5.78}$$

Now we substitute the radial null geodesic equation (5.76) and perform a change of variables $dH = d(M-\omega) = -d\omega$, since the change on the Hamiltonian H is equal to minus the energy ω of the emitted particle. With this we have

$$\mathrm{Im}S = -\mathrm{Im}\int_0^{\omega} d\omega \int_{r_{in}}^{r_{out}} \frac{4}{\left(1-\frac{2M(v)}{r}+\frac{r^2}{l^2}\right)} dr\,. \tag{5.79}$$

A first approximation considers the near horizon limit of the geodesic equation at equal times [69]. For the geodesic equation (5.76) that approximation is given by

$$\frac{dr}{dv} = \kappa_g(v=cte)(r-r_+)\,. \tag{5.80}$$

and

$$\mathrm{Im}S = -\mathrm{Im}\int_{r_{in}}^{r_{out}} \frac{2\omega}{\kappa_g(v=cte)(r-r_+)} dr\,. \tag{5.81}$$

The complex integral has a pole in $r = r_+$ In order to solve this integral it is used a Feynman prescription and after complex integration we get:

$$\mathrm{Im}S = \frac{4\pi\omega}{\kappa_g} = \frac{2\omega}{T}\,. \tag{5.82}$$

With the tunneling probability defined by (5.75) this gives the thermal Boltzmann factor $\Gamma \sim \exp(-\omega/T)$. This initial approximation ignores both the backreaction of the metric and the time dependency of the temperature. We can take into account the effect of the evaporation on the black hole by subtracting the particle energy ω from the black hole mass. Considering a black hole of initial (Misner-Sharp) mass $M_{ms} = M(v,r)$ and final mass $M_{ms} = M(v,r) - \omega$ where ω is the energy of the tunneled particle we have

$$\mathrm{Im}S = \mathrm{Im}\int_{r-\delta r}^{r+\delta r} \frac{2\omega}{\left(1-\frac{2(M(v,r)-\omega)}{r}\right)} dr\,. \tag{5.83}$$

The complex integral has a pole when r is equal to the trapping horizon $r = 2(M(v,r)-\omega)$. After complex integration we obtain the following result:

$$\mathrm{Im}S = 8\pi\omega\left[M(v,r_+) - \frac{\omega}{2}\right]\,. \tag{5.84}$$

If compared with the entropy variation of the process due to the emission of a particle with energy ω:

$$\Delta S = \pi(r_f^2 - r_i^2) = 4\pi\omega(\omega - 2M)\,, \tag{5.85}$$

where $r_i = r_+(M)$ and $r_f = r_+(M-\omega)$ correspond to the trapping horizon radius before and after the tunneling of a particle of energy ω, we get for the tunneling probability (5.75) the following distribution depending on the entropy change $\Delta S(\omega)$ of the process:

$$\Gamma \sim e^{-2\mathrm{Im}S} = e^{\Delta S(\omega)/2}\,. \tag{5.86}$$

For small ω the probability (5.86) approximates the Boltzmann distribution $\exp(\omega/T)$ [57].

To study the effects of tunneling and backreaction as the black hole radiates mass we use the distribution (5.86) of the Vaidya-AdS metric to obtain the black hole luminosity [70, 17]. The Planck distribution for an idealized blackbody considers radiation at every frequency ω. However, when it comes to black holes, not only do they lose mass as they evaporate but also the temperature changes during the process. In order to account for energy conservation it is imposed that no quanta is emitted with energy ω larger than the initial black hole mass, With this consideration the black hole luminosity will be obtained as:

$$L(M) = \frac{A}{4\pi^2}\int_0^M d\omega \frac{\omega^3}{e^{2\mathrm{Im}S}-1}\,. \tag{5.87}$$

In figure 5.10 we illustrate the difference between the luminosity of a blackbody, proportional to T^d, and the luminosity of a black hole when energy conservation is considered. The graphic refers to the integral in (5.87) with the Boltzmann distribution function

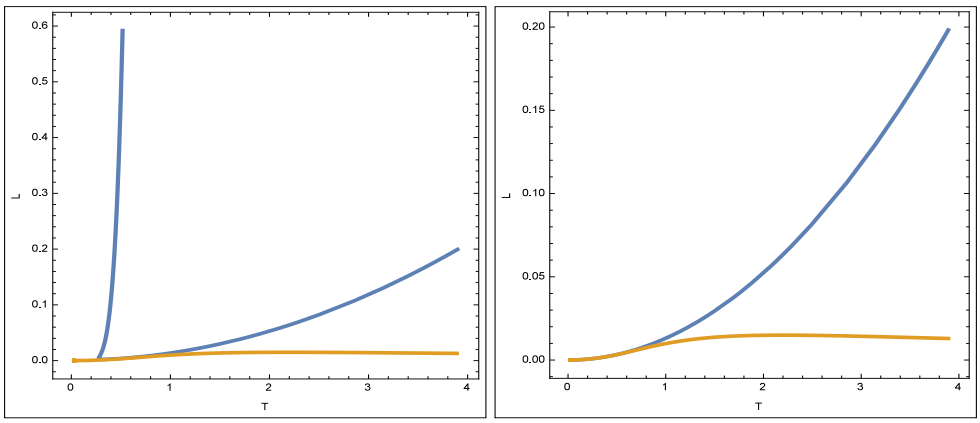

(A) (B)

FIGURE 5.10: Luminosity as a function of temperature. The blue line considers the Boltzmann distribution integrating over all values of frequency ω. In yellow we consider energy conservation and integrate to the value of the initial mass of the black hole. (A) Large black hole with $M_0 = 10$ and $l = 1$. (B) Small black hole with $M_0 = 5$ and $l = 10$.

In order to characterize the time dependency of the black hole luminosity we use the mass function $M(v)$ given in (5.36) with $M_0 > M_f$.

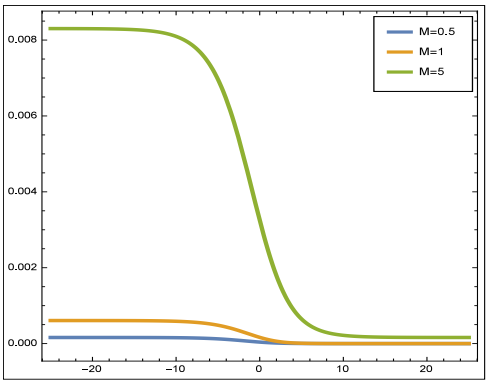

FIGURE 5.11: Black hole luminosity from tunneling process for different masses with $l = 1$.

For large black holes we will assume that the mass shrinks to a value $M_f \approx l$, whereas for small black holes $M_f \to 0$ We proceed to illustrate the difference between the black hole luminosity for the usual Boltzmann distribution and for the tunneling distribution (5.86) in figure 5.11. The tunneling probability accounts for the mass and temperature loss of the black hole during the process.

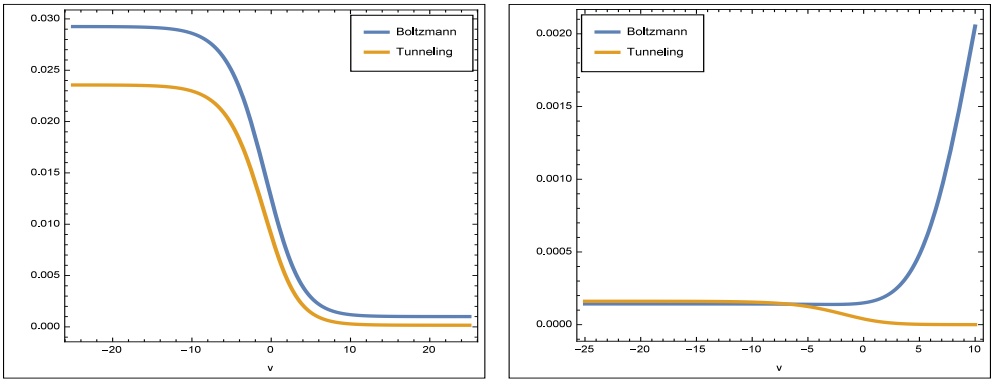

(A) (B)

FIGURE 5.12: Comparison between luminosity for the Boltzmann distribution and the tunneling distribution for (A) Initial mass $M_0 = 10$ (B) $M_0 = 0.55$.

The time-dependent behaviour of the luminosity function will allow us to compare the numerical results obtained for the tunneling process with the behaviour expected of a idealized blackbody satisfying the Stefan-Boltzmann law. In figure 5.12 we study the tunneling process for the Vaidya-Anti de Sitter black hole with mass function $M(v)$ given in (5.36) with $M_f \to 0$ for two different values of initial black hole mass $M_[0$ representing the small and large black hole mass regimes. In the graphic (A) of figure 5.12 we present the numerical results for the tunneling process of a large AdS black hole. In this case the time-dependent behavior approximates in a reasonable fashion the behaviour of the Stefan-Boltzmann law. For large AdS

black holes both temperature and horizon area decrease as the black hole radiates energy. On the contrary, in small Anti-de Sitter black holes the evaporation process the temperature increases as the black hole radiate. In the graphic (B) of figure 5.12 we present the same analysis for the tunneling process of a small AdS black hole. It is obtained that the luminosity from the luminosity process does not increase as the temperature rises. This is a different behavior when compared with the Stefan-Boltzmann law for idealized blackbodies, the luminosity obtained from the tunneling of particles through the horizon of a Vaidya black hole takes into consideration the change of temperature as the black hole radiates.

Chapter 6

Anti-de Sitter Black Holes and Gauge Duals

Following the duality between gravitational and field theories suggested by the AdS/CFT correspondence, we study the thermodynamics of five dimensional Anti-de Sitter black holes and the corresponding dual field theory: the $\mathcal{N} = 4$ supersymmetric Yang-Mills theory. At finite temperature the dual to the $\mathcal{N} = 4$ SYM theory is a black hole in $AdS_5 \times S^5$. From a time dependent black hole we characterize the thermalization process of the field theory.

6.1 Phase Transitions of $\mathcal{N} = 4$ super Yang-Mills theory

A characteristic of $SU(N)$ gauge theories is the confinement/deconfinement phase transition. The most familiar case is the gauge theory $SU(3)$, better known as *quantum chromodynamics* (QCD). In this theory the fundamental degrees of freedom are quarks and gluons. At high energy quarks behave as free particles and become strongly coupled at low energies. Thus $SU(3)$ as a gauge theory is said to be confining at low energy and deconfined at high energy. The $\mathcal{N} = 4$ SYM theory as a conformal theory has no bound states in $\mathbb{R}^3$ and the theory does not have a confining phase. In fact, since in conformal field theories the temperature can always be rescaled, they cannot have phase transitions on $\mathbb{R}^3$, that is, on an infinite volume [71, 72].

Phase transitions on $\mathcal{N} = 4$ super-Yang Mills theory are only possible when the theory is defined on $\mathbb{R} \times S^3$ [71, 72]. Normally, phase transitions on a compact space are not possible since there are only a finite number of degrees of freedom: on a sphere, charged physical states of a gauge theory are not allowed due to the finite spatial volume. This is what is referred to as confinement in $\mathcal{N} = 4$ SYM, in the sense that there are only $\mathcal{O}(1)$ physical states at low energies. The confinement/deconfinement phase transition on $\mathcal{N} = 4$ does not have the same interpretation as it does in QCD. In the confining phase of a $SU(N)$ gauge theory, the physical states are color singlets, and the free energy is of order $\mathcal{O}(1)$. The confinement/deconfinement phase transition is only possible when the large N limit

is taken. In the deconfined phase, the states are gauge bosons (gluons), with free energy of order $\mathcal{O}(N^2)$ [71, 72].

In the context of the AdS/CFT correspondence, the gravitational dual of the confinement/ deconfinement phase transition is the collapse of thermal Anti-de Sitter to a Schwarzchild anti-de Sitter black hole [73]. This thermal phase transition of the gauge theory resembles the Hawking-Page phase transition, therefore the confined phase of the gauge theory is identified with thermal AdS space and the deconfined phase with an AdS black hole.

A criterion to determine whether the dual field theory is in a confining phase or a deconfining phase is based on taking the free energy of the black hole as an order parameter [61]. When the theory is confining, the free energy is expected to have a low temperature phase with a free energy of order $\mathcal{O}(1)$, meaning that the contribution comes from the color singlet hadrons.

$$\frac{F}{N^2} \to 0\,, \quad N \to \infty\,. \tag{6.1}$$

On the other hand, the deconfining phase corresponds to a high temperature phase with a free energy of order $\mathcal{O}(N^2)$, since the contribution corresponds to that of gauge fields, (i.e. gluons).

6.1.1 Free energy of $\mathcal{N} = 4$ SYM theory

In the weak coupling limit of the $\mathcal{N} = 4$ Super Yang Mills theory the free energy can be obtained from perturbative calculations as a series of the t'Hooft coupling λ in the large N limit of the gauge group $SU(N)$. At leading order the free energy corresponds to that of non-interactive massless degrees of freedom and is obtained from one loop Feynman diagrams of each of the fields of the theory, that is, a gauge bosons, a gaugino, three adjoint fermions, and three adjoint scalars, together with the non-physical ghosts degrees of freedom that appear in the quantization of a gauge field. The free energy is obtained from the sum of all such diagrams with final result [74]

$$F_0(T) = -\frac{\pi^2}{6} N^2 T^4\,. \tag{6.2}$$

The following contribution of order $\mathcal{O}(g^2_{YM})$ is obtained from two-loop Feynman diagrams [74, 75]

$$F(T) = -\frac{\pi^2 N^2 T^4}{6}\left[1 - \frac{3}{2\pi^2 L^2 T^2} + \mathcal{O}\left(\frac{1}{L^6 T^6}\right)\right]\,. \tag{6.3}$$

At strong coupling λ a perturbative calculation of the free energy is not possible. Following the AdS/CFT correspondence, the free energy of the $\mathcal{N} = 4$ super Yang-Mills theory at strong coupling is obtained from the gravitational dual. Following references [75, 76] , the leading contribution to the free energy F for an Anti-de

Sitter black hole can be obtained from the (euclidean) gravitational action I times the temperature as $I=\beta F$, with β the inverse of the temperature.

The result obtained has the form

$$F(T)=-\frac{\pi^2N^2T^4}{8}\mathcal{F}\left(\frac{1}{T^2L^2}\right). \tag{6.4}$$

where the function $\mathcal{F}(x)$ is

$$\mathcal{F}(x)=\frac{1}{16}\left[1+\left(1-\frac{2x}{\pi}\right)^{\frac{1}{2}}\right]^2\left\{\left[1+\left(1-\frac{2x}{\pi}\right)^{\frac{1}{2}}\right]^2-\frac{4x}{\pi^2}\right\}, \tag{6.5}$$

with the following expansion in the limit $x\ll 1$:

$$\mathcal{F}(x)=1-3\left(\frac{x}{\pi^2}\right)+\frac{3}{2}\left(\frac{x}{\pi^2}\right)^2+\frac{1}{4}\left(\frac{x}{\pi^2}\right)^4+\dots \tag{6.6}$$

To compare the free energy obtained from the gravitational dual with the perturbative expansion in the weak coupling limit, given by (6.3), equation (6.4) is expanded in the high temperature limit $TL\gg 1$

$$F(T)=-\frac{\pi^2N^2T^4}{8}\left[1-\frac{3}{\pi^2L^2T^2}+\frac{3}{2\pi^4L^4T^4}+\mathcal{O}\left(\frac{1}{L^6T^6}\right)\right], \tag{6.7}$$

with the leading term in the free energy is

$$F_0(T)=-\frac{\pi^2}{8}N^2V_3T^4. \tag{6.8}$$

The leading order contribution to the free energy in the weak coupling limit (6.2) and strong coupling limit (6.8) also hold a proportionality relation by a factor of $3/4$. In general the free energy of the $\mathcal{N}=4$ SYM theory must have a form (at high temperature) [75]:

$$F(T)=-\frac{\pi^2N_c^2T^4}{6}\sum_{n=0}^{\infty}b_n(\lambda)\left(\frac{1}{L^2T^2}\right)^n. \tag{6.9}$$

with $b_n(\lambda)$ an unspecified function of λ.

6.1.2 Gravitational dual to $\mathcal{N} = 4$ SYM theory

In the context of the AdS/CFT correspondence, the $AdS_5 \times S^5$ geometry is referred as the bulk. The 5-dimensional Anti-de Sitter space is a solution of the 5-dimensional Einstein-Hilbert action (obtained from the 10-dimensional type IIB supergravity action compactifyied on S^5):

$$I = -\frac{1}{16\pi G_5}\int d^d x\sqrt{-g}\,(R - 2\Lambda) + \text{boundary terms}\,, \tag{6.10}$$

where G_5 is the 5-dimensional Newton constant, R is the Ricci scalar and $\Lambda = -6/L^2$ is the cosmological constant in five dimension. The Schwarzschild-Anti-de-Sitter solution in five dimensions is

$$ds^2 = -\left(1 - \frac{\mu}{r^2} + \frac{r^2}{L^2}\right)dt^2 + \left(1 - \frac{\mu}{r^2} + \frac{r^2}{L^2}\right)^{-1} dr^2 + r^2 d\Omega_3^2\,. \tag{6.11}$$

The black hole horizon $r = r_+$ satisfies $r_+^4 + r_+^2 L^2 = \mu\, L^2$, with solution

$$r_+^2 = \frac{L^2}{2}\left(-1 + \sqrt{1 + \frac{4\mu}{L^2}}\right)\,. \tag{6.12}$$

The parameter μ in (6.11) is proportional to the ADM mass of the black hole:

$$M = \frac{3Vol(S^3)}{16\pi\, G_5}\mu = \frac{3Vol(S^3)}{16\pi\, G_5} r_+^2\left(1 + \frac{r_+^2}{L^2}\right)\,. \tag{6.13}$$

In the limit $r \to \infty$ the metric (6.11) reduces to the following conformal metric:

$$ds^2 = \frac{r^2}{L^2}\left(-dt^2 + L^2 d\Omega_3^2\right)\,, \tag{6.14}$$

meaning that the dual field theory is defined on S^3 with radius L.

From the expression for the horizon radius (6.12) the thermodynamical quantities of the 5-dimensional Schwarzschild Anti-de Sitter black hole are readily obtainable. The horizon temperature is:

$$T = \frac{2r_+^2 + L^2}{2\pi r_+ L^2}\,, \tag{6.15}$$

with a minimum temperature $T_0 = L/\sqrt{2}$. The black hole entropy and heat capacity are respectively:

$$S = \frac{A}{4G_5} = \frac{\pi^2 r_+^3}{2G_5}\,. \tag{6.16}$$

$$C = \frac{\partial M}{\partial T} = \frac{3Vol(S^3)}{16\pi\, G_5}\left(\frac{4r_+^3}{L^2} + 2r_+\right)\left(\frac{1}{\pi L^2} - \frac{1}{2\pi r_+^2}\right)^{-1}\,. \tag{6.17}$$

The heat capacity is positive for $r_+^2 > L^2/2$, corresponding to the large black hole

regime, and negative for black holes with $r_+^2 < L^2/2$, making them thermodynamically unstable. The free energy of the black hole is defined by $F = M - TS$. From the expressions of temperature (6.15) and entropy (6.16) we get

$$F_{BH} = \frac{\pi r_+^2}{8G_5}\left(1 - \frac{r_+^2}{L^2}\right) . \tag{6.18}$$

The gravitational action is $I = \beta F$, where β is the inverse of the temperature

$$I_{BH} = \frac{\pi^2 r_+^3}{4G_5}\frac{\left(1 - \frac{r_+^2}{L^2}\right)}{\left(1 + \frac{2r_+^2}{L^2}\right)} \tag{6.19}$$

If r_+ is less than $r_+ = L$ the free energy and the gravitational action are positive. The temperature at which the free energy changes from positive to negative corresponds to the temperature of the Hawking-Page transition

$$T_{HP} = \frac{3}{2\pi L} . \tag{6.20}$$

For $r_+ > L$ the preferred state is a large black hole whereas for $r_+ < L$ the preferred state is thermal AdS. The larger radius is therefore always a thermodynamical stable configuration, but need not always be the most favorable.

6.2 Non-equilibrium analysis on $\mathcal{N} = 4$ super Yang-Mills

In the AdS/CFT correspondence, non-equilibrium states of the gauge theory can be described by a time-dependent geometry on the gravity side, specifically, a time-dependent Vaidya metric should describe a thermalization process on the dual field theory [77, 78]. In asymptotically $AdS_5 \times S^5$ the Vaidya AdS line element is:

$$ds^2 = -F(v,r)dv^2 + 2dvdr + r^2 d\Omega^2 + L^2 d\omega^5 \,, \tag{6.21}$$

where

$$F(v,r) = 1 - \frac{2M(v)}{r^2} + \frac{r^2}{L^2} \,. \tag{6.22}$$

In certain occasions it will be useful to express (6.21) in the Poincaré coordinate system introduced in section 3.2:

$$ds^2 = \frac{L^2}{z^2}\left[-(1 - M(v)z^d)dv^2 - 2dzdv + dx^2\right] \,. \tag{6.23}$$

In this coordinate system the conformal boundary corresponds to $z = 0$. The metric (6.23) corresponds to a non-vacuum solution of Einstein's field equations with an energy-momentum tensor $T_{\mu\nu}$ describing a massless null fluid

$$8\pi G_N^{(d+1)} T_{\mu\nu} = \frac{d-1}{4} z^{d-1} \frac{dM(v)}{dv} k_\mu k_\nu \,, \tag{6.24}$$

with $M(v)$ a function of the advanced time v. Since we are interested in comparing the thermodynamical properties of the geometry with the large N limit of a gauge theory, we take the entropy as the main thermodynamical variable and subsequent thermodynamical quantities are to be expressed as functions of the entropy S and gauge color N. According to the AdS/CFT correspondence the Anti-de Sitter L radius and the number of gauge colors are related by

$$L^4 = \frac{\sqrt{2} N \ell_p^4}{\pi^2} \,, \tag{6.25}$$

where ℓ_p is the 10-dimensional Planck-length, related to the 10-dimensional Newton constant by $G_{10} = \ell_p^8$. The compactification into five dimensions relates the gravitational constants by $G_5 = G_{10}/(\pi^3 L^5)$ [79]. With that the black hole mass and temperature are given as a function of S and N:

$$M(S,N) = \frac{3m_p}{4}\left[N^{\frac{5}{12}}\left(\frac{S}{\pi}\right)^{2/3} + N^{\frac{-11}{12}}\left(\frac{S}{\pi}\right)^{4/3}\right] \,. \tag{6.26}$$

$$T(S,N) = \left.\frac{\partial M}{\partial S}\right|_N = \frac{m_p}{2\pi}\left[N^{\frac{5}{12}}\left(\frac{S}{\pi}\right)^{-1/3} + 2N^{\frac{-11}{12}}\left(\frac{S}{\pi}\right)^{1/3}\right] \,. \tag{6.27}$$

with $m_p = \sqrt{\pi}\ell_p^7/(2^{1/8}G_{10})$ the 10-dimensional Planck mass. For our numerical analysis we set $m_p = 1$.

The trapping horizon of (6.21) is given by the condition $F(v, r_h) = 0$. To study the transition from thermal Anti-de Sitter to Anti-de Sitter black hole we use the following mass function

$$M(v) = \lim_{M_0 \to 0} M_0 + \frac{M_f - M_0}{2}\left[1 + \tanh\left(\frac{v}{v_0}\right)\right]. \tag{6.28}$$

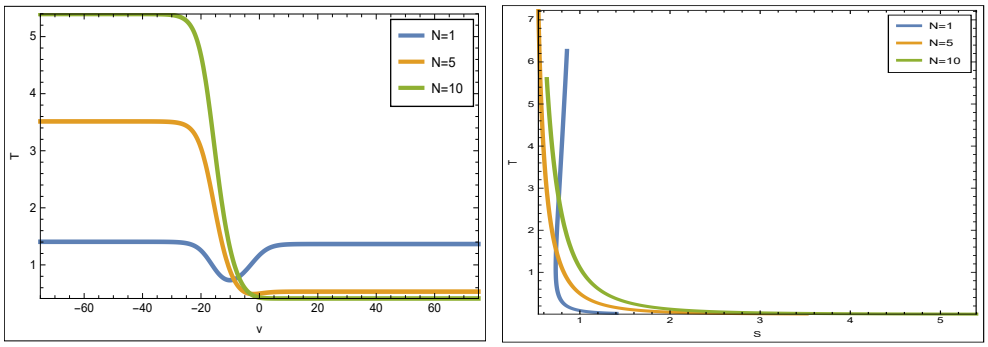

(A) (B)

FIGURE 6.1: (A) Temperature as a function of v ($M_f = 50$). (B) Temperature as a function of S

The heat capacity is obtained from the temperature as a function of entropy (6.27) while keeping N fixed, that is

$$C = T\frac{\partial S}{\partial T}\bigg|_N = \frac{3S(N^{4/3}\pi^{2/3} + 2S^{2/3})}{2S^{2/3} - N^{4/3}\pi^{2/3}}. \tag{6.29}$$

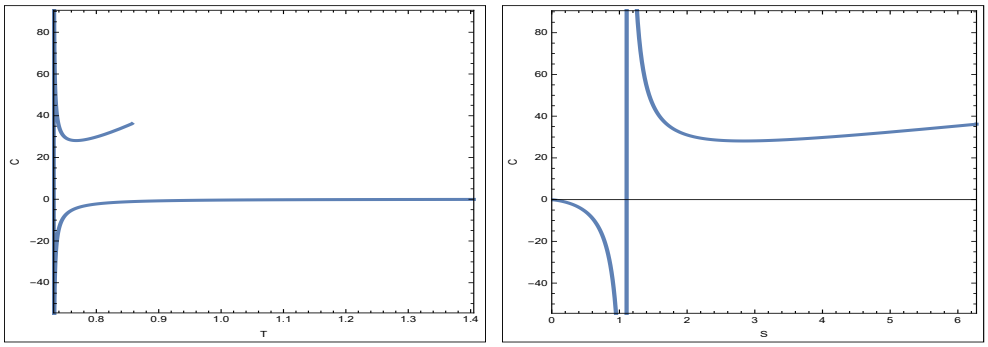

(A) (B)

FIGURE 6.2: (A) Heat capacity as a function of temperature (B) Heat capacity as a function of entropy.

The behavior of the free energy of the Anti-de Sitter black hole and the Hawking page phase transition will correspond to the process of deconfinement in the strong

coupling limit of the gauge theory. The free energy of the Vaidya AdS black hole (6.21) as a function of entropy and number of colors N is:

$$F(S,N) = M - TS = \frac{m_p}{4}\left[N^{\frac{5}{12}}\left(\frac{S}{\pi}\right)^{2/3} - N^{\frac{-11}{12}}\left(\frac{S}{\pi}\right)^{4/3}\right]. \tag{6.30}$$

In figure 6.3 we have the behavior of the free energy corresponding to the mass function $M(v)$ given in (6.28) as function of the time coordinate v for different values of M_f. The free energy becomes negative only when the final mass is large enough that the temperature of the black hole reaches the value corresponding to the Hawking-Page temperature (6.20).

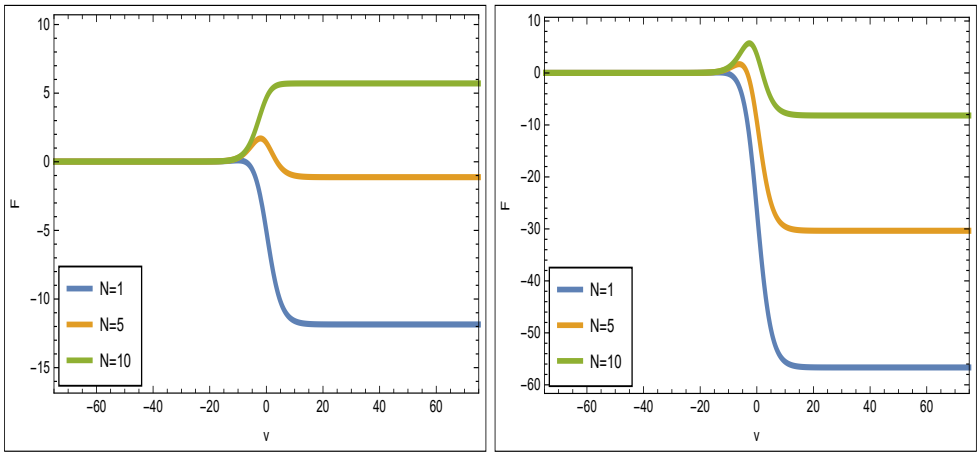

(A) (B)

FIGURE 6.3: Free energy as a function of advanced time for various values of N (A) $M_f = 50$, (B) $M_f = 200$.

In figure 6.4 we have the free energy as a function of temperature and entropy considering different values of N. As a function of temperature there are two branches, one with positive free energy and other with negative free energy, and the derivative of the free energy with respect to temperature presents a discontinuity between the branches of positive and negative free energy, indicating a first order phase transition. Only when the black undergoes the phase transition with a sufficiently large black hole mass M_f the negative values of the free energy are reached.

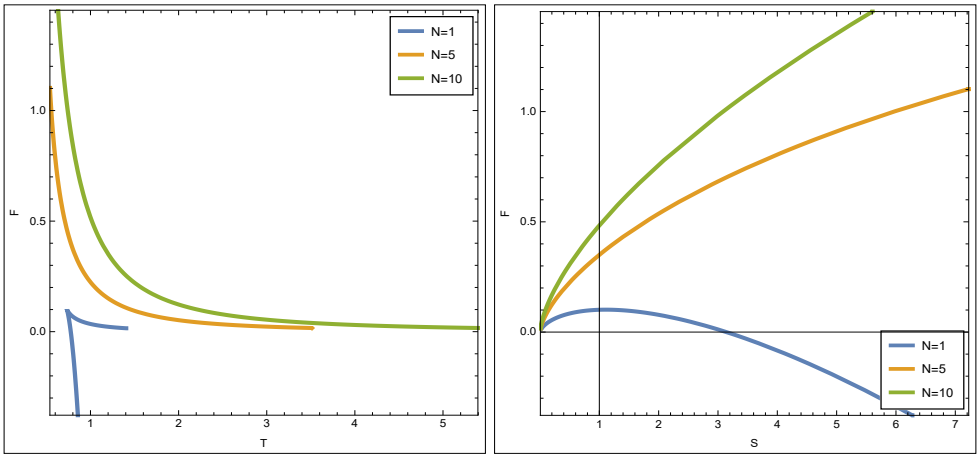

(A) (B)

FIGURE 6.4: (A) Free energy as a function of temperature. (B) Free energy as function of entropy. Final value of mass $M_f = 5$.

The behavior of the free energy when varying N will quantify whether a phase transition occurs in the strongly coupled theory or not at large N^2. In figure 6.5 we display the behavior of the free energy as a function of N for different scenarios of final black hole mass. In the limit $v \to -\infty$, before the transition occurs, the free energy is equal to zero. The final state corresponds to the curve $v \to +\infty$.

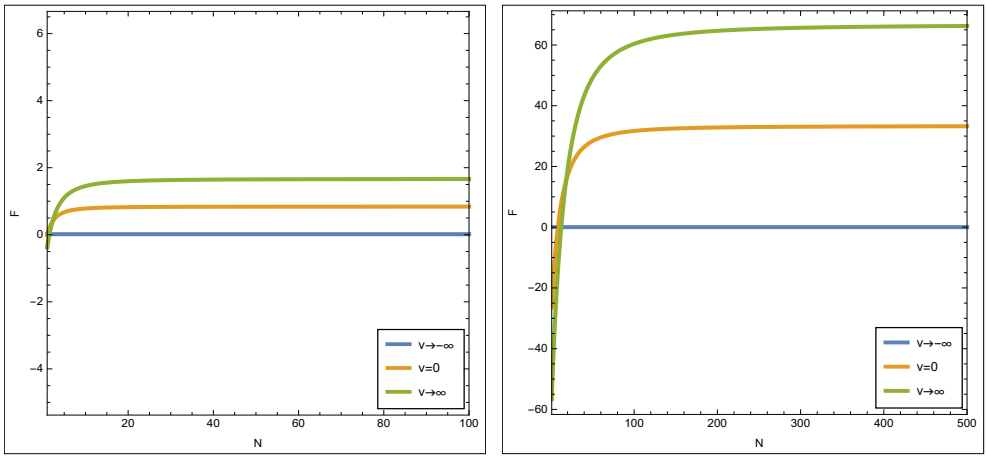

(A) (B)

FIGURE 6.5: Free energy as a function of N for different times. (A) $M_f = 5$ (B) $M_f = 500$.

In figure (6.6) we show how the free energy behaves as a function of M_f for different values of N. Increasing the value of M_f implies that the phase transition will require a greater value of N in order to occur. An important conclusion is that for the free energy to be of order N^2 the final mass value should both of order N^2 and greater than M_{HP}.

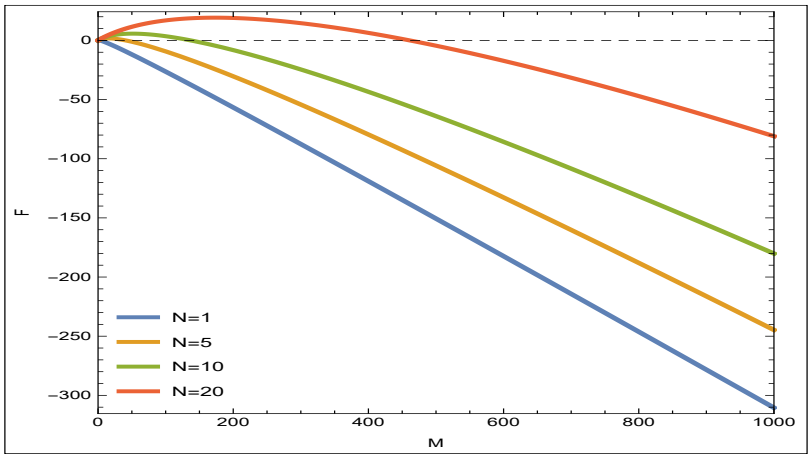

FIGURE 6.6: Free energy as a function of M_f for different values of N.

We proceed to compare the free energy of the Vaidya-Anti-de Sitter black hole for increasing values of N with the weakly coupled limit of a gauge theory, where the free energy is given by (6.2). In the mass function (6.28), the limit $M_0 \to 0$ is taken to replicate a initial state of thermal AdS. A caveat is that there is a time lapse where the heat capacity is negative. As it was mentioned previously, Anti-de Sitter black holes with negative heat capacity are unstable. In the AdS/CFT correspondence such unstable states do not correspond to equilibrium states in the CFT. Instead of the limit $M_0 \to 0$ in (6.28) we consider an initial mass corresponding to the mass value where the heat capacity diverges (6.29) (Any value of mass such that $M_* \leq M(v) < M_{HP}$ should suffice)

$$M_* = \frac{3Vol(S^3)}{16\pi G_5}\frac{3}{4}L^2\,. \tag{6.31}$$

Taking this restriction guarantees that (i) the heat capacity is always positive, (ii) the temperature is monotonically increasing and (iii) the black hole undergoes the Hawking-Page phase transition. In figure 6.7 we compare the free energy of the Vaidya metric obtained from equation (6.30) with the corresponding result obtained for the strong coupling limit in (6.4). Numerically, the results seem to agree better if the mass is taken large but of the same order as N

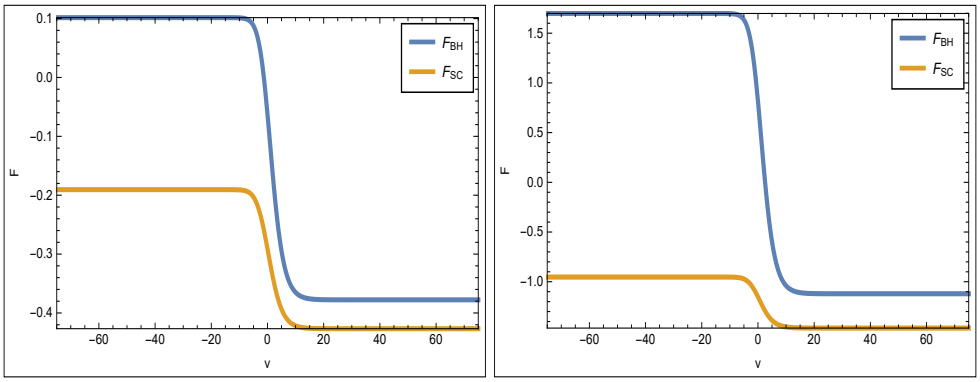

(A) (B)

FIGURE 6.7: Comparison of the free energy of the Vaidya Anti-de Sitter metric (F_{BH}) and the strong coupling limit of the $\mathcal{N} = 4$ SYM denoted by (F_{SC}). (A) $M_f = 5$ and $N = 1$ (B) $M_f = 50$ and $N = 5$.

Finally, we compare the free energy results with the free energy of weak coupling limit at the leading and first orders, given in (6.2) and (6.3) respectively. We obtain confirmation that the free energy of the black hole is proportional to the free energy of the weak coupling limit by a factor of $4/3$.

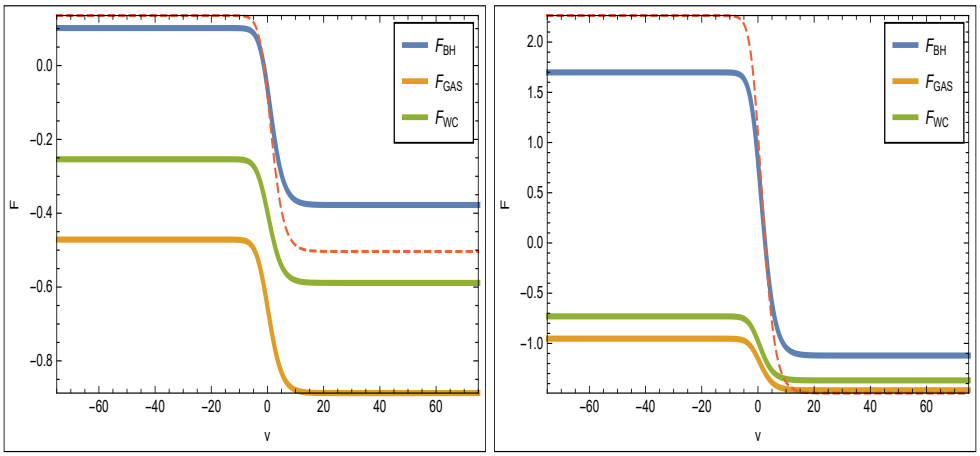

(A) (B)

FIGURE 6.8: Comparison of the free energy of the Vaidya Anti-de Sitter metric (F_{BH}), the free energy of free massless particles (F_{GAS}) and the weak coupling limit of the $\mathcal{N} = 4$ SYM denoted by (F_{WC}). (A) $M_f = 5$ and $N = 1$ (B) $M_f = 50$ and $N = 5$. The dashed line corresponds to multiply F_{BH} by a factor of $4/3$.

6.3 Boundary energy-momentum tensor

The AdS/CFT correspondence is usually used to study a strongly coupled gauge theory by identifying the gravitational dual and relate the physical observables associated with the field theory, for example correlation functions, with the proper geometric equivalent. The converse to this procedure would be, given an arbitrary asymptotically Anti-de Sitter geometry, what can be said about a field theory on the boundary. The answer to this question is a procedure known as holographic renormalization, and allows to obtain the energy-momentum tensor on the conformal boundary from the metric of the gravitational.

Following the AdS/CFT the boundary energy-momentum tensor of asymptotically Anti-de Sitter geometry is dual to vacuum expectation value of the energy-momentum tensor of the CFT. Any asymptotically Anti-de Sitter spacetime can be expressed in the so-called Fefferman-Graham coordinates (z, x) as

$$ds^2 = \frac{L^2}{z^2}\left[g_{\mu\nu}(z,x)dx^\mu dx^\nu + dz^2\right] , \tag{6.32}$$

Near the boundary $z = 0$ the induced metric $g_{\mu\nu}(z, x)$ can be expanded in the following form:

$$g_{\mu\nu}(z,x) = g_{\mu\nu}(x) + z^2\, g^{(2)}_{\mu\nu}(x) + z^d g^{(d)}_{\mu\nu}(x)\,. \tag{6.33}$$

where $g_{\mu\nu}(x) = g_{\mu\nu}(0, x)$ is the metric on the boundary Then the expected value of the energy-momentum tensor is:

$$\langle T_{\mu\nu}\rangle = \frac{d\, L^{d-1}}{16\pi G_N^{(d+1)}}\left[g^d_{\mu\nu}(x) + X^{(d)}_{\mu\nu}(x)\right] , \tag{6.34}$$

where $X^{(d)}_{\mu\nu}(x)$ is equal to zero for d odd and for d even is given by

$$X^{(2)}_{\mu\nu}(x)) = -g_{\mu\nu}g^{(2)\alpha}_{\alpha}\,, \tag{6.35}$$

$$X^{(4)}_{\mu\nu}(x)) = -\frac{1}{8}\mu\nu\left[(g^{(2)\alpha}_{\alpha})^2 - g^{(2)\beta}_{\alpha}g^{(2)\alpha}_{\beta}\right] - \frac{1}{2}g^{(2)\alpha}_{\mu}g^{(2)}_{\alpha\nu} + \frac{1}{4}g^{(2)}_{\mu\nu}g^{(2)\alpha}_{\alpha}\,, \tag{6.36}$$

To obtain the corresponding metric for the Schwarzschild-Anti-de Sitter black hole in the Fefferman-Graham coordinates we follow the procedure outlined in [80, 81]. Even if the black hole is non-stationary it is possible to consider a static boundary. Introduce coordinate [80]:

$$\frac{dz}{z} = -\frac{2}{L}\frac{dr}{\sqrt{F(r)}}\,, \tag{6.37}$$

where $F(r)$ is the function characterizing he Schwarzschild-AdS black hole in static coordinates.

$$F(r) = 1 - \frac{\mu}{r^2} + \frac{r^2}{L^2}\,. \tag{6.38}$$

Integration of equation (6.37) gives

$$z^4 = \frac{16}{4+\mu}\frac{r^2+\frac{1}{2}-r\sqrt{f(r)}}{r^2+\frac{1}{2}+r\sqrt{f(r)}}\,, \tag{6.39}$$

which can be inverted to yield r as a function of z:

$$r^2 = \frac{1-\frac{1}{2}z^2+\gamma z^4}{z^2}\,, \quad \gamma = \frac{1+4\mu}{16}\,. \tag{6.40}$$

With this coordinate transformation the metric for the Schwarzchild- AdS metric is put into the form (6.32) with

$$ds^2 = \frac{L^2}{z^2}\left[dz^2 - \frac{(1-\gamma z^4)^2}{1-\frac{1}{2}z^2+\gamma z^4}dt^2 + (1-\frac{1}{2}z^2+\gamma z^4)d\Omega_3^2\right]\,. \tag{6.41}$$

Having the metric expressed in Fefferman-Graham coordinates allows to obtain the obtain the expected value of the energy-momentum tensor from equation (6.34), giving the following components:

$$\langle T_{tt}\rangle = \frac{3\gamma}{4\pi G_5}\,, \quad \langle T_{ii}\rangle = 3\langle T_{tt}\rangle\,. \tag{6.42}$$

Corresponding to a fluid of density $\rho = \langle T_{tt}\rangle$. In the weakly coupled limit of the gauge theory the relation between the components of the energy - momentum tensor and temperature must have the form:

$$T_{\mu\nu}^{(eq)} = \frac{\pi^2 N^2 T^4}{8} diag(3,1,1,1)\,. \tag{6.43}$$

In figure 6.9 we compare the component $\langle T_{tt}\rangle$ of the energy-momentum tensor (6.42) with the energy density from the weak coupling limit of the gauge theory:

$$U_{WC} = \frac{\pi^2\, N^2 T^4}{8}\,. \tag{6.44}$$

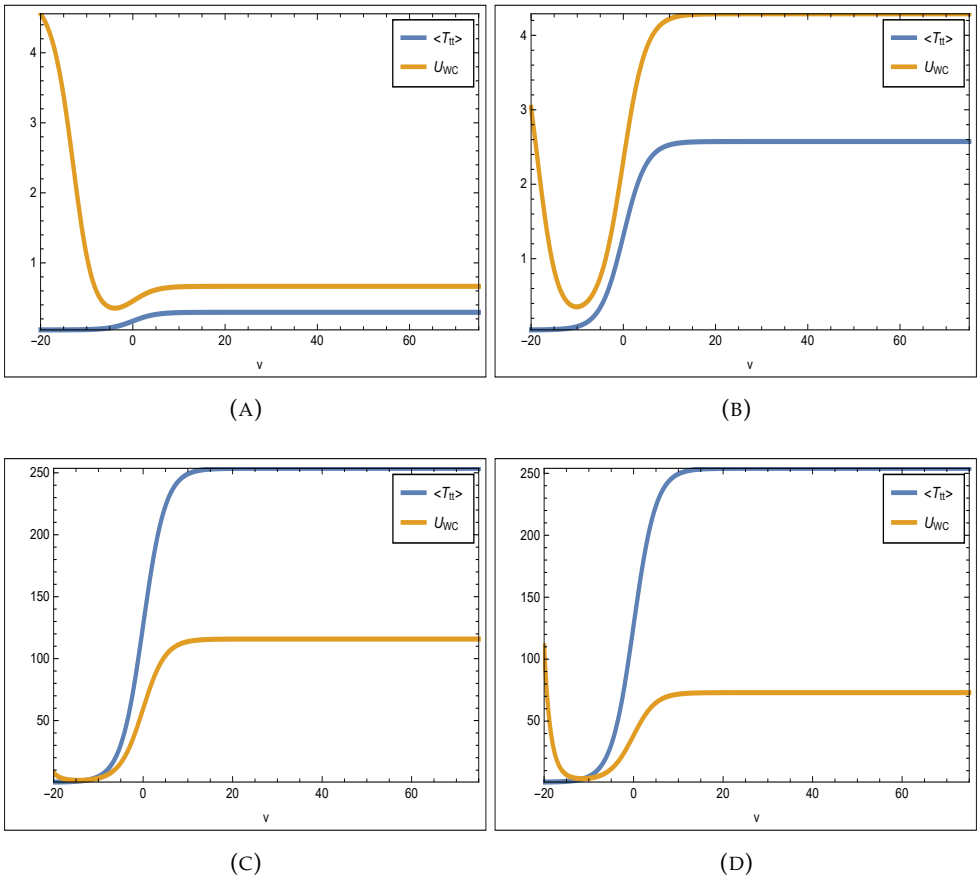

FIGURE 6.9: Energy densities obtained from the boundary energy-momentum tensor and leading order of free energy of the Yang-Mills theory. (A) $M_f = 5$ and $N = 1$. (B) $M_f = 200$ and $N = 1$. (C) $M_f = 5000$ and $N = 5$. (D) $M_f = 5000$ and $N = 10$.

The discrepancy at early times in the first example corresponds to the fact that since small Anti-de Sitter black holes are thermodynamically unstable they do not correspond to equilibrium states in the boundary CFT. For latter times after the black hole is sufficiently large the functions share a similar behavior. Regarding the numerical evaluation, for increasing values of N it is necessary to increase in a large proportion the value of the final mass in order to compare both functions, implying that such comparison is only possible for large black holes with high temperature.

Chapter 7

Final Remarks

One of the main motivations behind this thesis has been the study of aspects of the AdS/CFT correspondence and gauge/gravity dualities focusing on the gravitational side. For Anti-de Sitter black holes the main interest has been the description of the processes of black hole radiation and phase transitions from the time evolution of the relevant thermodynamical quantities. For that purpose we have implemented a generalization of black hole thermodynamics introduced by Hayward as an extension of black hole to non-stationary and non-asymptotically flat spacetimes. In this formalism the thermodynamical quantities are associated to a trapping horizon and not to an event horizon.

The second line of work has been the investigation on the perturbative dynamics of spacetimes where the dynamics can be approximated by potentials of the Pöschl-Teller kind, where we have obtained that it is possible to associate an underlying symmetry to the field equations of motion. The Pöschl-Teller-type potentials considered were shown to be associated to a representation of the algebra $\mathfrak{sl}(2)$, allowing us to to obtain quasinormal modes and frequencies, which are inherent elements of the perturbative dynamics, by algebraic methods. Also we have discussed their role in the associated Cauchy initial value problem.

In order to provide a specific model for the dynamical processes of Anti-de Sitter black holes we have employed a Vaidya-AdS geometry. The Vaidya geometries are null dust solution of general relativity associated to massless radiation and the black hole solution is characterized by a time dependent mass, providing a useful setting to characterize the thermodynamics involved in the process of black hole radiation and transitions between different states. Whether the mass function is able to replicate the phase transition of a black hole depends significantly on the range of the mass function with respect to the value of the Anti-de Sitter radius and the rate of change of the function.

A more involved description of black hole radiation is given by semiclassical arguments, considering the Hawking radiation of a black hole as an atmosphere associated to a quantum field evolving in a fixed background. One of the main results of this thesis concerns the semiclassical description of black hole radiation by tunneling methods, where the black hole radiation is explained as quanta of massless

particles tunneling through the horizon. The probability of emission is found to be dependent on the entropy change before and after emission of a particle, and corrections are found compared with the Stefan-Boltzmann law describing blackbody radiation. The study of the tunneling process on a time-dependent background geometry has provided us with additional insight on the behaviour of the black hole during the evaporation process. We have found differences in the evolution of the tunneling process between AdS black holes of small and large mass, and an initial conclusion is that only the latter case seems to approximate the Stefan-Boltzmann law.

In the context of the AdS/CFT correspondence, we have studied the thermodynamical properties of the Schwarzschild Anti-de Sitter geometry in five dimensions in order to compare with the thermodynamical behaviour of the the corresponding gauge dual, the $\mathcal{N} = 4$ super Yang-Mills theory. The confinement/deconfinement phase transition of the gauge theory is related to the Hawking-Page phase transition of the black hole. The free energy of the Anti-de Sitter black hole is taken as an order parameter to characterize the phase transition. We have used a time-dependent Vaidya Anti-de Sitter black hole as a dual to non-equilibrium configuration of a strongly coupled field theory in order to evaluate the time evolution of the phase transition in the gauge theory. A significant space of parameters was explored and one of the main conclusions obtained was that with an increasing number of gauge color N it is necessary to set up a larger black hole mass in the final state in order to perceive a phase transition. Finally, from the Anti-de Sitter geometry it is obtained the boundary energy-momentum tensor by methods of holographic renormalization and the results are compared with the weak coupling limit of the dual gauge theory.

Appendix A

Useful coordinate systems

In this appendix we will elaborate on some coordinate systems that are commonly used in the description of the different spherically symmetric geometries that are used in this work. The causal structure of a spacetime is dictated by the behavior of light cones, which can be obtained from the set of radial null curves, that is, curves for which $ds^2 = 0$ and θ, ϕ are constant. For metrics of the form

$$ds^2 = -F(r)dt^2 + \frac{1}{G(r)}dr^2 + r^2 d\Omega^2 \,, \tag{A.1}$$

those curves are given by the condition

$$\frac{dt}{dr} = \pm \frac{1}{\sqrt{F(r)G(r)}} \,, \tag{A.2}$$

which is equivalent to the geodesics of massless particles

$$\frac{dt}{d\tau} = \frac{1}{\sqrt{F(r)G(r)}} \quad \text{and} \quad \frac{dr}{d\tau} = \pm 1 \,. \tag{A.3}$$

In Minkowski spacetime $dt/dr = \pm 1$, that is, light cones form a angle of 45 degrees at every point. However, equation (A.2) indicates that if the metric coefficients depend on r the light cones slope will be different at each point of spacetime. Motivated from this observation, it is convenient to define a new coordinate x, called tortoise coordinate, by

$$\frac{dx}{dr} = \frac{1}{\sqrt{F(r)G(r)}} \,, \tag{A.4}$$

such that the temporal coordinate t and the new tortoise coordinate are related in the form

$$dt = \pm dx + \text{ constant } \,, \tag{A.5}$$

implying that for radial null curves $dt = \pm dx$. In the coordinate system (t, x, θ, ϕ) the metric (A.1) becomes

$$ds^2 = \mathcal{F}(x)\left(-dt^2 + dx^2\right) + r^2(x)d\Omega^2 \,, \tag{A.6}$$

where $\mathcal{F}(x) = A(r(x))$. In this particular coordinate system (t, x, θ, ϕ) the metric is characterized by the functions $\mathcal{F}(x)$ and $r(x)$.

Another important coordinate systems are based on the advanced time u and retarded time v, defined as

$$du = dt - dx\,, \tag{A.7}$$

$$dv = dt + dx\,. \tag{A.8}$$

Null geodesics with u constant satisfy $dt = dx$ whereas null geodesics with v constant satisfy $dt = -dx$. The coordinate systems (u, r, θ, ϕ) and (v, r, θ, ϕ) are called *ingoing* and *outgoing Eddington-Finkelstein coordinates* respectively [82]. In the coordinate system (v, r, θ, ϕ), the metric (2.19) adopts the following form

$$ds^2 = -F(r)dv^2 + \sqrt{\frac{F(r)}{G(r)}}(dvdr + drdv)r^2 d\Omega^2\,, \tag{A.9}$$

while in the coordinate system (u, r, θ, ϕ) a similar expression is obtained

$$ds^2 = -F(r)du^2 - \sqrt{\frac{F(r)}{G(r)}}(dudr + drdu) + r^2 d\Omega^2\,, \tag{A.10}$$

It is possible to define another coordinate system using both the retarded and advanced times u, v. From the form of the metric tensor in the coordinates (t, x, θ, ϕ) given by (A.6) and the replacements

$$dt = \frac{1}{2}(du + dv), \quad dx = \frac{1}{2}(dv - du)\,. \tag{A.11}$$

we get the following expression for the metric

$$ds^2 = -\mathcal{F}(x(u, v))dudv + r^2(x(u, v))d\Omega^2\,, \tag{A.12}$$

with the particularity that there are no quadratic terms in du or dv. The coordinates (u, v) are well suited to describe radial null geodesics, since the condition $ds^2 = 0$ implies that massless particles propagate at either u constant or v constant, which are null curves.

Appendix B

Blackbody radiation

Starting from the concept of a black hole as a compact spacetime region able to absorb all forms of infalling matter, a black hole can be modelled of as a blackbody. A blackbody is an idealized physical body that absorbs all incident electromagnetic radiation, independent of frequency or angle of incidence. A blackbody in thermal equilibrium emits electromagnetic radiation with a spectrum determined only by its temperature.

A blackbody will spontaneously emit thermal radiation at a frequency ω with a probability determined by Boltzmann's distribution:

$$\rho(\omega) = \mathrm{e}^{\hbar\omega/k_B T}\,, \tag{B.1}$$

where k_B is the Boltzmann constant and T is the temperature of the blackbody. The probability of emission of a photon with energy $E_n = n\hbar\omega$ is then

$$p(n) = \frac{\mathrm{e}^{-E_n/kT}}{\sum_{n=0}^{\infty} \mathrm{e}^{-E_n/(kT)}}\,. \tag{B.2}$$

The average energy of a photon with frequency ω is

$$\bar{E}(\omega) = \sum_{n=0}^{\infty} E_n p(n) = \frac{\sum_{n=0}^{\infty} n\hbar\omega e^{-n\hbar\omega/kT}}{\sum_{n=0}^{\infty} \mathrm{e}^{-n\hbar\omega/(kT)}}\,. \tag{B.3}$$

The result of this sum is:

$$\bar{E}(\omega) = \frac{\hbar\omega}{e^{\hbar\omega/(kT)} - 1}\,. \tag{B.4}$$

The number of modes in the frequency interval ω to $\omega + d\omega$ is:

$$dN = \frac{8\pi\omega^2}{c^3} d\omega\,, \tag{B.5}$$

and with that, the energy density of radiation per unit of frequency is

$$u(\omega)d\omega = \frac{8\pi\omega^2}{c^3}\bar{E}d\omega\,. \tag{B.6}$$

This results in the Planck's distribution function:

$$I(\omega, T) = \frac{\hbar\omega^3}{4\pi^3 c^2} \frac{1}{e^{\hbar\omega/(kT)} - 1} \,. \tag{B.7}$$

The quantity $I(\omega, T)\, A\, d\omega\, d\Omega$ is the power radiated by a surface of area A through a solid angle $d\Omega$ in the frequency range between ω and $\omega + d\omega$. The total energy radiated per unit area is obtained by integrating over angular frequency for all values of frequency and over solid angle for the half-sphere due to blackbodies obeying Lambert's cosine law

$$\frac{P}{A} = \int_0^\infty d\omega \int d\Omega \cos\theta\, I(\omega, T) = \frac{\hbar}{4\pi^2 c^2} \int_0^\infty \frac{\omega^3}{e^{\frac{\hbar\omega}{kT}} - 1}\, d\omega \,. \tag{B.8}$$

The integral is solved by a change of variables $x = \hbar\omega/(kT)$:

$$\frac{P}{A} = \frac{\hbar}{4\pi^2 c^2} \left(\frac{kT}{\hbar}\right)^4 \int_0^\infty \frac{x^3}{e^x - 1}\, du. \tag{B.9}$$

The value of the integral is given by the Riemann zeta function $\zeta(4) = \pi^4/15$. With this the total power emitted per unit area by a perfect blackbody surface is

$$\frac{P}{A} = \sigma T^4 \,, \qquad \sigma = \frac{\pi^2 k^4}{60\hbar^3 c^2} \,. \tag{B.10}$$

This is the Stefan-Boltzmann law for the luminosity of a blackbody.

The total energy density U can be similarly calculated from the Planck distribution (B.7) by integrating the solid angle over the whole sphere. The resulting energy flux is divided by c to give the energy density U:

$$U = \frac{1}{c} \int_0^\infty d\omega \int d\Omega I(\omega, T) \,. \tag{B.11}$$

Integration over the whole sphere gives an extra factor of 4:

$$U = \frac{4}{c}\, \sigma\, T^4 \,. \tag{B.12}$$

Both luminosity and energy density are proportional to T^4.

Appendix C

Phase transitions in gauge theories

In a physical system that admits different equilibrium states, a phase transition is essentialy a change between two states of a physical system in order to minimize the action. The AdS/CFT correspondence establishes a relation between the action/partition function of the CFT and the gravity theory [36]:

$$Z_{CFT}(\mathcal{C}) = Z_{gravity}(\mathcal{M})\,, \tag{C.1}$$

where $\mathcal{C} = \partial\mathcal{M}$ is the boundary of the manifold $\mathcal{M}$ that is a solution of the gravitational action. Considering a saddle-point approximation this relation between partition functions becomes

$$Z_{CFT}(\mathcal{C}) = e^{\mathcal{I}_{gravity}(\mathcal{M})}\,, \tag{C.2}$$

where $\mathcal{I}_{gravity}(\mathcal{M})$ is the gravitational functional action of the manifold $\mathcal{M}$. In the large N limit $\mathcal{I}_{gravity}(M) = N^2 F(\mathcal{M})$, where $F(\mathcal{M})$ is a non-specified action defined on $\mathcal{M}$ [36]. Then the partition function of the CFT will be given by a sum over all geometries $\mathcal{M}_i$ with the same boundary $\mathcal{C}$

$$Z_{CFT}(\partial\mathcal{M}) = \sum_i \exp\left[N^2 F(\mathcal{M}_i)\right]\,. \tag{C.3}$$

In the large N limit the partition function will be dominated by the geometry with the smallest $F(\mathcal{M}_i)$.

The phase transition of gauge theories can be observed from the behavior of the Wilson-Polyakov loop [73]. For a gauge field A_μ this operator is defined as [83]:

$$W_C = \mathrm{Tr}\left(\mathcal{P} e^{i\int_C A_\mu dx^\mu}\right)\,. \tag{C.4}$$

where $\mathcal{P}$ is the path ordering operator, C denotes a closed curve in spacetime and the trace is taken over the fundamental representation of the gauge group. Any combination of Polyakov loops with non-vanishing center-charge must have vanishing expectation value. The vanishing of the expected value of the Polyakov loop indicates confinement, a non-vanishing Polyakov loop represents deconfinement [84, 83]. The

expected value of the Wilson-Polyakov loop is related to the free energy F by [85]

$$e^{-\beta F} = \langle \mathrm{Tr}\left(\mathcal{P} e^{i\int_C A_\mu dx^\mu}\right)\rangle\,. \tag{C.5}$$

In the AdS/CFT correspondence the expected value of a Wilson loop is related to the partition function of a string world sheet Σ in the bulk ending on a loop C on the boundary [86]:

$$\langle W_C\rangle = \int \mathcal{D}\Sigma e^{-\mathcal{A}(\Sigma)}\,. \tag{C.6}$$

The functional integration is carried over all inequivalent worldsheets Σ with boundary C. In the strongly coupled limit it is considered a saddle-point approximation, where the partition function is dominated by the string world sheet Σ_0 minimizing the area surface $\mathcal{A}$ and whose whose endpoint constitute the Wilson loop C on the AdS boundary

$$\langle W_C\rangle = e^{-\mathcal{A}(\Sigma_0)}\,. \tag{C.7}$$

According to the AdS/CFT duality, the expectation value of the Wilson loop of the boundary field theory, in the saddle approximation, is dual to the area of a two-dimensional extremal surface in the bulk that is attached to the conformal boundary by the loop.

Bibliography

[1] James M Bardeen, Brandon Carter, and Stephen W Hawking. The four laws of black hole mechanics. *Communications in Mathematical Physics*, 31(2):161–170, 1973.

[2] Jacob D Bekenstein. Black holes and entropy. *Physical Review D*, 7(8):2333, 1973.

[3] Stephen W Hawking. Particle creation by black holes. *Communications in mathematical physics*, 43(3):199–220, 1975.

[4] Steven Frautschi. Entropy in an expanding universe. *Science*, 217(4560):593–599, 1982.

[5] Don N Page. Particle emission rates from a black hole: Massless particles from an uncharged, nonrotating hole. *Physical Review D*, 13(2):198, 1976.

[6] Gary T Horowitz and Joseph Polchinski. Gauge/gravity duality. *Approaches to Quantum Gravity, Editor D. Oriti, Cambridge University Press, Cambridge*, pages 169–186, 2009.

[7] Joseph Polchinski. Introduction to gauge/gravity duality. 2010.

[8] Juan Maldacena. The large-N limit of superconformal field theories and supergravity. *International journal of theoretical physics*, 38(4):1113–1133, 1999.

[9] Stephen W Hawking and Don N Page. Thermodynamics of black holes in Anti-de Sitter space. *Communications in Mathematical Physics*, 87(4):577–588, 1983.

[10] Sean A Hayward. General laws of black hole dynamics. *Phys.Rev.*, D49:6467–6474, 1994.

[11] Sean A Hayward. Gravitational energy in spherical symmetry. *Phys. Rev. D*, 53:1938–1949, 1996.

[12] Sean A Hayward. Unified first law of black-hole dynamics and relativistic thermodynamics. *Classical and Quantum Gravity*, 15(10):3147, 1998.

[13] Charles W Misner and David H Sharp. Relativistic equations for adiabatic, spherically symmetric gravitational collapse. *Physical Review*, 136(2B):B571, 1964.

[14] Walter C Hernandez Jr and Charles W Misner. Observer time as a coordinate in relativistic spherical hydrodynamics. *The Astrophysical Journal*, 143:452, 1966.

[15] PC Vaidya. Nonstatic solutions of Einstein's field equations for spheres of fluids radiating energy. *Physical Review*, 83(1):10, 1951.

[16] Prahalad Chunnilal Vaidya. The gravitational field of a radiating star. *Proceedings Mathematical Sciences*, 33(5):264–276, 1951.

[17] Alessandro Fabbri and Jose Navarro-Salas. *Modeling black hole evaporation*. World Scientific, 2005.

[18] Sean A Hayward. Gravitational energy as Noether charge. *arXiv preprint gr-qc/0004042*, 2000.

[19] James B Hartle. *Gravity: an introduction to Einstein's general relativity*, volume 1. 2003.

[20] Sean Carroll. *Spacetime and Geometry: An Introduction to General Relativity*. Benjamin Cummings, 2003.

[21] Bernard Schutz. *A first course in general relativity*. Cambridge university press, 2009.

[22] Hans C Ohanian and Remo Ruffini. *Gravitation and spacetime*. Cambridge University Press, 2013.

[23] Robert M Wald. *General relativity*. University of Chicago press, 2010.

[24] Stephen W Hawking. *The large scale structure of space-time*, volume 1. Cambridge university press, 1973.

[25] Karl Schwarzschild. Über das gravitationsfeld eines massenpunktes nach der Einsteinschen theorie. *Sitzungsberichte der Königlich Preußischen Akademie der Wissenschaften (Berlin), 1916, Seite 189-196*, 1:189–196, 1916.

[26] Valerio Faraoni. Cosmological apparent and trapping horizons. *Physical Review D*, 84(2):024003, 2011.

[27] Hideo Kodama. Conserved energy flux for the spherically symmetric system and the backreaction problem in the black hole evaporation. *Progress of Theoretical Physics*, 63(4):1217–1228, 1980.

[28] Valerio Faraoni. Cosmological and black hole apparent horizons. *Lecture Notes in Physics (Springer International Publishing, 2015)*, 2015.

[29] Carsten Gundlach, Richard H Price, and Jorge Pullin. Late-time behavior of stellar collapse and explosions. I. Linearized perturbations. *Physical Review D*, 49(2):883, 1994.

[30] Jun John Sakurai. *Advanced quantum mechanics*. Addison Wesley, 1967.

[31] Kostas D Kokkotas and Bernd G Schmidt. Quasi-normal modes of stars and black holes. *Living Rev. Rel*, 2(2):262, 1999.

[32] Hans-Peter Nollert. TOPICAL REVIEW: Quasinormal modes: the characteristic 'sound' of black holes and neutron stars. *Class.Quant.Grav.*, 16:R159–R216, 1999.

[33] E.S.C. Ching, P.T. Leung, W.M. Suen, and K. Young. Quasinormal mode expansion for linearized waves in gravitational system. *Phys.Rev.Lett.*, 74:4588–4591, 1995.

[34] Willem De Sitter. On the curvature of space. In *Proc. Kon. Ned. Akad. Wet*, volume 20, pages 229–243, 1917.

[35] Akihiro Ishibashi and Robert M Wald. Dynamics in non-globally-hyperbolic static spacetimes: III. Anti-de Sitter spacetime. *Classical and Quantum Gravity*, 21(12):2981, 2004.

[36] Makoto Natsuume. *AdS/CFT duality user guide*, volume 903. Springer, 2015.

[37] David S Berman and Maulik K Parikh. Holography and rotating AdS black holes. *Physics Letters B*, 463(2-4):168–173, 1999.

[38] AF Cardona and C Molina. Quasinormal modes of generalized pöschl–teller potentials. *Classical and Quantum Gravity*, 34(24):245002, 2017.

[39] C. Molina. Quasinormal modes of d-dimensional spherical black holes with near extreme cosmological constant. *Phys. Rev.*, D68:064007, 2003.

[40] Vitor Cardoso and Jose P.S. Lemos. Quasinormal modes of the near extremal Schwarzschild-de Sitter black hole. *Phys. Rev.*, D67:084020, 2003.

[41] C. Molina and J.C.S. Neves. Wormholes in de Sitter branes. *Phys. Rev.*, D86:024015, 2012.

[42] Sean A Hayward. Wormhole dynamics in spherical symmetry. *Physical Review D*, 79(12):124001, 2009.

[43] Izrail S Gradshteyn and I_M Ryzhik. Table of integrals. *Series, and Products (Academic, New York, 1980)*, 1, 1980.

[44] Valeria Ferrari and Bahram Mashhoon. New approach to the quasinormal modes of a black hole. *Physical Review D*, 30(2):295, 1984.

[45] Da-Ping Du, Bin Wang, and Ru-Keng Su. Quasinormal modes in pure de Sitter spacetimes. *Physical Review D*, 70(6):064024, 2004.

[46] G Pöschl and Edward Teller. Bemerkungen zur quantenmechanik des anharmonischen oszillators. *Zeitschrift für Physik*, 83(3-4):143–151, 1933.

[47] Jürgen Fuchs and Christoph Schweigert. *Symmetries, Lie algebras and representations: A graduate course for physicists*. Cambridge University Press, 2003.

[48] Howard Georgi. *Lie algebras in particle physics: from isospin to unified theories*. CRC Press, 2018.

[49] Alfredo López-Ortega. Quasinormal modes of D-dimensional de Sitter spacetime. *General Relativity and Gravitation*, 38(11):1565–1591, 2006.

[50] ESC Ching, PT Leung, WM Suen, and K Young. Wave propagation in gravitational systems: Late time behavior. *Physical Review D*, 52(4):2118, 1995.

[51] Celso Molina, D Giugno, E Abdalla, and A Saa. Field propagation in de Sitter black holes. *Physical Review D*, 69(10):104013, 2004.

[52] Jiliang Jing. Dirac quasinormal modes of the Reissner-Nordström de Sitter black hole. *Physical Review D*, 69(8):084009, 2004.

[53] Roman A Konoplya and Carlos Molina. Ringing wormholes. *Physical Review D*, 71(12):124009, 2005.

[54] James M Bardeen. Black holes do evaporate thermally. *Physical Review Letters*, 46(6):382, 1981.

[55] Eric W Weisstein. Cubic formula. *omega*, 86:87, 2002.

[56] GW Gibbons, MJ Perry, and CN Pope. Partition functions, the Bekenstein bound and temperature inversion in Anti-de Sitter space and its conformal boundary. *Physical Review D*, 74(8):084009, 2006.

[57] Samuli Hemming and Larus Thorlacius. Thermodynamics of large AdS black holes. *Journal of High Energy Physics*, 2007(11):086, 2007.

[58] Rodrigo Aros, Ricardo Troncoso, and Jorge Zanelli. Black holes with topologically nontrivial AdS asymptotics. *Physical Review D*, 63(8):084015, 2001.

[59] Yen Chin Ong. Hawking evaporation time scale of topological black holes in Anti-de Sitter spacetime. *Nuclear Physics B*, 903:387–399, 2016.

[60] Don N Page. Finite upper bound for the Hawking decay time of an arbitrarily large black hole in Anti–de Sitter spacetime. *Physical Review D*, 97(2):024004, 2018.

[61] Rabin Banerjee, Sujoy Kumar Modak, and Dibakar Roychowdhury. A unified picture of phase transition: from liquid-vapour systems to AdS black holes. *Journal of High Energy Physics*, 2012(10):125, 2012.

[62] Gerardus t Hooft. The self-screening hawking atmosphere, a new approach to quantum black hole microstates. *Nucl. Phys. B, Proc. Suppl.*, 68(gr-qc/9706058):174–184, 1998.

[63] William A Hiscock. Models of evaporating black holes. I. *Physical Review D*, 23(12):2813, 1981.

[64] Steven M Christensen and Stephen A Fulling. Trace anomalies and the Hawking effect. *Physical Review D*, 15(8):2088, 1977.

[65] MI Beciu. Evaporating black hole in Vaidya metric. *Physics Letters A*, 100:77–79, 1984.

[66] Sean P Robinson and Frank Wilczek. Relationship between hawking radiation and gravitational anomalies. *Physical review letters*, 95(1):011303, 2005.

[67] Elias C Vagenas and Saurya Das. Gravitational anomalies, Hawking radiation, and spherically symmetric black holes. *Journal of High Energy Physics*, 2006(10):025, 2006.

[68] Maulik K Parikh and Frank Wilczek. Hawking radiation as tunneling. *Physical Review Letters*, 85(24):5042, 2000.

[69] Ren Jun, Zhang Jing-Yi, and Zhao Zheng. Tunnelling effect and Hawking radiation from a Vaidya black hole. *Chinese Physics Letters*, 23(8):2019, 2006.

[70] R Torres, F Fayos, and O Lorente-Espín. Evaporation of (quantum) black holes and energy conservation. *Physics Letters B*, 720(1-3):198–204, 2013.

[71] Bo Sundborg. The Hagedorn transition, deconfinement and $N = 4$ SYM theory. *Nuclear Physics B*, 573(1-2):349–363, 2000.

[72] Howard J Schnitzer. Confinement/deconfinement transition of large N gauge theories with N_f fundamentals: N_f/N finite. *Nuclear physics B*, 695(3):267–282, 2004.

[73] Edward Witten. Anti-de sitter space, thermal phase transition, and confinement in gauge theories. *arXiv preprint hep-th/9803131*, 1998.

[74] Chanju Kim and Soo-Jong Rey. Thermodynamics of large N super Yang Mills theory and AdS/CFT correspondence. *Nuclear Physics B*, 564(3):430–440, 2000.

[75] Clifford P Burgess, Neil R Constable, and Robert C Myers. The free energy of $N = 4$ super Yang-Mills and the AdS/CFT correspondence. *Journal of High Energy Physics*, 1999(08):017, 1999.

[76] Steven S Gubser, Igor R Klebanov, and Arkady A Tseytlin. Coupling constant dependence in the thermodynamics of $N = 4$ supersymmetric Yang-Mills theory. *Nuclear Physics B*, 534(1-2):202–222, 1998.

[77] Vijay Balasubramanian, Alice Bernamonti, Jan de Boer, N Copland, Ben Craps, Esko Keski-Vakkuri, Berndt Müller, Andreas Schäfer, Masaki Shigemori, and Wieland Staessens. Holographic thermalization. *Physical Review D*, 84(2):026010, 2011.

[78] Vijay Balasubramanian, Alice Bernamonti, Johannes de Boer, Neil Copland, Ben Craps, Esko Keski-Vakkuri, B Müller, Andreas Schäfer, Masaki Shigemori, and Wieland Staessens. Thermalization of strongly coupled field theories. *Physical review letters*, 106(19):191601, 2011.

[79] Jia-Lin Zhang, Rong-Gen Cai, and Hongwei Yu. Phase transition and thermodynamical geometry for Schwarzschild AdS black hole in $AdS_5 \times S^5$ spacetime. *Journal of High Energy Physics*, 2015(2):143, 2015.

[80] Karin Bautier, François Englert, Marianne Rooman, and Ph Spindel. The Fefferman-Graham ambiguity and AdS black holes. *Physics Letters B*, 479(1-3):291–298, 2000.

[81] Pantelis S Apostolopoulos, George Siopsis, and Nikolaos Tetradis. Cosmology from an Anti-de Sitter–Schwarzschild black hole via holography. *Physical review letters*, 102(15):151301, 2009.

[82] Eric Poisson. *A relativist's toolkit: the mathematics of black-hole mechanics*. Cambridge University Press, 2004.

[83] Alexander M Polyakov. Thermal properties of gauge fields and quark liberation. *Physics Letters B*, 72(4):477–480, 1978.

[84] Gianluca Grignani, Joanna L Karczmarek, and Gordon W Semenoff. Hot giant loop holography. *Physical Review D*, 82(2):027901, 2010.

[85] Juan Maldacena. Wilson loops in large N field theories. *Physical Review Letters*, 80(22):4859, 1998.

[86] Andreas Brandhuber, Nissan Itzhaki, Jacob Sonnenschein, and Shimon Yankielowicz. Wilson loops, confinement, and phase transitions in large N gauge theories from supergravity. *Journal of High Energy Physics*, 1998(06):001, 1998.